University of Benghazi

Faculty of Science

Department of Earth Sciences

Benghazi-Libya

Regional Subsurface Facies Distribution of Upper-Ordovician Memouniat Formation, Hamada (Ghadames) Basin, NW Libya.

A thesis is submitted to the Department of Earth Sciences as partial fulfillment of the requirements for the degree of Master of Sciences **(**M. Sc.**)** in geology.

by

Ali El. Younis

Supervised by

Dr. Omar Elfigih

Year

Fall 2012-2013

جامـــعة بنغـــــازي

كـــلية العلوم

قسم علوم الأرض

بنغازي ليبيا

مشروح دراسة مقدم لقسم علوم الارض جامعة بنغازي
لنيل درجة الماجستير

في علم الجيولوجيا (علوم الارض)

التوزيع الإقليمي التحت سطحي لسحنات العصر الاردوفيشي العلوي لطبقة الميمونيات، حوض غدامس، شمال غرب ليبيا.

مقدم من الطالب: علي السنوسي يونس الزوي

الرقم الدراسي: 1393

تحت اشراف الدكتور: عمر بوزيد الفقية

تاريخ المناقشة

2012/12/8

الخـــلاصـــــة

تحليل العينات الصخرية الاصطوانية والسرود الكهربائية المتوفرة لتسعة عشر بئر في حوض الحمادة (غدامس) وضح ان طبقه الميمونيات تتكون من ثلاث سحنات ترسيبية محدودة بعلامات طبقية زمنية.

في هذا التركيب الطبقي وبمعرفة تتابعاتة النسيجية الترسيبية والتريكبة والتي تدل على التغير الافقي الشامل للسحنات في اتجاه الشمال الغربي من سحنات نهرية الي سحنات ذات طبقات موجية رملية شاطئية الي سحنات طينية حوضية عميقه.

التحليل المجهري لبعض العينات لطبقة الميمونيات يبين بأن هذة الطبقة تتكون بنسبة عالية من الكوارتز بمعدل (92%) من المجموع الكلي للحبيبات الرملية المكونة لها ونسبة قليلة من حبيبات الفلدسبار والتي قد تشكل نحو (2%) وايضا بعض فتات الصخور والذي يشكل (6%) متضمنا الكوارتز متعدد البلورات والفتات الطيني.

التوزيع المساحي للسحنات المدروسة والمعرفة يمكن دراستها وتحليلها عن طريق بعض القطاعات الطبقية والتي توضح نسبة تمركز الطبقات الرملية ذات الطابع النهري وازديادها ومصدرها جنوبا، بينما تتركز طبقات الطين البحري شمالا بعيدا عن الشاطئ.

يمكن تمثيل او رسم اتجاهات الترسيب لطبقات الرمال (1-4) بواسطة خرائط طبقية حيث توضح تغيير مسار ترسيب هذه الوحدات الطبقية الرملية والذي يشير الي استقلالية محاور تزويد الرواسب وتوزيعها.

ABSTRACT

Analysis of available cores and wireline logs from 19 wells within the Hamada **(**Ghadames**)** Basin are demonstrated that the Memouniat Formation consisting of mainly three depositional facies bounded by time stratigraphic markers. Within this stratigraphic framework the identified sequences of sedimentary texture and structures indicates that the gross facies changed laterally northwestward from a fluvially-channelized dominated facies, to wavy laminated and bioturbated shoreface sands and eventually to basinal-offshore silt/shale.

Petrographic analysis reveals that the Memouniat Formation have a very high quartz contents, constituting of an average about **(**92%**)** of the total sand grains, sparse feldspar grains account for about **(**2%**)** and rock fragments of an average **(**6%**)** which include polycrystalline quartz and clay clasts.

The areal distribution of identified facies can be analyzed with the help of regional stratigraphic cross-section and fence diagram in which proportion of channelized type sands increase southward indicating that the source of channels lay in that direction. Marine shale predominated in the northwest, which direction lead increasingly further offshore.

The depositional sand trends in each mappable stratigraphic unit **(**1-4**)** are showing some offset from those in older units, where the pattern reveals the independence of the main sediment supply roots.

Acknowledgment

I thank Allah first for his help and guidance to finish this project. I am grateful to my supervisor Dr. Omar Elfigih for his patience, encouragement and support to present this work in a simple and an understandable way. I am extending my thanks to the management of the Exploration Department in the Arabian Gulf Oil Company, Benghazi, and Sirte Oil Company, El Bereqa Libya for providing the data upon which this study is based. I wish to express my gratitude to my parents and my family for their unlimited support and bidding to Allah to give me the success in my whole life. Thanks are due to all staff members of the Department of Earth Sciences in Benghazi University for their help and advices.

Contents

List of Figures

List of Tables

Chapter (1)
Introduction

In the last ten years exploration companies have accelerated efforts to tap the vest potential gas/oil reserves from the subsurface, upper Memouniat Formation in the Hamada **(**Ghadames**)** Basin, NW Libya. The area of study is a part of Hamada **(**Ghadames**)** Basin encompassing approximately an area of 150,000 km² **(**Fig. 1**)**.

Nineteen exploratory wells with little or no core control were used for multi-purposes, including preparing the isopach, structure, and isolith **(**facies**)** maps. The average density of cores in the studied area is 1.1 cored wells per concession **(**mainly concentrated in NC1 and NC8A concessions**)** or 3.1 wells per concession if all control points were taken into account.

1.1 Location of the study area.

The study area is a part of Hamada **(**Ghadames**)** Basin, it is located in the NW portion of Libya between latitudes 28°00 N to 32º20' N and longitudes 10°00E to 14º00E **(**Fig. 1**)** and covering an area of about 150,000Km².

Hamada **(**Ghadames**)** Basin has been the focus of hydrocarbon exploration since the early of 1970s, with the discovery of El Hamra and Emgayt Fields in concession NC8A and Al Kabier Field in concession NC7A in the southern part of the basin. The Arabian Gulf Oil Company **(**AGOCO**)** has continued exploration activities in this basin included several thousand kilometers of seismic lines **(**2D & 3D**)** and drilling of many wells.

1.2 Objectives of this study.

The specific objectives of this study were to:

- **a)** Identify the main environmental facies package of Memouniat Formation.
- **b)** Utilize well data for the recognition of plaeogeography through establishing time-stratigraphic framework and areal distribution of facies in Memouniat Formation.

c) Map the trends of the principle recognized facies in Memouniat Formation.

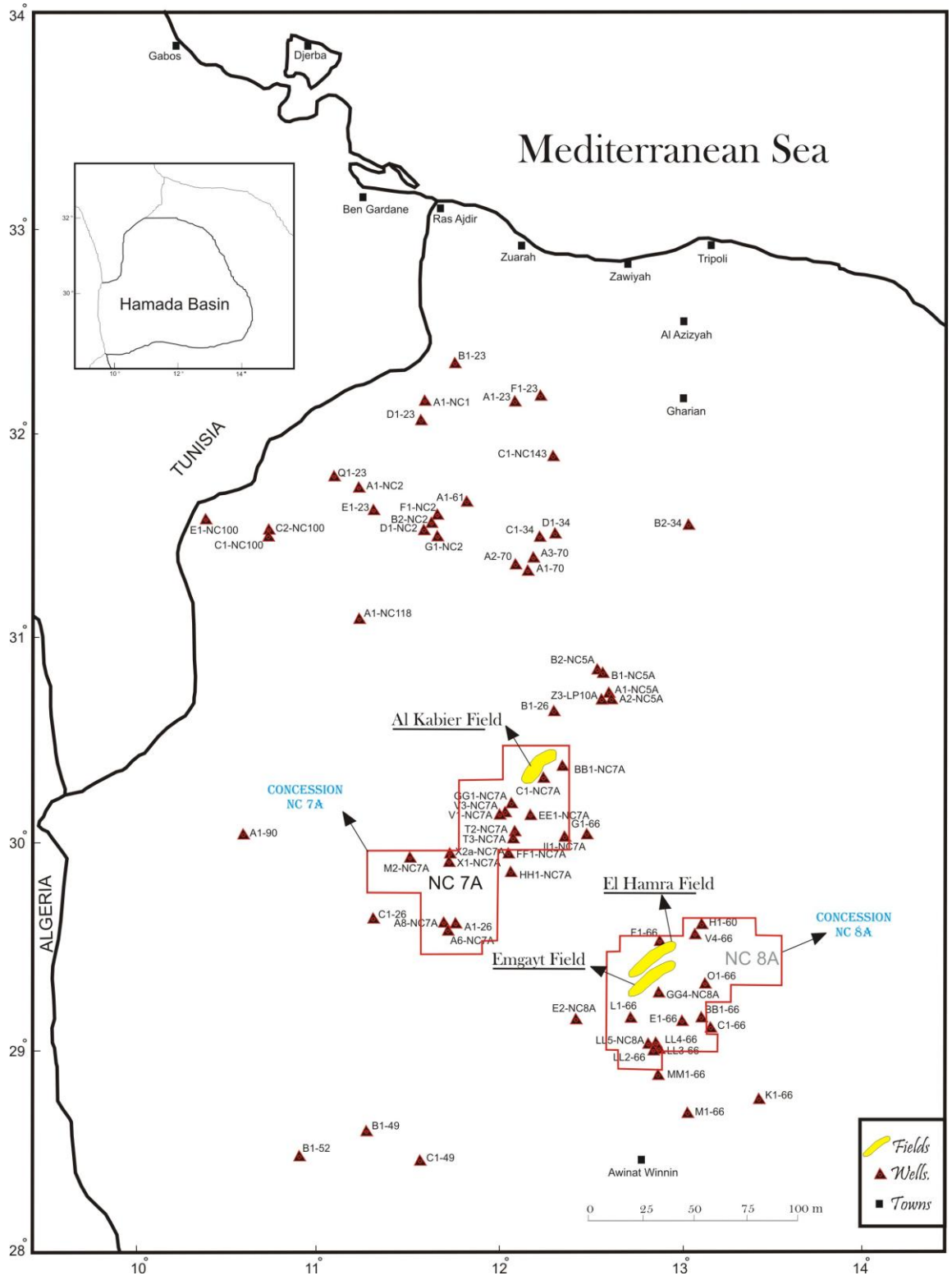

Figure 1. Location map of the study area, Hamada **(**Ghadames**)** Basin, NW Libya **(**Elfigih, 2000**)**.

1.3 Scientific Problems.

The term facies refers to a body of rock with specified characteristics. In the case of sedimentary rocks, it is defined on the basis of colour, bedding, composition, texture, fossils and sedimentary structures **(**Reading, 1978**)**. Stratigraphically could be defined in terms of sequential ordering of different depositional fashions from basin margin to basin depocentre. Also, the facies could be addressed in terms of energy levels and of tectonic subsidence and uplifts **(**Elfigih, 2000**)**.

The intracratonic Hamada **(**Ghadames**)** Basin was slowly subsiding, the subsurface environments may be regarded as dynamic system in which fluid continuously move along with some sediment compaction. Considerable sediment modification can be attributed in regional scale to the nature of facies changes **(**Elfigih, 2000**)**.

The exploration for the Memouniat Formation has faced many drilling difficulties for being deep-seated reservoirs and their possible facies heterogeneity and reservoir quality variation from one location to the other were very pronounced.

In this thesis and as data permits us, we will be dealing with the regional subsurface distribution of Memouniat facies throughout the Libyan part of the Hamada **(**Ghadames**)** Basin, to possibly address some scientific problems that could be raised regarding comparative study between facies types of Memouniat Formation intermes of their areal distribution, facies changes and heterogeneity.

1.4 Previous Work.

In the Hamada **(**Ghadames**)** Basin, the basic stratigraphy, structural picture, sedimentology, geochemistry of some rocks and some palaeontological studies are very well known through several studies, e.g. Massa and Collomb **(**1960**)**, Bellini and Massa **(**1980**)**, and Massa **(**1988**)**, Bergstrom and Massa, **(**1991**)**, Belhaj **(**1996**)**, Rubino, **(**2000**)**, Sikander **(**2000**)**, Wanis Elruemi **(**2000**)**, Youssif and Abugares **(**2000**)**, Ameed Ghori and Rajab, Mohammed **(**2000**)**, Marco Vecoli, Marco Tongiorgi, Marco Quintavalle and Dominique Massa **(**2000**)**, Wanis Elrumi **(**2000**)**.

Some studies have dealt with Memouniat Formation and its strato/structural fashion in some local areas in the Hamada **(**Ghadames**)** Basin and Murzuq Basin **(**El

Hawat, 2003**)**, Sikander **(**2000**)**, Howlett **(**2000**),** Jean-Loup Rubinoo, Remy Anfrayo , Christina Blanpiedo , Jean-Franconis Ghienne[2] and Gianreto Manatschal[2] **(**2000**)**. Nothing is known about the regional subsurface facies distribution of the Memouniat Formation.

An attempt should be taken in this thesis to present the possible facies characterizing this formation, their distribution and stratigraphic values in exploring throughout the Hamada **(**Ghadames**)** Basin.

Chapter (2)

Regional Geological Setting of the Hamada (Ghadames) Basin

2.1 Regional tectonic.

The Ghadames Basin is a large intracratonic sag basin developed on the passive northern margin of Gondwana. It covers an area of 350,000km², with the basin centre located in Algeria. The Libyan portion represents the eastern flank of the basin, rising towards the Tripoli-Tibisti Uplift, with a small sub-basin, the Zamzam Depression **(**ZZD**)** extending towards Misratah **(**Fig. 2**)**. The Libyan portion of this basin contains more than 16000ft **(**4877m**)** of Paleozoic-Mesozoic sediments. The basin is bounded in the west by the Amguid-El Biod Uplift in Algeria, to the south by the Hoggar Massif in Algeria. **(**Don Hallett, 2004**)**. In Libya the Hamada **(**Ghadames**)** Basin is shown in figure 2, occupies the northwestern part of Libya and is structurally bounded from the north by Nafusa Uplift, from the south by Qarqaf Arch from the east by Tripoli Soda Arch and from west partially bounded by Tihemboka Uplift.

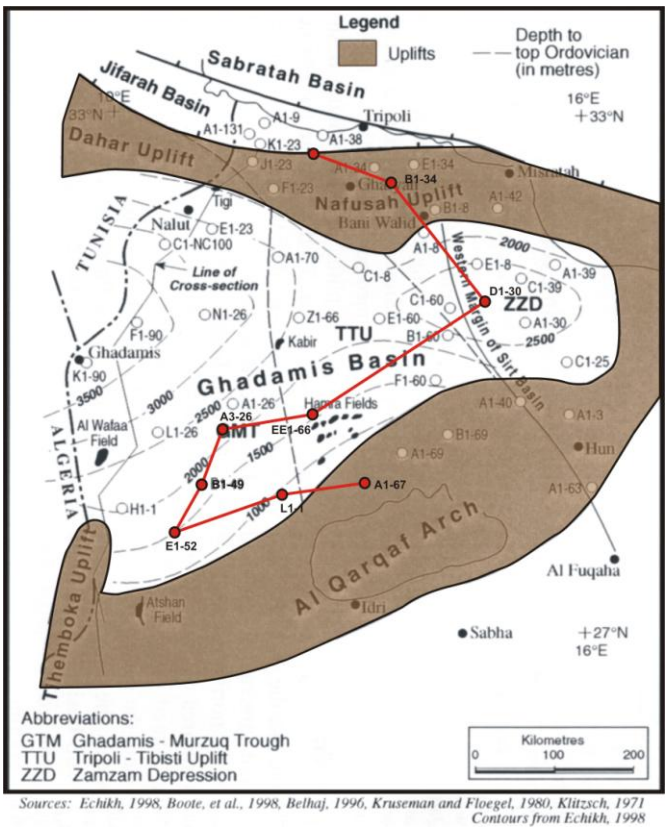

Figure 2. Tectonic Elements of Hamada **(**Ghadames**)** Basin, **(**Modified after Don Hallett, 2004**)**.

2.1.1 Ghadames basin evolution.

The early Palaeozoic history of the basin was controlled by the northwest-southeast Pan-African tectonic trend **(**Fig. 3**)**. The basin narrows southwards, confined between the Tripoli-Tibisti and Tihemboka Uplifts, into the Murzuq Basin. To the east the Palaeozoic section pinches-out against the Tripoli-Tibisti Uplift, but to the west the Tihemboka Uplift did not extend further north than the Edjeleh field, and the basin widened into a broad depocentre extending into Tunisia and Algeria west of the Tihemboka Uplift **(**Klitzsch, 1971**)**.

The final pulses of Pan-African tectonism continued into the Ordovician. During Llandeilian times, uplift and erosion occurred on the Tihemboka Arch and the Ahara Uplift in Algeria, and during the Caradocian, folding, faulting, uplift and erosion occurred which removed much of the Early and Middle Ordovician section on the Dahar Uplift in Tunisia. It was onto this irregular surface that the Late Ordovician ice-sheet encroached from the south **(**Echikh, 1998**)**.

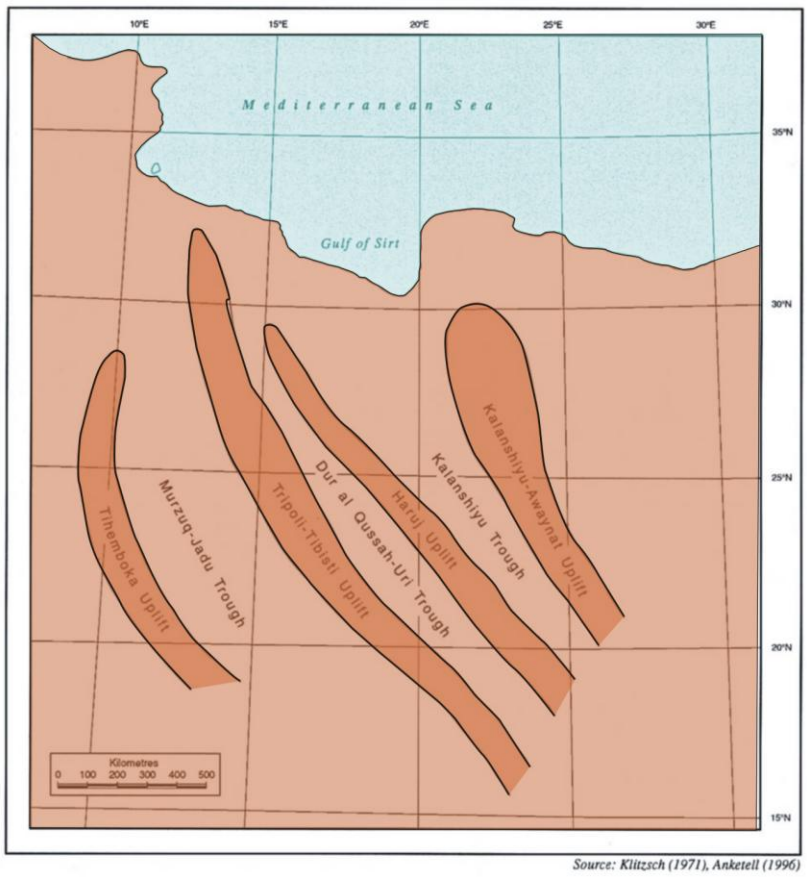

Figure 3. Post Pan-African structural trends in Libya, **(**Modified after Don Hallett, 2004**)**.

The Hercynian orogeny reached its peak during the Late Carboniferous and major new tectonic elements were formed as, including the Qarqaf and Nafusah Uplifts in Libya. The entire area was uplifted and subjected to intense erosion during the Permian which left the basin surrounded by highs which, in the case of the Nafusah and Qarqaf Arches, were eroded to their Cambro-Ordovician roots **(**Fig. 4**)**. Within the Libyan part of the basin structural trends with a northeast-southwest alignment were formed during the Hercynian orogeny **(**Fig. 5**)**.

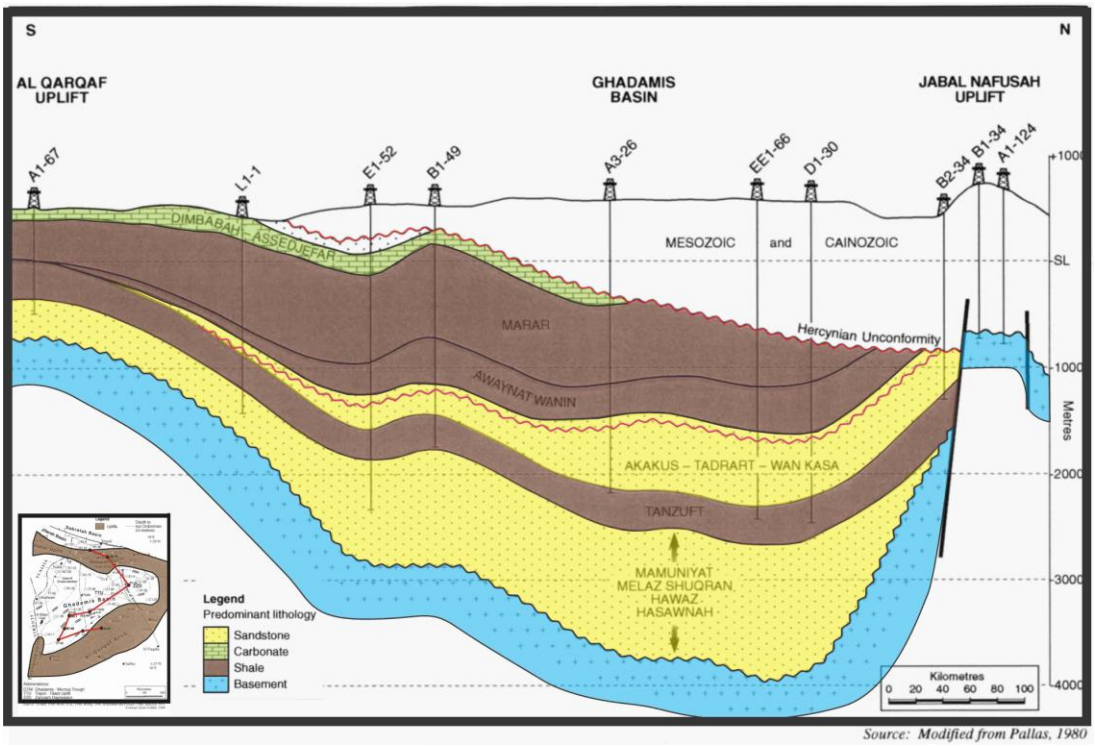

Figure 4. N-S Structural Cross-Section illustrates the Palaeozoic succession in the Ghadames Basin, and the effect of the Hercynian unconformity, **(**Modified after Don Hallett, 2004**)**.

Thick successions of Mesozoic continental deposits, including Triassic sandstones and evaporites, were deposited in the post-Hercynian sag basin **(**known as the Triassic Basin in Algeria and the Hamada Basin in Libya**)** in which the depocentre was located much further north than during the Palaeozoic **(**Fig. 6**) (**Echikh, 1998**)**.

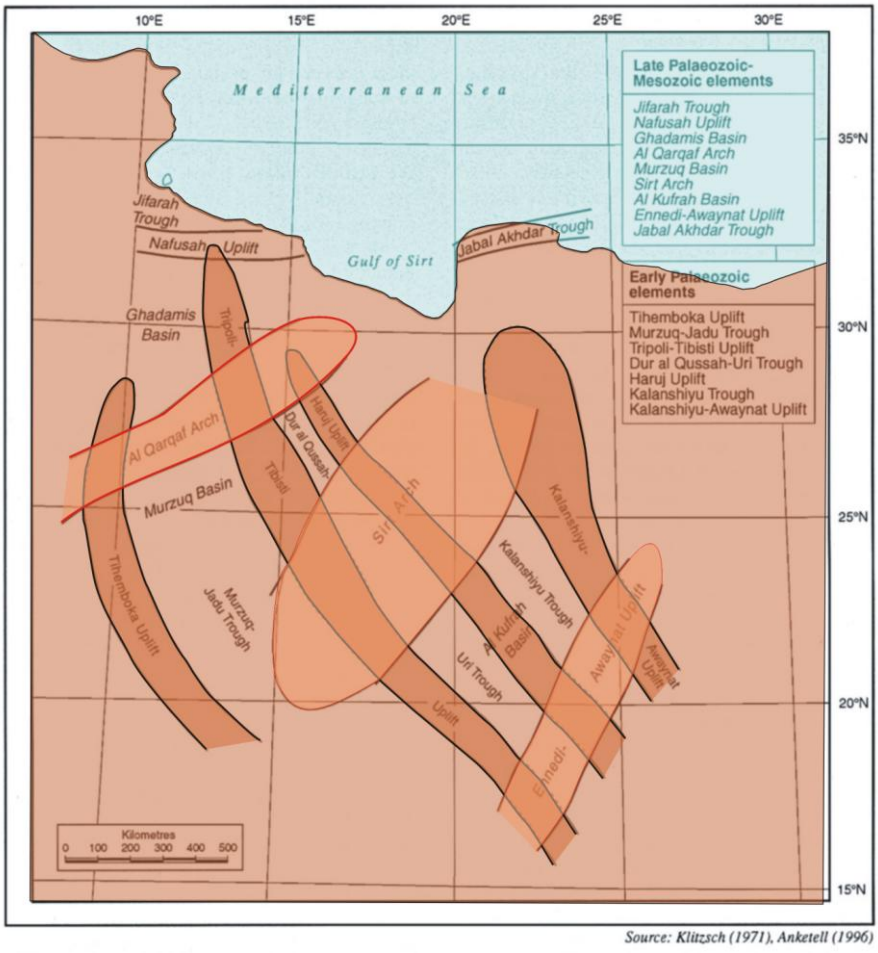

Figure 5.Hercynian Structural Trends, **(**Modified after Don Hallett, 2004**)**.

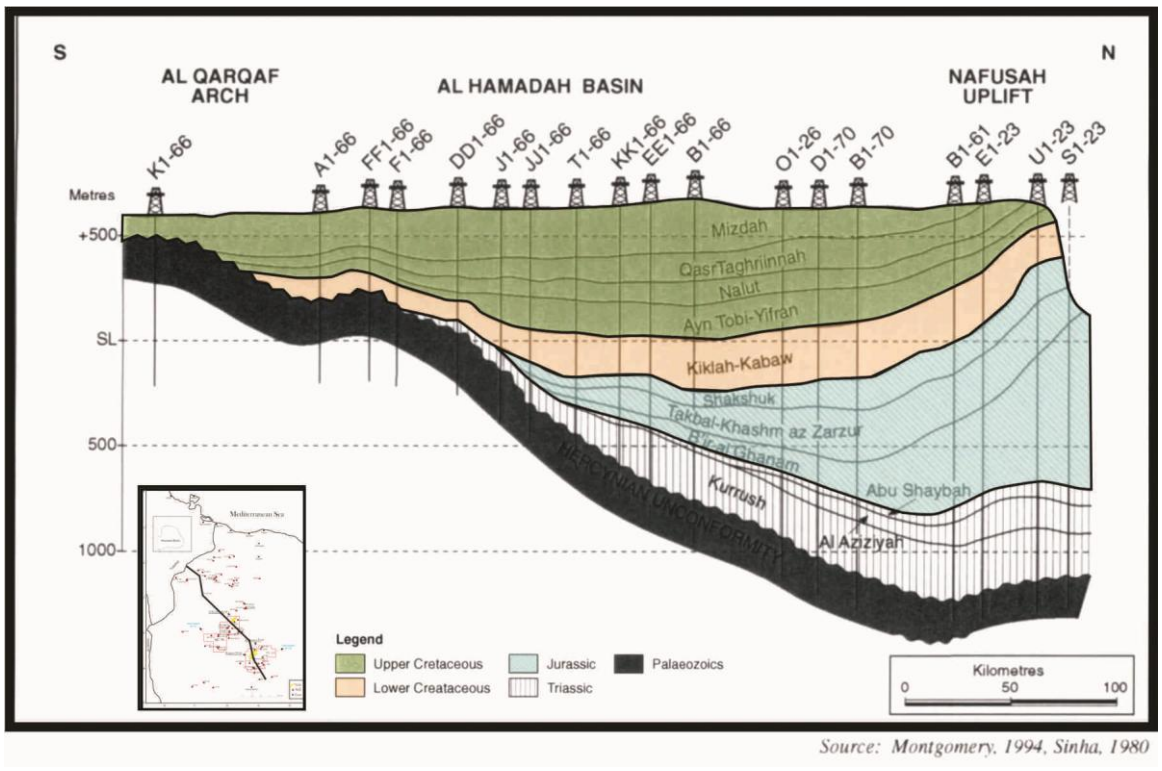

Figure 6. N-S Structural Section showing Mesozoic sediment package which overlies the Palaeozoic sediment package **(**Modified after Don Hallett, 2004**)**.

2.1.2 Late Ordovician glaciation.

During the early Palaeozoic western Gondwana was located close to the south pole, figure 7 is showing the palaeogeographic reconstruction of Gondwana and showing the extent of the Late Ordovician ice sheet and the palaeo-ice flow during the late Ordovician.

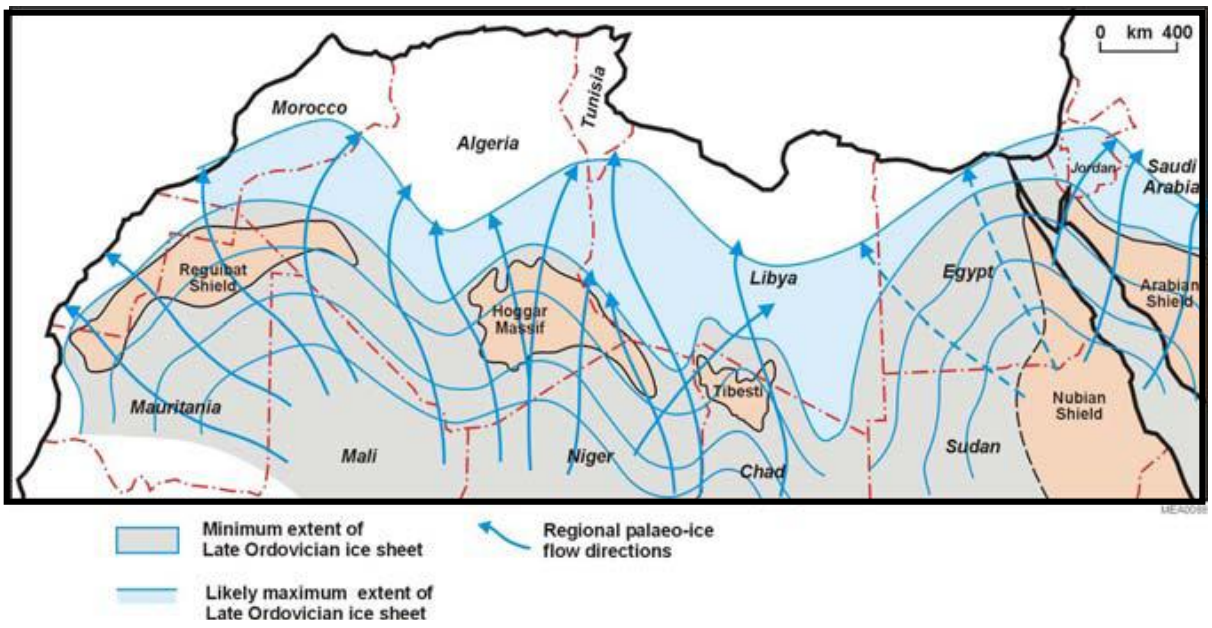

Figure 7. Palaeo-ice flow during the Late Ordovician glaciation of west Gondwana. **(**Modified after Vaslett, 1990**)**.

The glacial episode was very short lived, and was followed by a major flooding event during which Early Silurian seas spread across much of North Africa. Thick black shales were deposited in these seas which form the major source rocks for the Palaeozoic oil accumulations of north Africa **(**Luning, et al. 2000**)**.

Thereafter western Gondwana drifted northwards towards more temperate latitudes and the lapetus Ocean separating Gondwana from Laurentia gradually closed. Throughout the Palaeozoic much of the interior of Gondwana was the site of widespread erosion and continental deposition, but shallow-shelf seas continued to occupy the northern margin, **(**Boote, et al. 1998**)**, figure 8 shows the major distribution of upper Ordovician glacigenic rocks in North Africa.

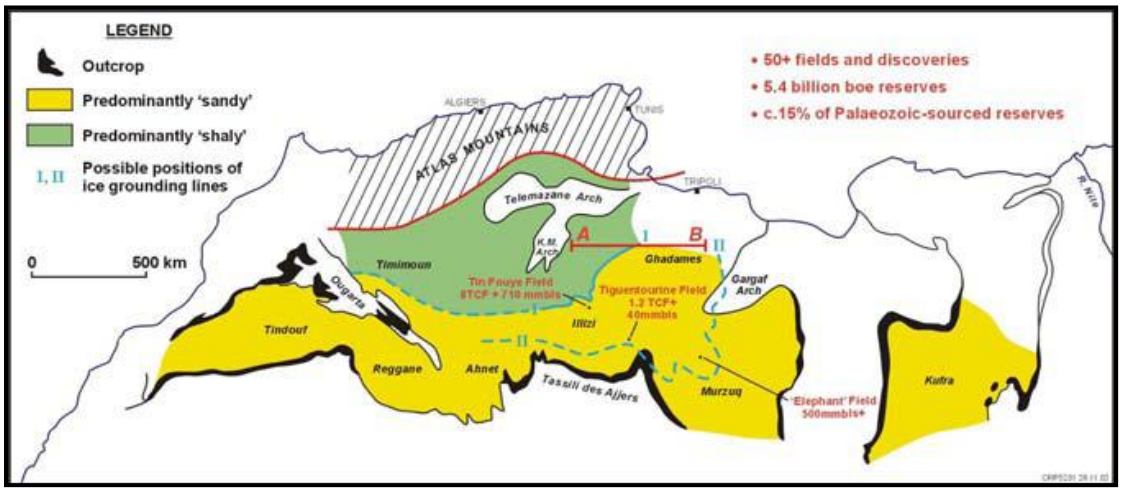

Figure 8. Distribution of Upper Ordovician Glacigenic Rocks in North Africa **(**Boote, et al., 1998**)**.

The Late Palaeozoic tectonism caused a major marine regression in North Africa. Most of Libyan territory became emergent and extensive erosion and continental deposition took place in the interior **(**Klitzsch, 1971**)**.

2.1.3 Taconic Unconformity.

Early Ordovician time was characterized by a tectonic instability **(**Attar 1987**)** indicated by the absence of the Cambrian over the main uplifts, e.g. the Ahara Uplift and the Tihemboka Arch. Peak activity occurred during Llandeilo time, when there was substantial activity, particularly on the southern rim of the Ghadames Basin, in Illizi and close to the Qarqaf Uplift. Active fault uplifts caused erosion and the creation of a series of overlapping deep erosional troughs, which were later filled by periglacial deposits. The folds created at this time are broad, with active faulting controlling thickness and facies distribution in syn- and post-tectonic formations.

The Taconic unconformity is illustrated by a cross-section though the Dahar High **(**Fig. 9**)**, where successive units of the Early Ordovician are seen to be overlain by the Late Ordovician Microconglomeratic Shales.

In Libya, deep troughs were formed close to the Qarqaf Uplift **(**Echikh 1992**)** and were filled with the periglacial facies of the Bir Tlacsin and Memouniat Formations.

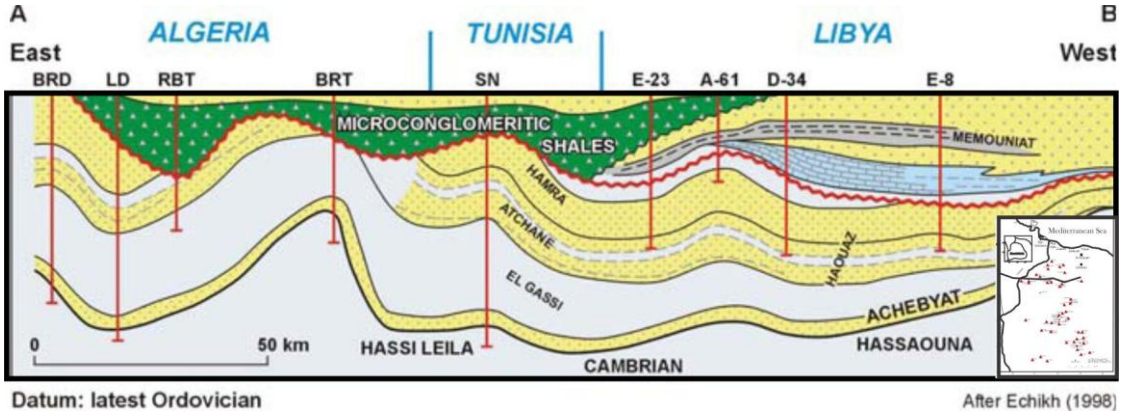

Figure 9. Geological cross-section through Ordovician formations of north Africa illustrating the erosional effects of the Taconic event. **(**After Echikh, 1998**)**.

2.2 Regional stratigraphy.

The Hamada **(**Ghadames**)** Basin of NW Libya is an intracratonic basin in which a thick sequence of clastic rocks of marine and non-marine origin were deposited in different sequences during the Paleozoic. These sedimentary sequences encompassing three stages during their development which are:

- The first stage corresponds to non-marine to shallow marine deposits forming the basal transgressive, deltaic to fluviatile sandstones of the Ordovician Memouniat Formation.
- The second stage is represented by the marine transgressive unit of Tanezzuft shale.
- The third stage represented by regressive sediments of Acacus Tadrart sandstones.

The Hamada **(**Ghadames**)** Basin spans from Cambrian to Carboniferous and is characterized by five regional unconformities representing emergent periods that may be related to sea level changes across the cratons **(**Fig. 10**)**, these unconformities could be timed as follows:

*1- Early Cambrian Unconformity **(**PANAFRICAN**)**.*

*2- Late Ordovician Unconformity **(**TACONIAN**)**.*

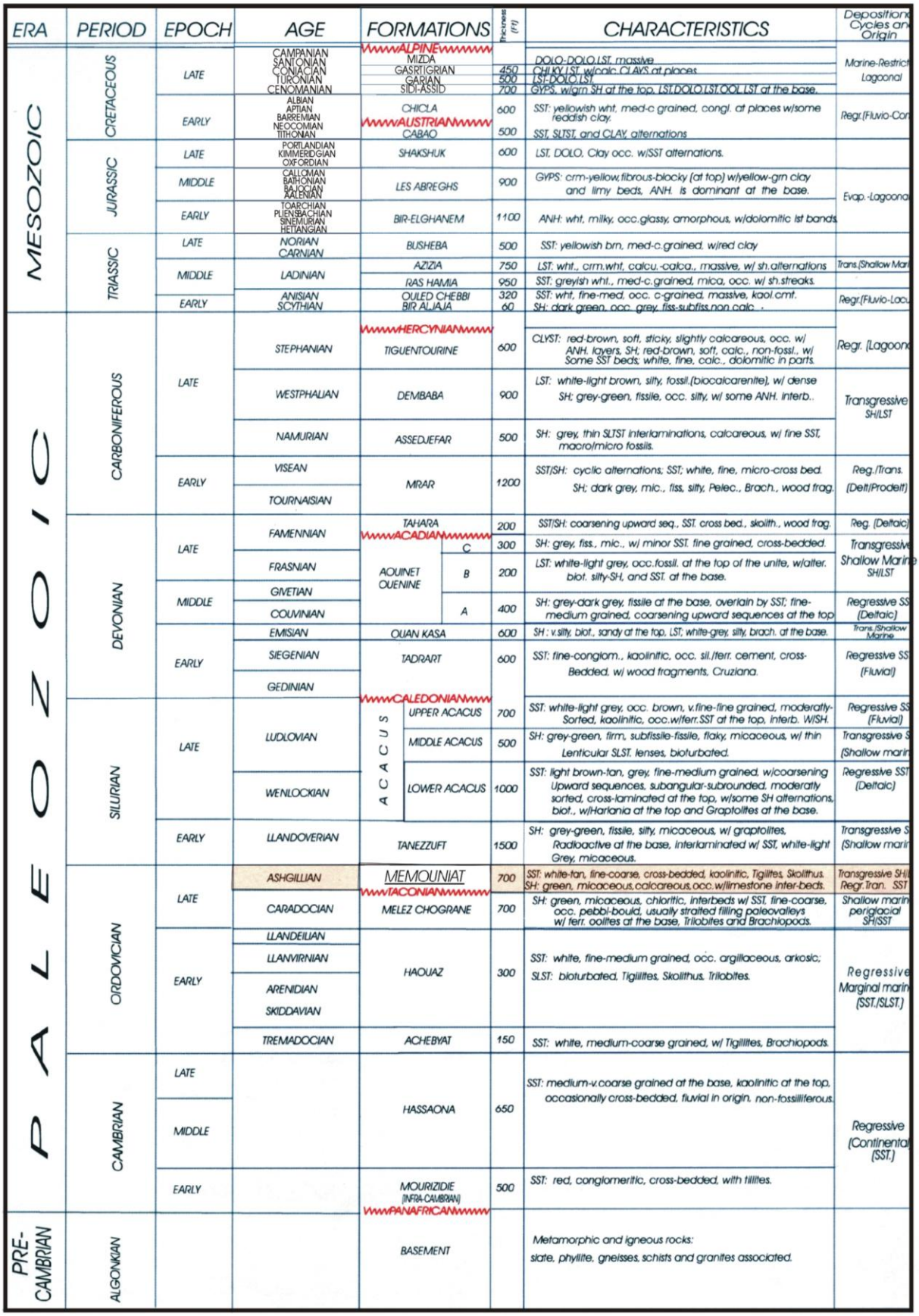

Figure 10. Paleozoic stratigraphic framework, Hamada **(**Ghadames**)** Basin. **(**Elfigih, 2000**)**.

3- Late Silurian Early Devonian Unconformity (CALEDONIAN).

4- Late Devonian Early Carboniferous Unconformity (ACADIAN).

5- Late Carboniferous. Eperrian Unconformity (HERCYNIAN).

The Paleozoic stratigraphic succession of the Hamada (Ghadames) Basin is summarized in figure 10, (Elfigih, 2000). This study deals with the stratigraphy of the Late Ordovician section of Memouniat Formation.

The Memouniat Formation was first described by Massa and Collomb from outcrops on the Al Qarqaf Arch (Fig. 11). A type section was selected by Parizek in the Idri area (Massa and Collomb, 1960). It has a wide distribution in the Murzuq, Al Kufrah and Ghadames Basins. It comprises 100 to 140m of massive, cross-bedded sandstones, representing a basal lowstand system. Rubino, reported a complex meander belt in the lower part of the Memouniat Formation which can be traced over a distance of 12km (Don Hallett, 2004).

The lower contact is unconformable and often ferruginous. The sandstone is generally medium- to coarse-grained, and frequently conglomeratic. It is friable, with a high percentage of kaolinitic cement. It contains occasional fine-grained sandstone and siltstone stringers. The Memouniat Formation contains rare *Tigillites* and fragmentary brachiopods and pelecypods. Palynological evidence suggests a Caradocian age for the Memouniat Formation whilst the brachiopod evidence indicates an Ashgillian age (Collomb, 1962, Havlicek and Massa, 1973). Additionally, the brachiopod fauna suggests a periglacial environment, and other evidence shows that at this period western Gondwana was located very close to the South Pole (Don Hallett, 2004).

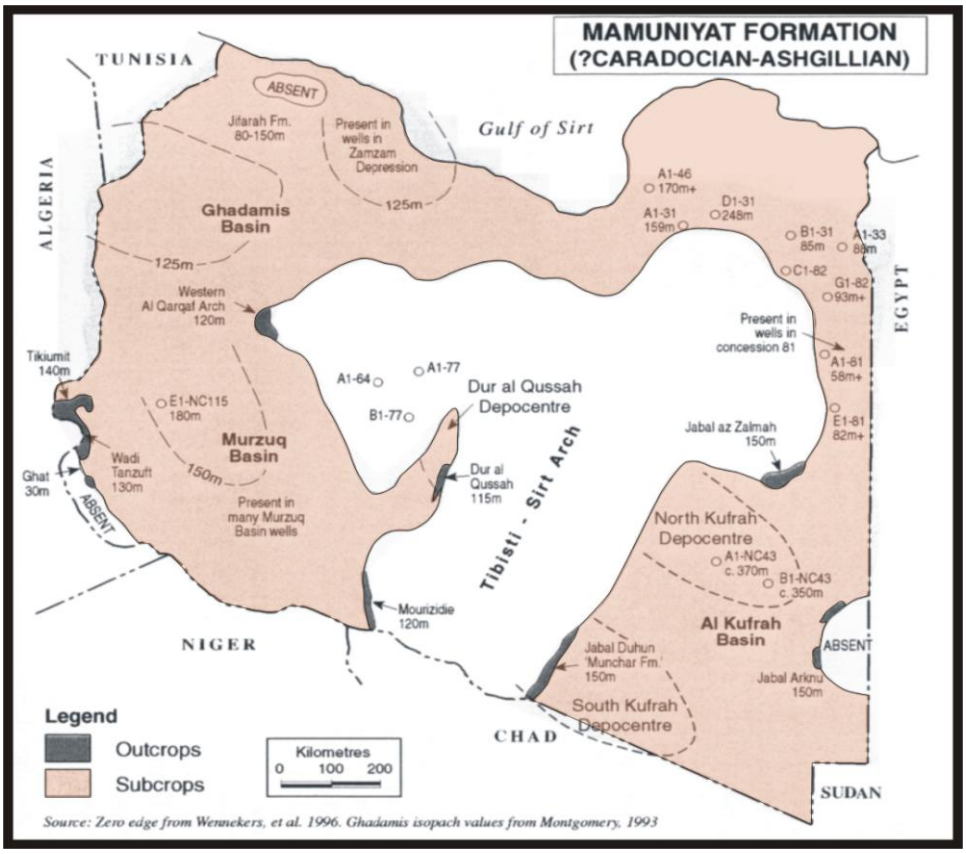

Figure 11. Memouniat Formation distribution in Libya, **(**Modified after Don Hallett, 2004**)**.

2.3 Geological setting of the study area.

The Upper Ordovician Memouniat Fromation in the study area is about **(**70 to 720ft**)** thick. The lower boundary is erosive with underlain Melez Chograne Formation, its upper boundary is unconformable with the Silurian Tanezzuft Formation, **(**Fig. 10**)**.

The isopach map of Memouniat Formation, **(**Fig. 12**)** indicates a rapid increase in thickness in the **(**NW**)** direction of the study area, as the responding to the structurally low basin area **(**Fig. 13**)**. However relative decrease of thickness much more pronounced in the NE direction here probably where the upper Ordovician Memouniat strata may onlap a NE striking paleogeographic high rising from the underlying erosional Melez Chograne surface. The present depth to the top of the Memouniat Formation is in the order of -1880 to -12500ft **(** -573 to -3810m**)**, while the maximum present depth of burial of Memouniat Formation in the study area is attaining more than -12500ft, this deep burial accounts for the relatively high consolidation nature of these sands.

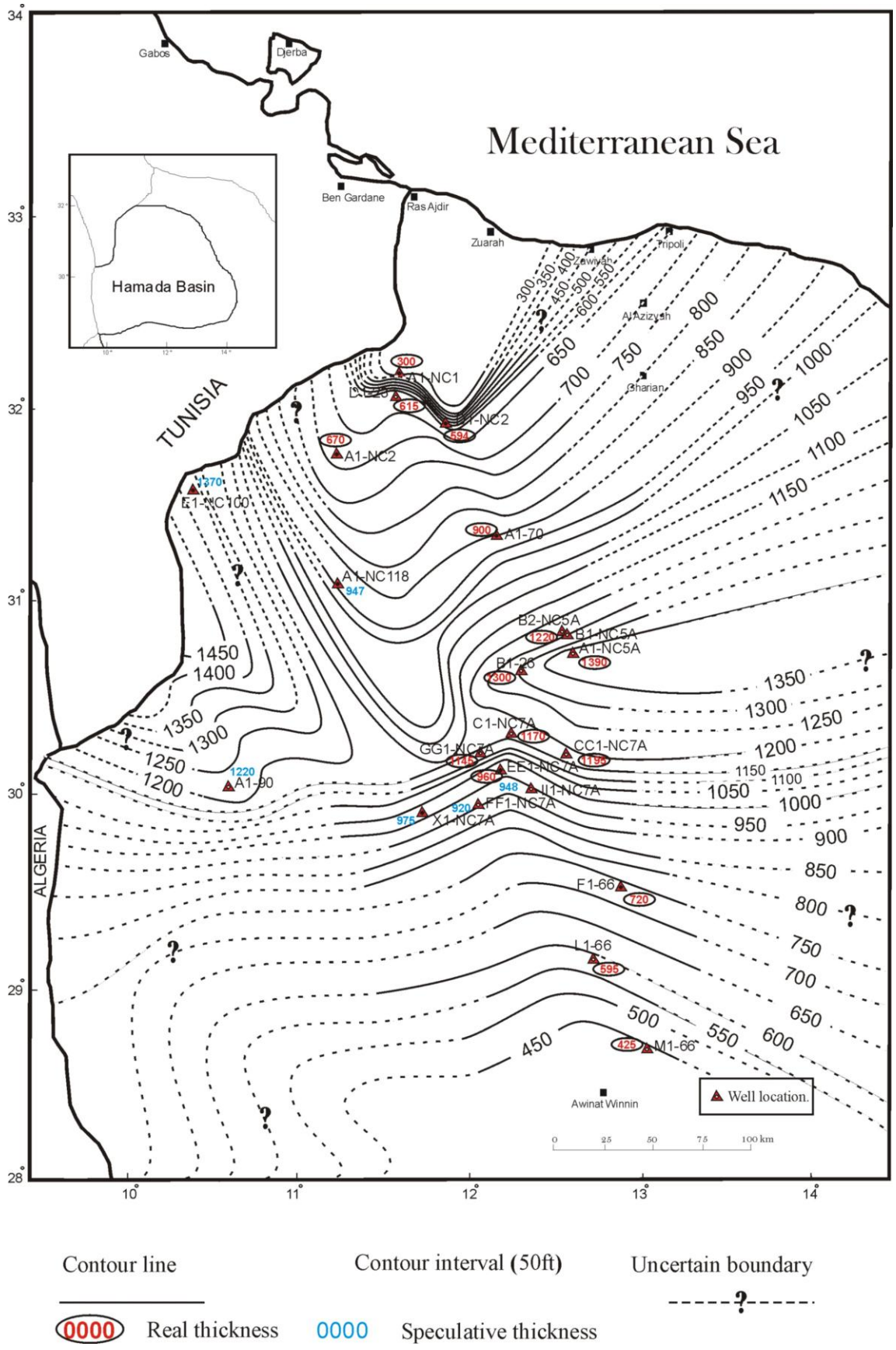

Figure 12. Isopach map of Memouniat Formation, Hamada **(**Ghadames**)** Basin.

Distinction between the Memouniat and Tanezzuft Formations is always possible and clear **(**in all well-logs**)** by referring to the relatively high radioactive basal part of Tanezzuft Fromation which has been used as a datum in this study. Structure map on the top of Ordovician **(**Fig. 13**)** shows that the strata dip generally westward at a rate of approximately **(**16ft/1km**)**.

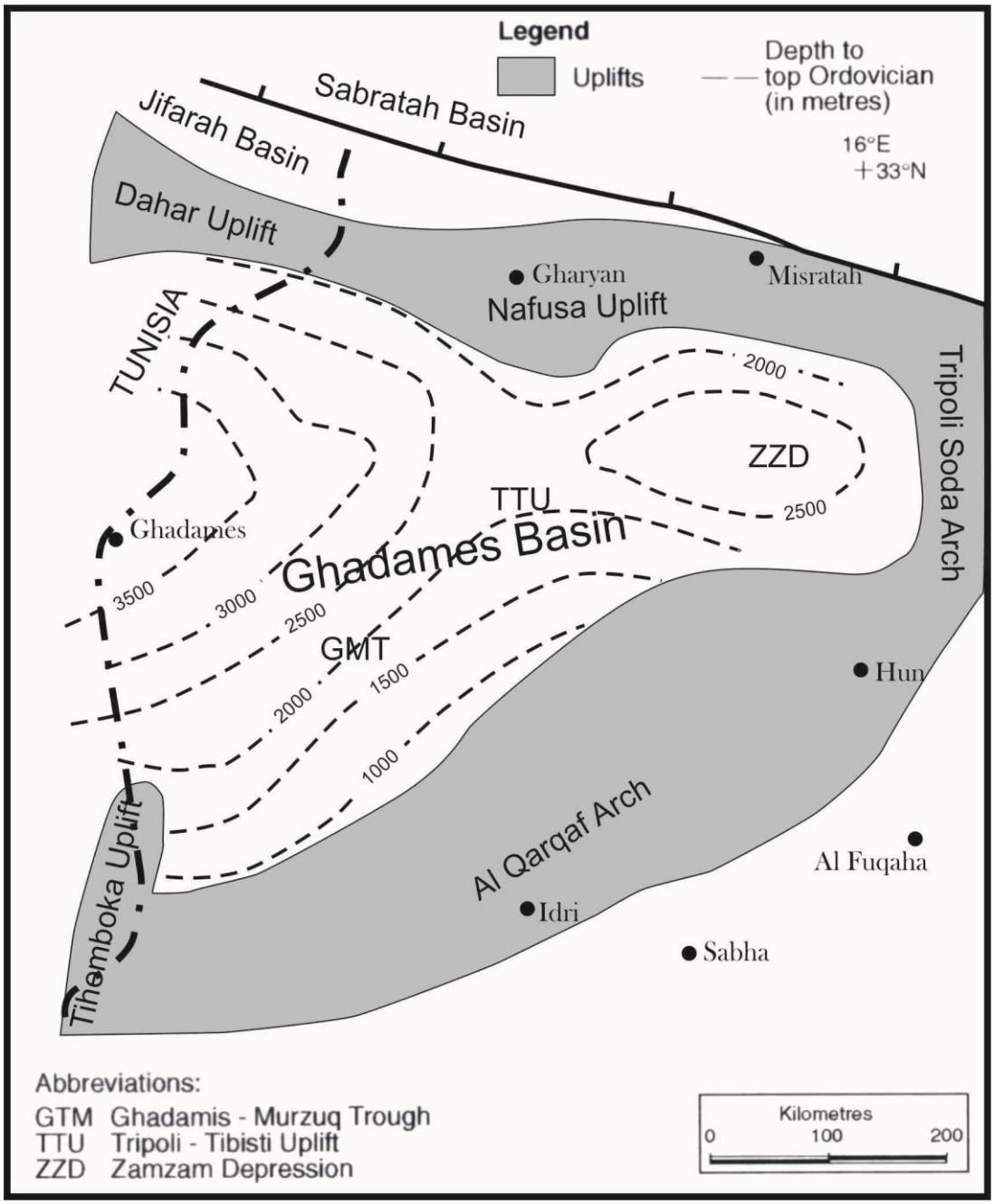

Figure 13. Structure map on top of Ordovician **(**Modified after Don Hallett, 2004**)**.

Chapter (3)

Methods of Study

The recovered 201ft of cores from targeted wells **(**Table 1**)**, **(**Fig. 14**)** were described by using a graphic logging form **(**Fig. 15**)**, in which, a vertical scale of 1cm to 4ft was selected, so that the graphic log could be compared directly with the wireline logs.

The principle attributes used to interpret environment shows in logging form are:

1- Gross lithology.

2- Associated sedimentary structures.

3- Vertical variation of grain sizes.

Well No.	***Well Name***	***Available cores at Mem. Fm.***	***Available well-log Suites***
1	D1-23	✓	SP.
2	B1-26	**X**	SP.
3	F1-66	✓	SP.
4	GG1-66	✓	SP.
5	L1-66	**X**	SP.
6	M1-66	**X**	SP.
7	A1-70	**X**	SP.
8	A1-90	**X**	SP.
9	E1-NC100	**X**	SP. & GR
10	A1-NC118	**X**	SP. & GR
11	A1-NC1	✓	SP. & GR
12	A1-NC2	**X**	SP.
13	D1-NC2	**X**	SP. & GR
14	A1-NC5A	**X**	GR
15	B1-NC5A	**X**	SP. & GR
16	B2-NC5A	**X**	SP. & GR
17	C1-NC7A	**X**	SP. & GR
18	CC1-NC7A	**X**	SP. & GR
19	EE1-NC7A	**X**	SP. & GR

Table 1. Targeted wells used in multi purposes in the study area.

A column was added to show the variation in oil shows obtained from core analysis. At the time of core examination the cores were found to be in good condition, core samples were arranged in a sequence and partially slabbed. As a result the sedimentary structures were preserved and the sands were very well consolidated and of quartzose nature.

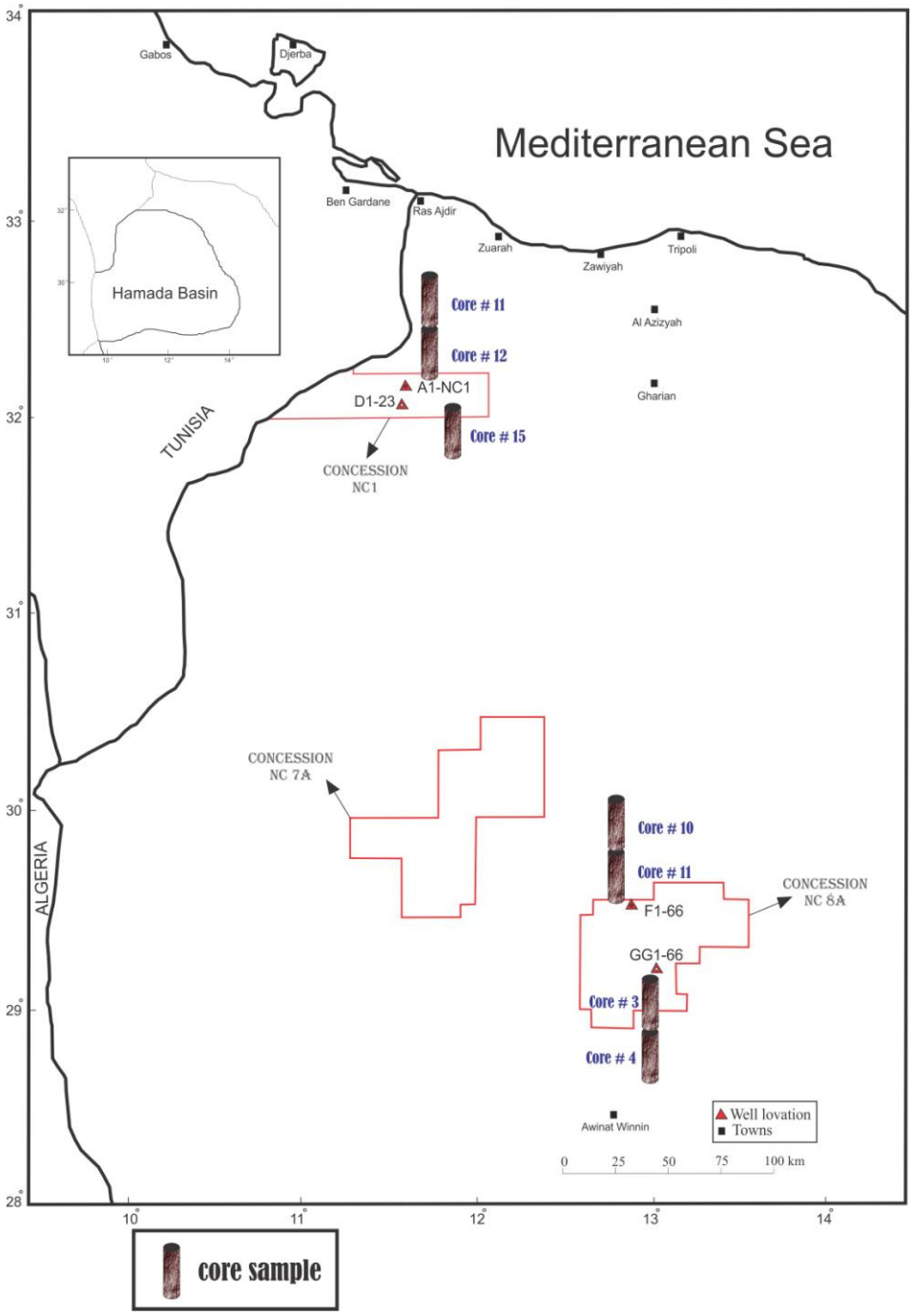

Figure 14. Base map for available cored wells **(**GG1-66, F1-66, D1-23, and A1-NC1**)** in the study area.

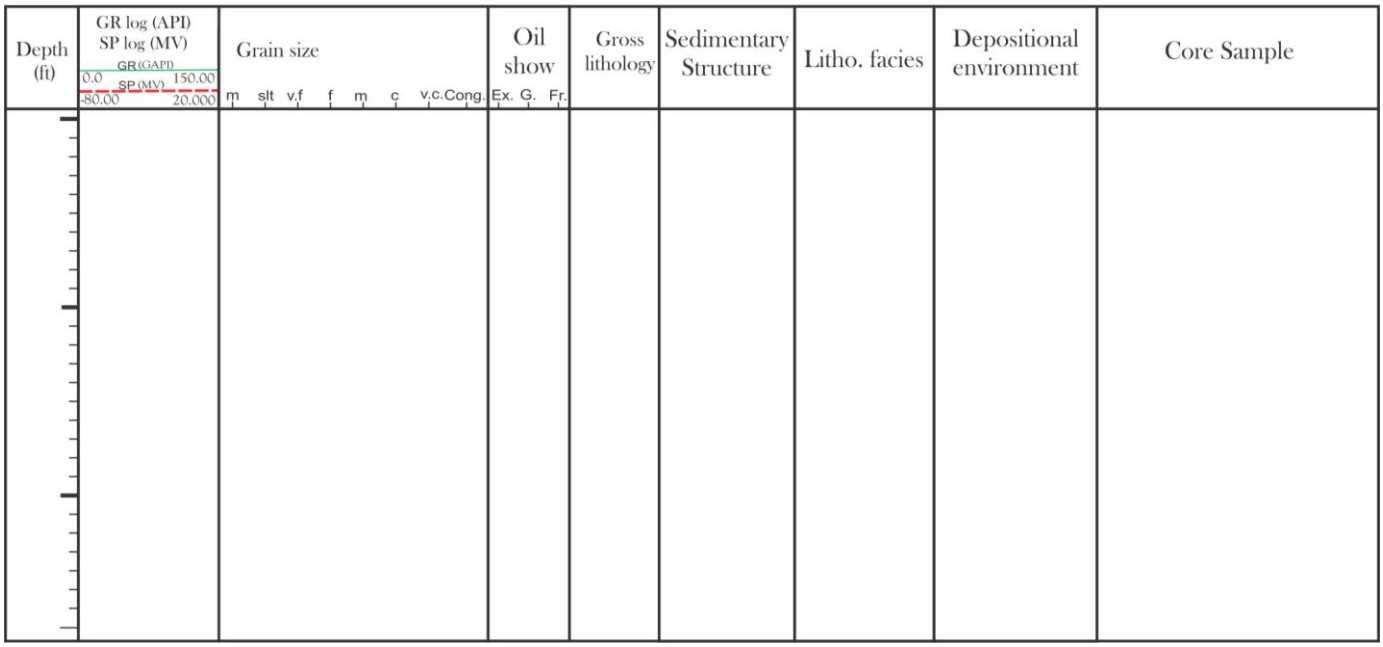

Figure. 15. Graphic facies log form, which used to show some low and high sandstone heterogeneity of Memouniat Formation, Hamada **(**Ghadames**)** Basin.

Following the detailed core description, the lateral facies relationships were investigated with the aid of well log suites to generate cross sections and fence diagram covering the whole study area. Wireline log data were incorporated into a basinwide assessment of the Memouniat sands lithofacies because they are widespread than core data. The well-to-well best correlation approaches were used to establish a stratigraphic framework within which possible lateral facies changes could be examined and mapped.

About seventeen thin sections were selected from different sandstone intervals of Memouniat Formation for petrographic examination.

Finally a series of log-facies maps obtained from wireline-log analysis to show possible trends of reservoir facies of Memouniat Formation were also prepared.

Chapter (4)

Lithofacies Analysis of Memouniat Formation

4.1 Environmental facies recognition through cores examination.

Sedimentary structures are the larger-scale features of sedimentary rocks. The majority of structures form by physical processes, before, during and after sedimentation, whereas others result from organic and chemical processes. Sedimentary structures, particularly those formed during sedimentation, have a variety of uses: for interpreting the depositional environment in terms of processes, water depth wind strength etc: for determining the way up of a rock sequence in area of complex folding and for deducing the palaeocurrent pattern and palaeogeography **(**Tucker 1991**)**.

4.1.1 Primary sedimentary structure and texture.

The observed sedimentary structures and textures in the examined cores indicate that there was an interplay between fluvio-channel and marine processes in the study area.

Three possible facies channel fill sands **(**Fig. 16**)**, proximal sands **(**Fig. 17**)** and basinal silt /shale **(**Fig. 18**)**, have been recognized.

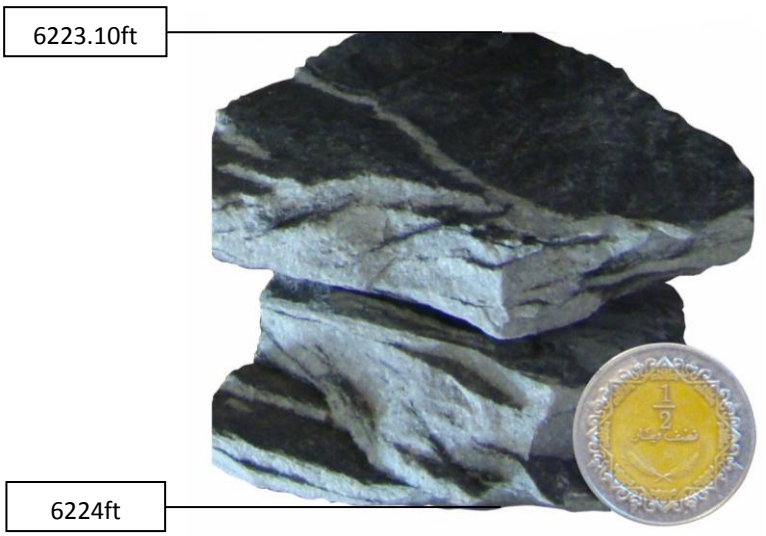

Figure 16. Channel fill sands in channel fill facies predominated sector, core #4 **(**6187-6224ft**)** in well GG1-66.

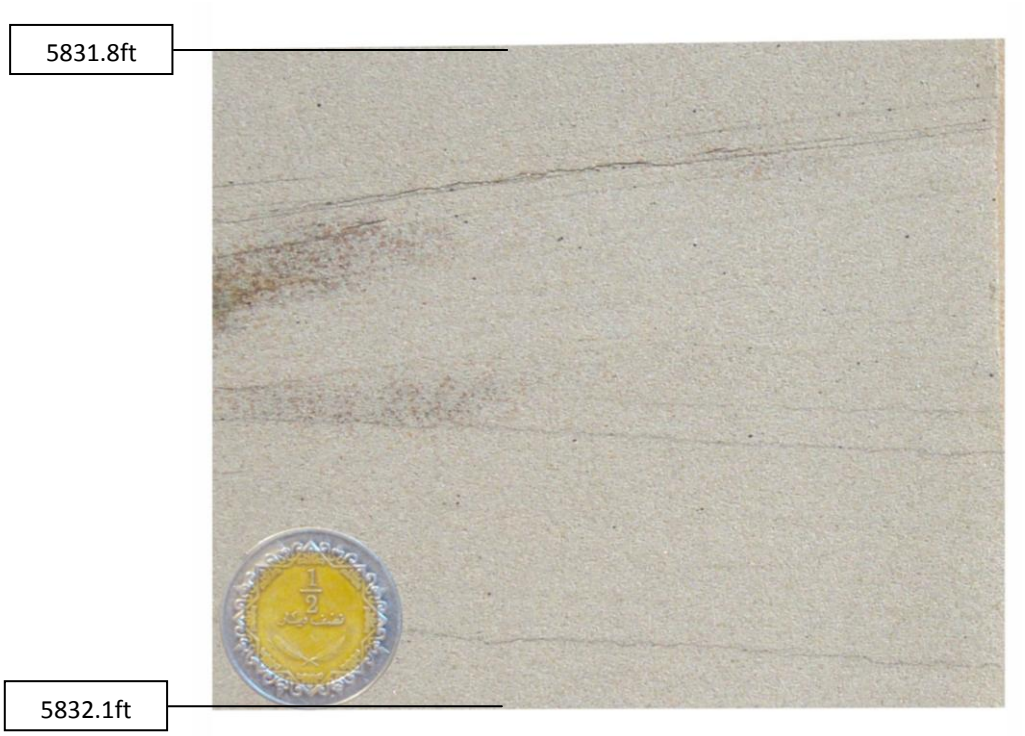

Figure 17. Proximal sands in proximal facies predominated sector, core #12 **(**5828.8-5843.8ft**)** in well A1-NC1.

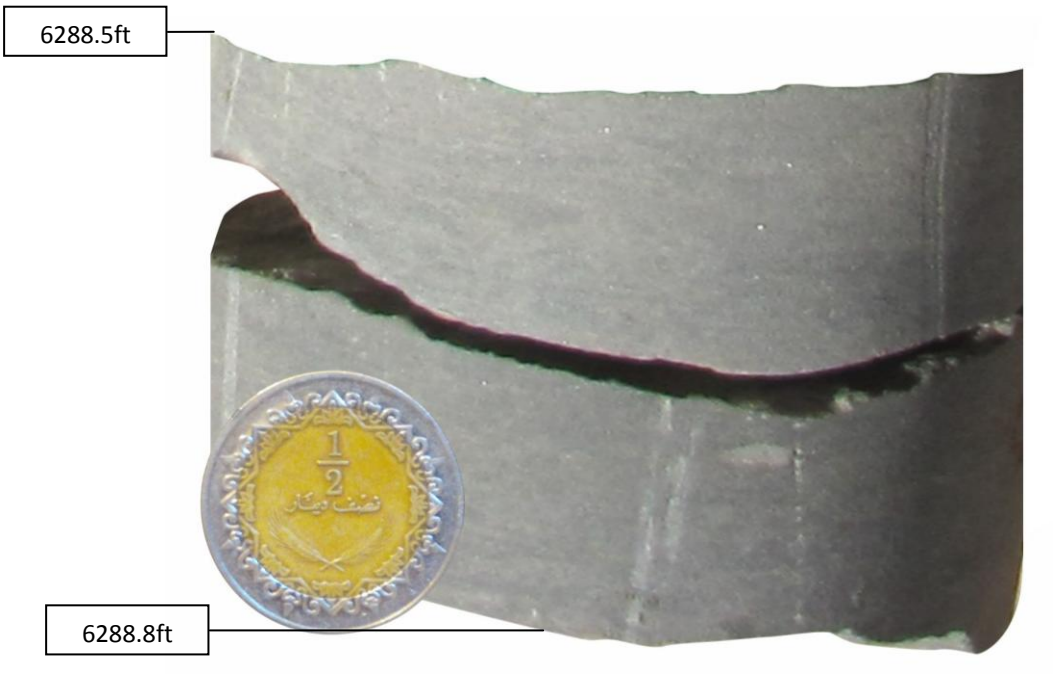

Figure 18. Basinal **(**offshore**)** silt/shale facies predominated sector, core #15 **(**6256-6311.6ft**)** in well D1-23.

4.1.1.1 Channel fill sandstone lithofacies:

The channels fill sand facies **(**Figs. 19, 20, 21, 22**)** consists of occasionally trough x-lamination **(**Fig. 23**)**, basal scours and rip-up clasts **(**Fig. 24**)**,. Horizontal lamination associated with wavy lamination may be observed at some levels of the sand-fill sequence which may suggests periods of variation in energy conditions **(**Fig. 25**)**.

Some evidences may suggest tidal processes may affect sedimentation like flaser-sands structures could be seen at some places **(**Fig. 26**)**. Bioturbations are less abundant in this facies, but may be present at some levels **(**Fig. 27**)**.

The grain size of this facies tends to be from medium to coarse grained, where the relative abundance of clay clasts is higher.

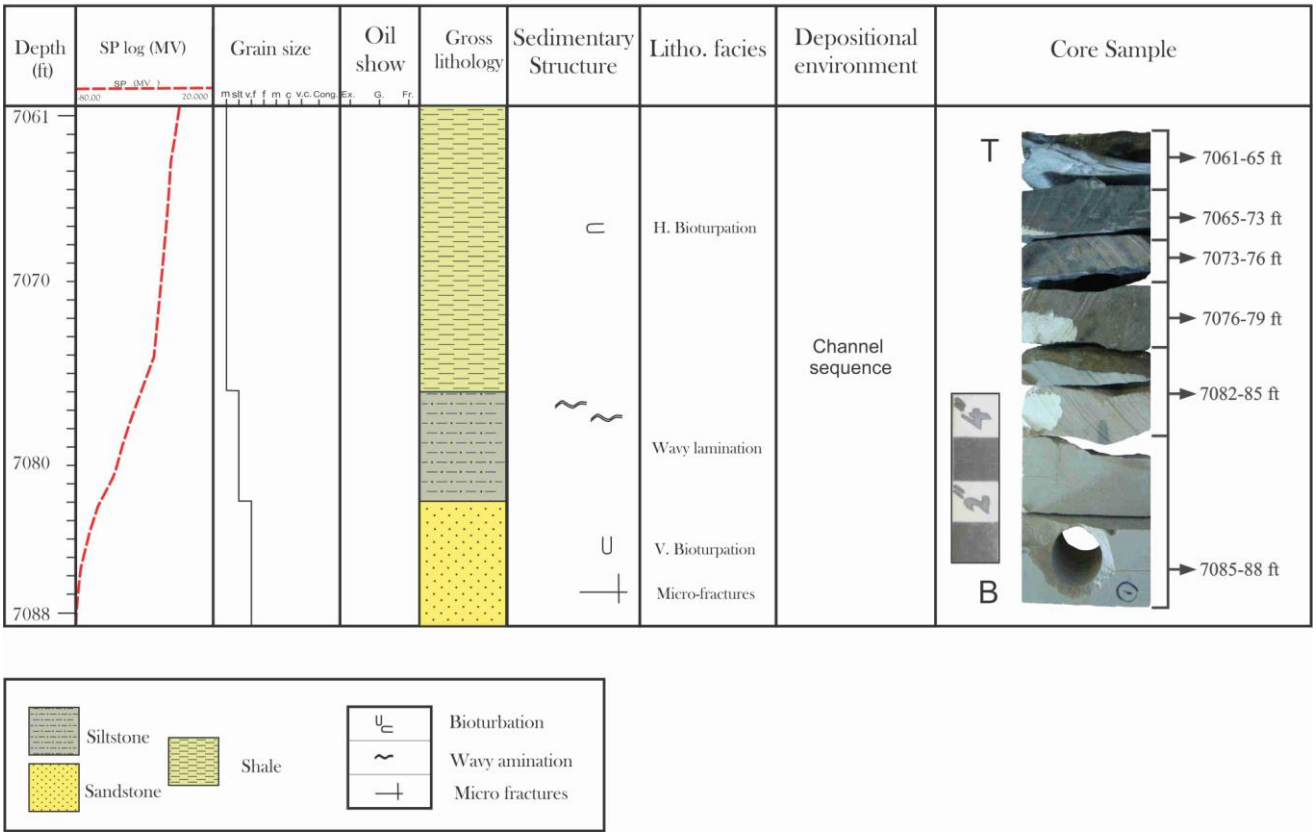

Figure 19. Graphic facies log of core #10, at interval **(**7061-7088ft**)**, in well F1-66, illustrating sequence grading upward from v.bioturbated, m-c grained sands at the base to H. bioturbated, f. grained sands at top, channel fill sands facies, Memouniat Formation, Hamada **(**Ghadames**)** Basin.

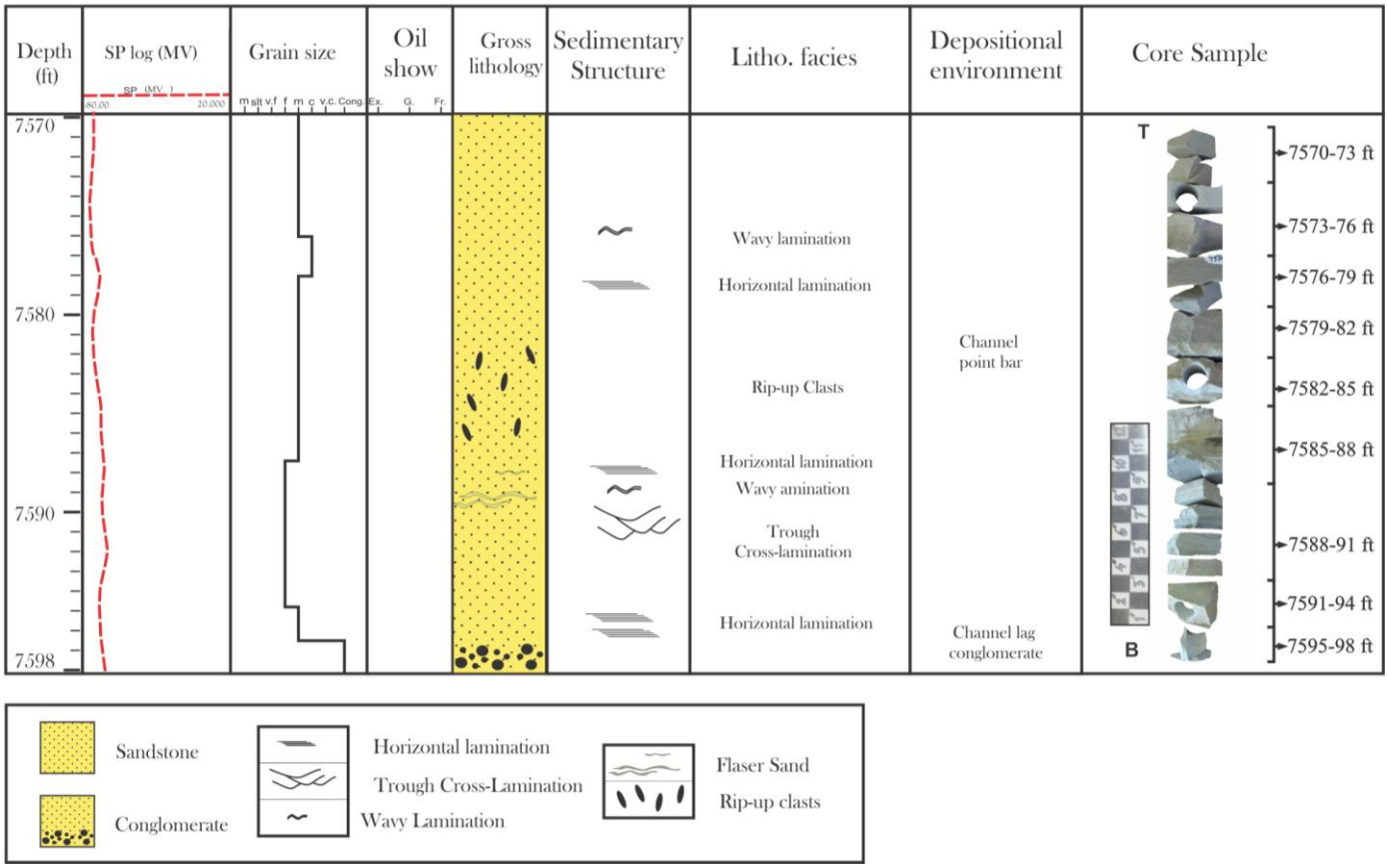

Figure 20. Graphic facies log of core #11, at interval **(**7570-7598ft**)**, in well F1-66, showing sequence grading upward from horizontal to trough x-lamination, coarse grained sands at the base to horizontal laminated, wavy laminated, m. grained sands at top. Suggesting proximity to point bar deposits, channel fill sands facies, Memouniat Formation, Hamada **(**Ghadames**)** Basin.

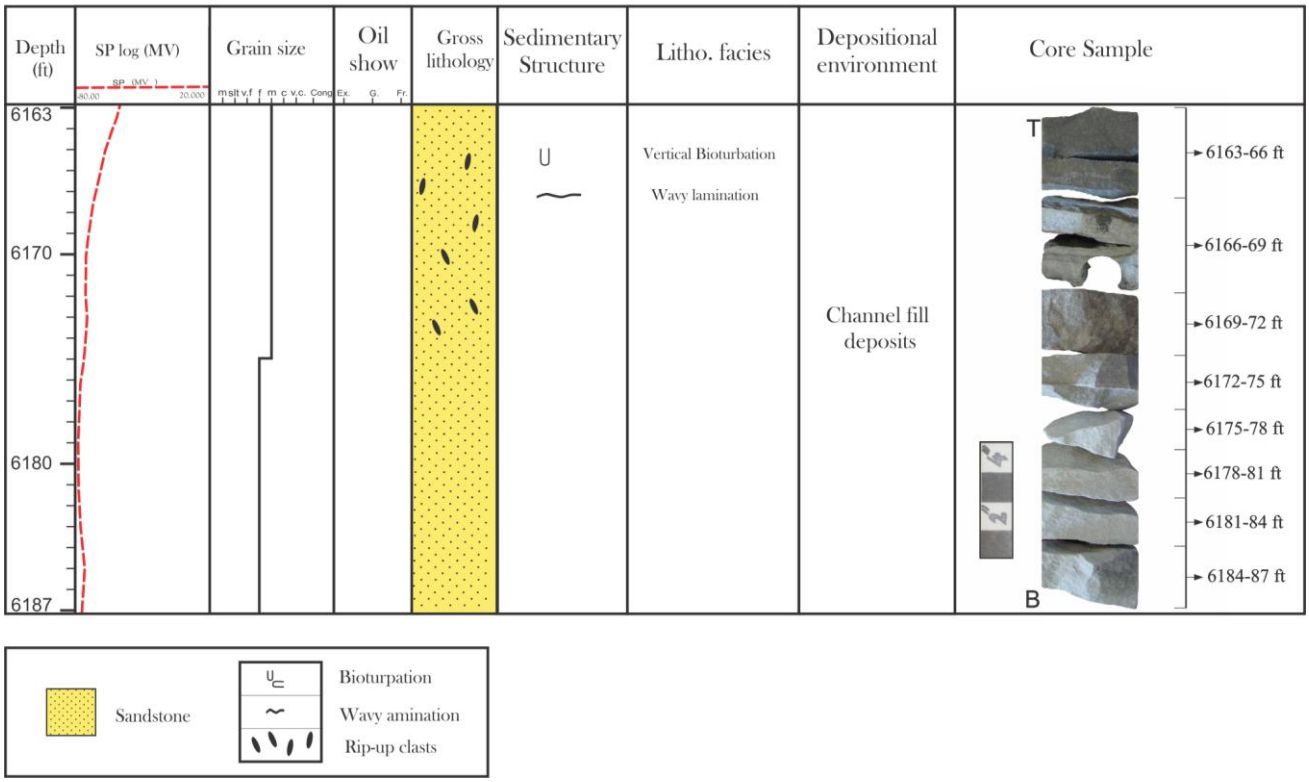

Figure 21. Graphic facies log of core #3, at interval **(**6163-6187ft**)**, in well GG1-66, showing f-m. sands characterized by rip-up clasts, some wavy lamination and v. bioturbation at top, channel fill sands facies, Memouniat Formation, Hamada **(**Ghadames**)** Basin.

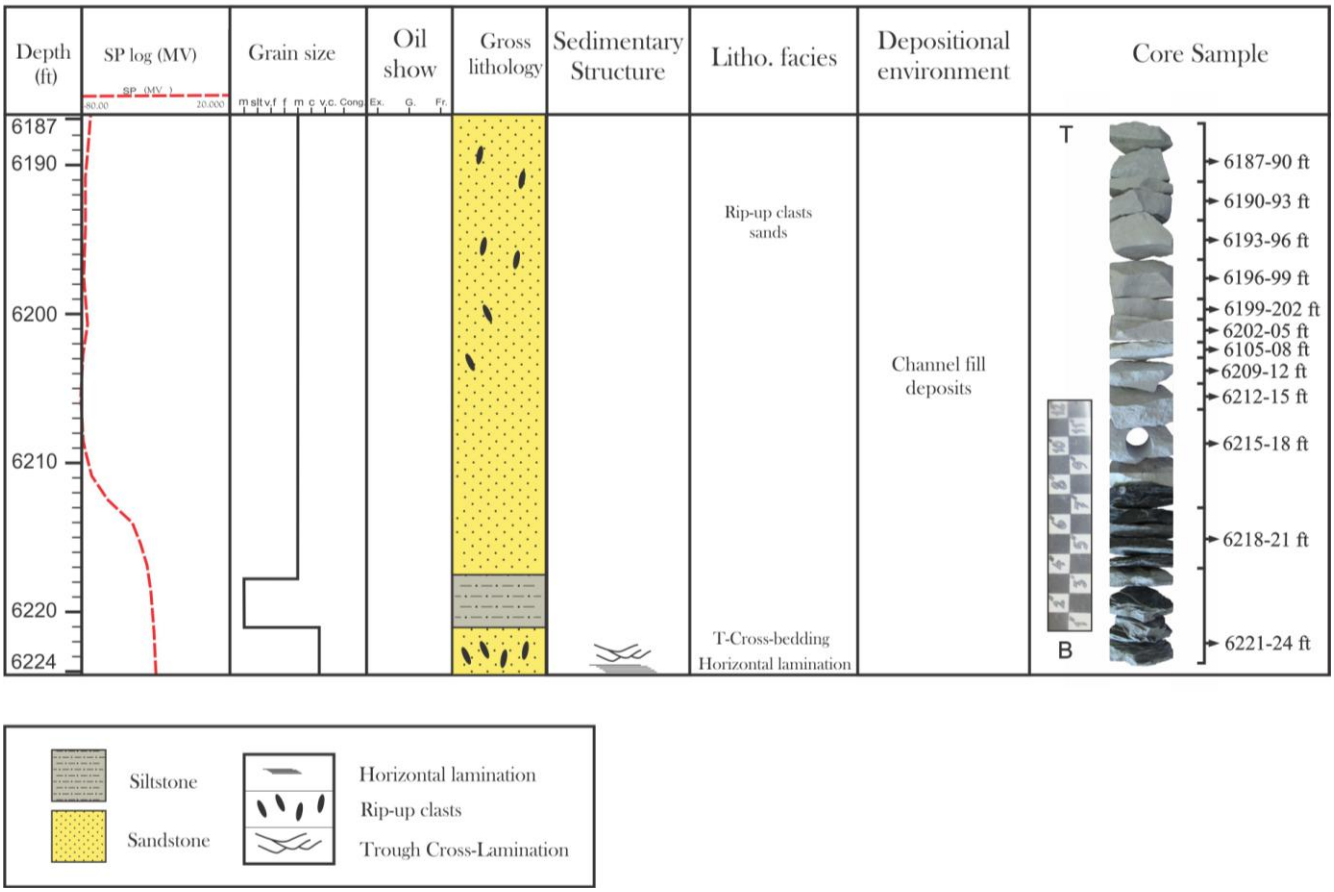

Figure 22. Graphic facies log of core #4, at interval **(**6187-6224ft**)**, in well GG1-66, illustrating a sequence of fining upward grain size, characterized by trough x-lamination at base **(**scour nature**)** and of rip-up clasts sands at top, channel fill sands facies, Memouniat Formation, Hamada **(**Ghadames**)** Basin.

Figure 23. Trough x-lamination in channel fill sands facies predominated sector, core #11 **(**7598-7570ft**)** in well F1-66.

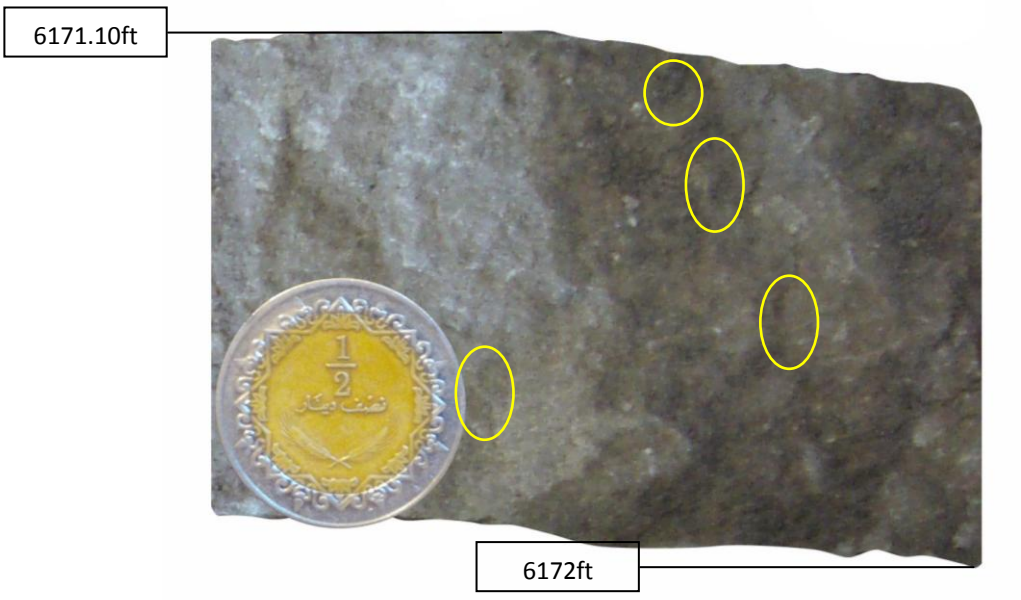

Figure 24. Rip-up clasts in channel fill sand facies predominated sector, core #3 **(**6163-6187ft**)** in well GG1-66.

Figure 25. Horizontal and wavy lamination primary sedimentary structures in channel fill sands facies predominated sector, core #11 **(**7570-7598ft**)** in well F1-66.

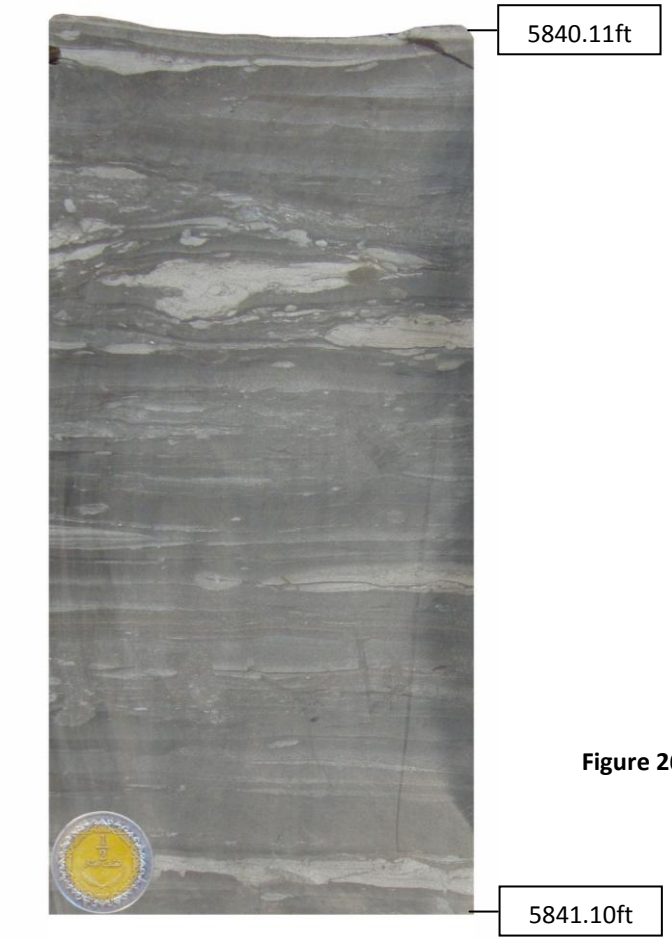

Figure 26. Flaser-sands structures in proximal sands facies predominated sector, core #12 **(**5828.8-5843.8ft**)** in well A1-NC1.

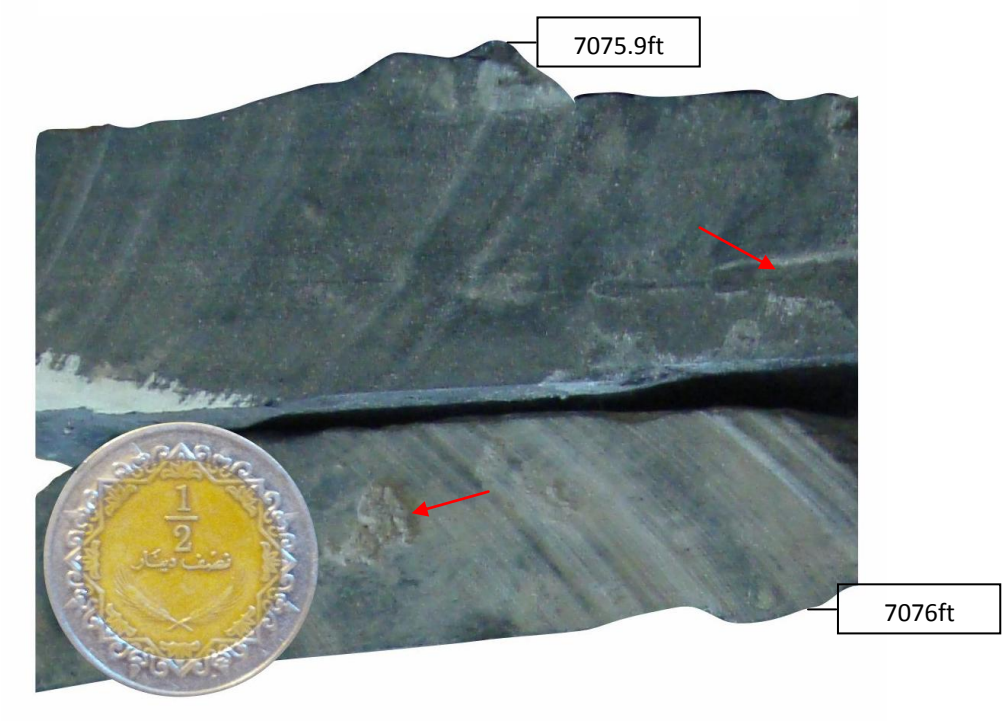

Figure 27. Bioturbation **(**indicated by arrows**)** in channel fill sands facies, core #10 **(**7061-7088ft**)** in well F1-66.

4.1.1.2 Proximal (shoreface) sand facies:

The proximal sand facies **(**shoreface**) (**Figs. 28 and 29**)**, was deposited basin ward from the channel fill facies in a shallow marine water environment in which wave processes predominated. Parallel lamination associated with wavy lamination **(**Fig. 30**)**, occasionally with truncated surface **(**Fig. 31**)**, may be seen in this facies reflecting periodic variation in wave energy through agitated environment. Bioturbation is more severs in shaly parts in this facies, where high water turbulence effects on sandy facies.

Sedimentation rate could restrict faunal diversity in this proximal **(**shoreface**)** sand facies. The mean grain size tends to be of fine sands.

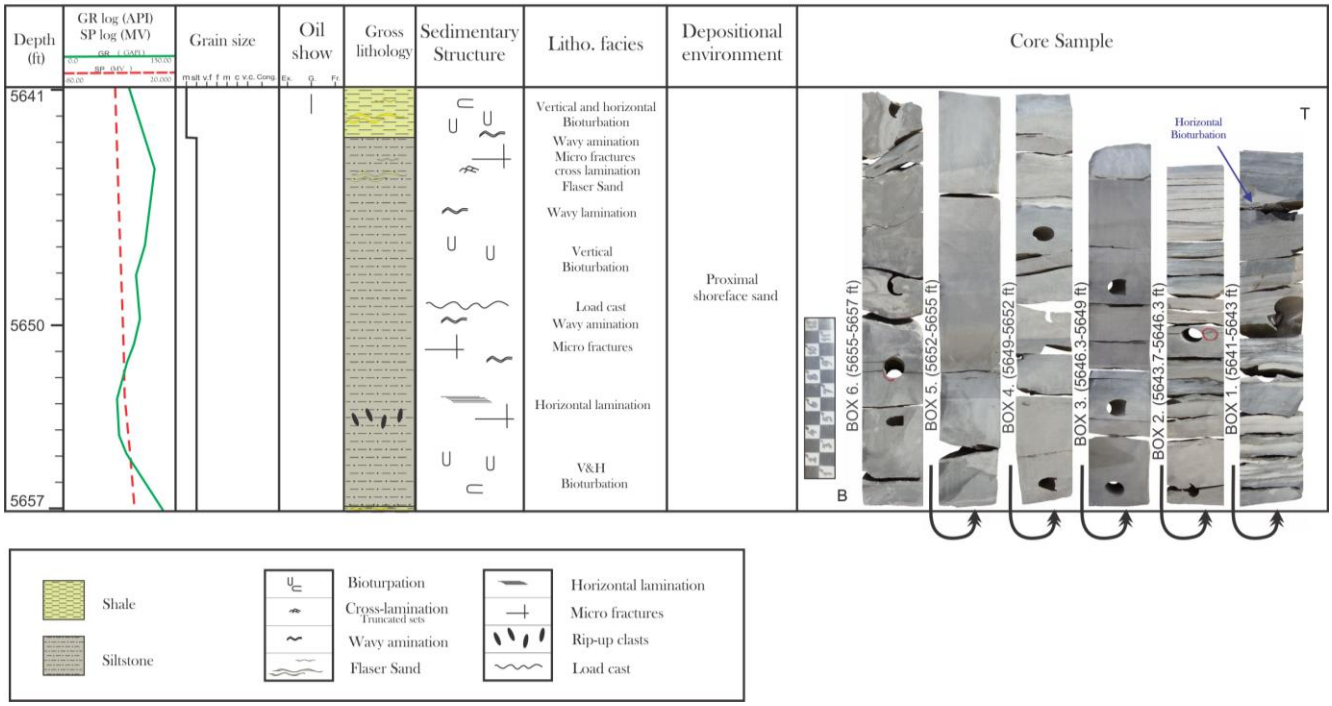

Figure 28. Graphic facies log of core #11, at interval **(**5641-5657ft**)**, in well A1-NC1, showing proximal shoreface sandstone heterogeneity where sands have been reworked by marine processes, Memouniat Formation, Hamada **(**Ghadames**)** Basin.

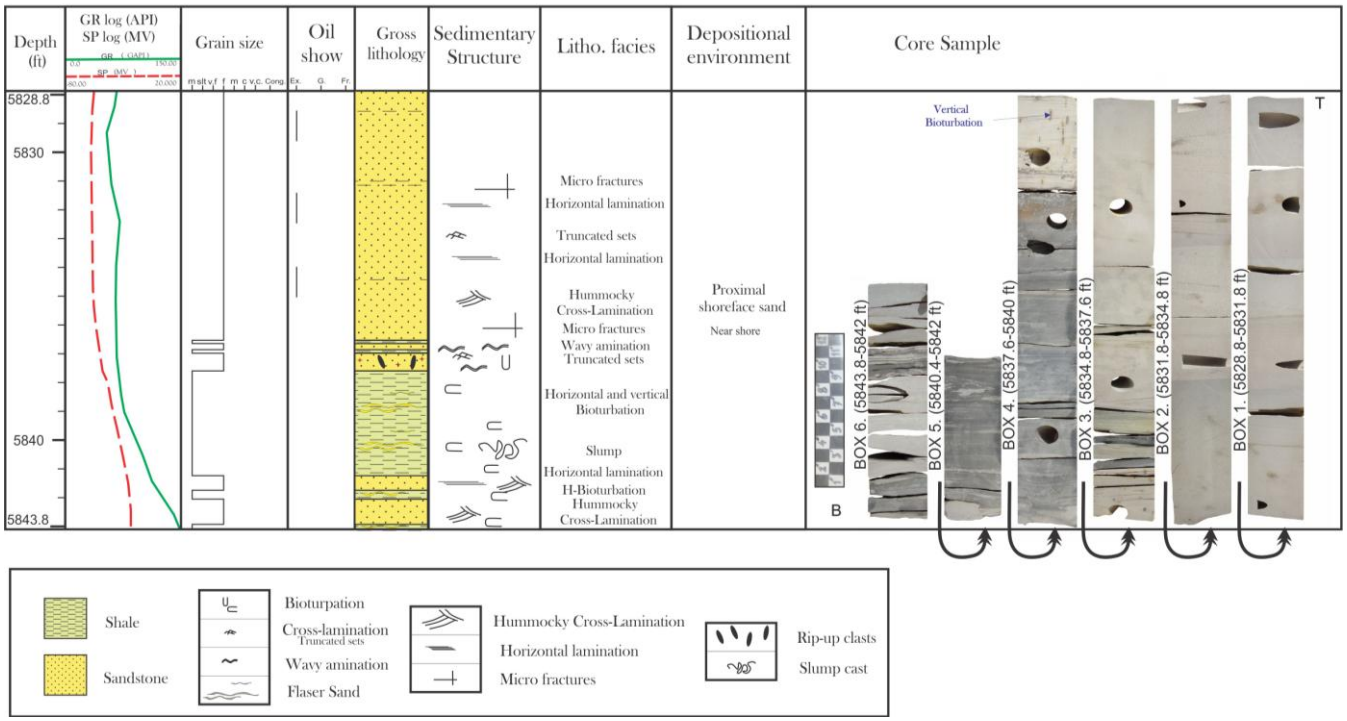

Figure 29. Graphic facies log of core #12, at interval **(**5828.8-5843.8ft**)**, in well A1-NC1, showing some reworked sandstone as indicated by some sedimentary structures and grain sizes, proximal shoreface facies, Memouniat Formation, Hamada **(**Ghadames**)** Basin.

Figure 30. Horizontal and wavy lamination primary sedimentary structures in proximal sands predominated sector, core #12 **(**5828.8-5843.8ft**)** in well A1-NC1.

Figure 31. Truncated surface primary sedimentary structures in proximal sands predominated sector, core #12 **(**5828.8-5843.8ft**)** in well A1-NC1.

4.1.1.3 Basinal (offshore) silt/shale facies:

The basinal offshore silt/shale facies **(**Fig. 32**)** characterized by lenticuler silt/sands and muds **(**Fig. 33**)** occasionally with parallel lamination **(**Fig. 34**)** and of intensive bioturbation **(**Fig. 35**)**. The mean grain size of this facies tends to be fine silt and mud.

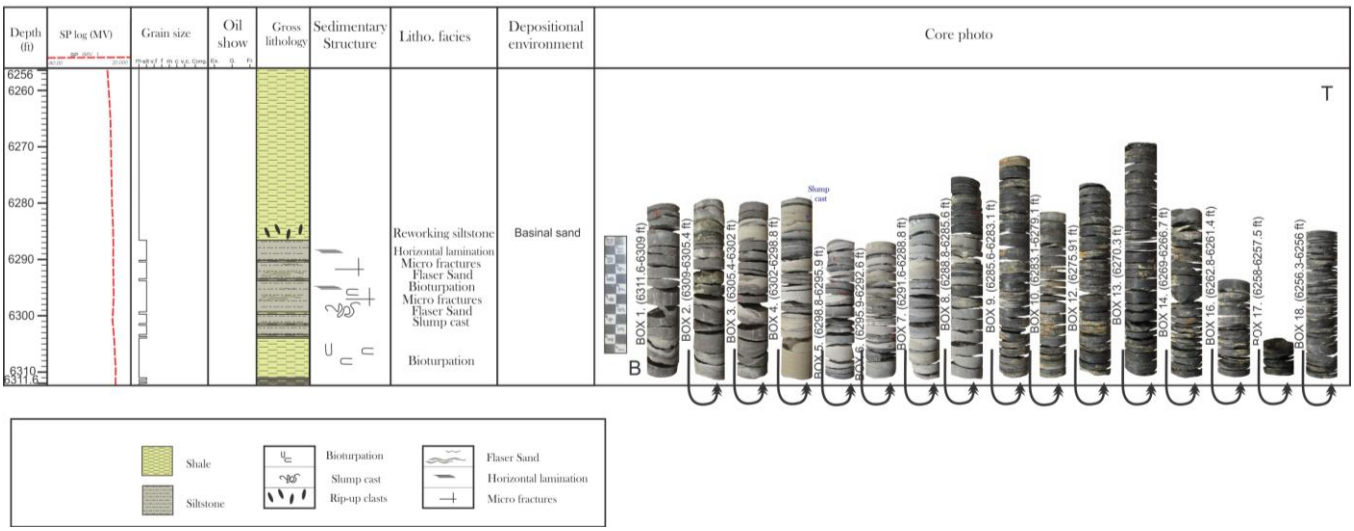

Figure 32. Graphic facies log of core #15, at interval **(**6256-6311.6ft**)**, in well D1-23, showing extensive bioturbation in silty-shaly sandstone of basinal offshore facies, Memouniat Formation, Hamada **(**Ghadames**)** Basin.

Figure 33. Lenticuler silt/sands and muds in basinal predominated sector, core #15 **(**6256-6311.6ft**)** in well D1-23.

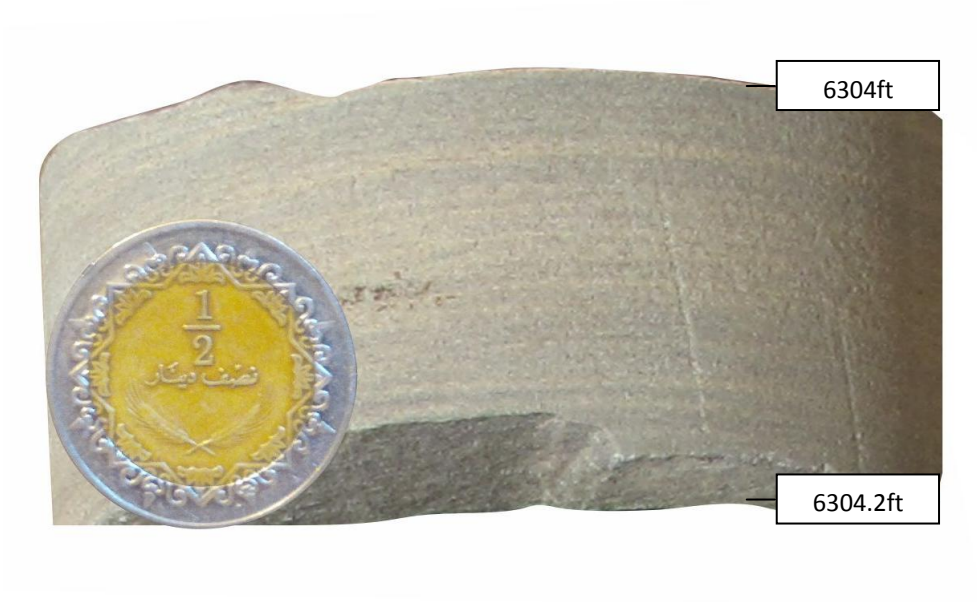

Figure 34. Horizontal lamination in basinal silt/shale predominated sector, core #15 **(**6256-6311.6ft**)** in well D1-23.

Figure 35. Bioturbation in basinal silt/shale predominated sector core #15

4.1.2 Secondary sedimentary structure.

The modification of primary sedimentary structures by sediment loading and differential compaction or possibly by deep-seated basement faulting has been observed at many levels of the examined cores.

Sediment loading slump-like features **(**Fig. 36**)** and some micro factures **(**Figs. 37 and 38**)** are the most evidences of postdepositional **(**secondary**)** sedimentary structures in the studied cores. There microfractures may suggest that this rock have experienced some deformation in moderate to deep burial. Many questions remained unsolved regarding these fractured sandstone. Moreover, the potential is obvious for effective fractures and their characterization to have an application in exploration and development of the Memouniat Formation.

Figure 36. Slump like structure in basinal silt/shale predominated sector, core #15 **(**6256-6311.6ft**)** in well D1-23.

Figure 37. Micro fracture structures **(**indicated by arrows**)** in channel fill sand predominated sector, core #10 **(**7061-7088ft**)** in well F1-66.

Figure 38. Micro fracture structures **(**indicated by arrows**)** in proximal sand predominated sector, core #11 **(**5641-5657ft**)** in well A1-NC1.

4.2 Wireline-Log Characteristic.

As cores are not available on many of the studied wells, other type of data must be used to identify the environmental facies and characterization of the sandstones of Memouniat Formation. Wireline logs which are run routinely on most wells were examined as facies tools for identifying sand-body types. Well logs types of the Memouniat Formation can be seen in **(**Fig. 39**)** in which different sand types are defining their dominating sectors. The main observation made-out of the GR **(**Gama Ray**)** and SP **(**Spontaneous Potential**)** curves are:

a) Trend of the curves is it inclined to the right **(**decreasing in clay contents upward**)**, or inclined to the left **(**increase clay contents upward**),** or some times of blocky nature **(**clay contents are uniform**)**, or spiky-nature of the fining or coarsing upward grain size.

b) Nature of the basal contacts of the studied sandstone **(**is it gradational or sharp?**)**.

c) The general appearance of the curve, is it smooth or serrated as interbedded with some shale?

The observed GR-SP log characteristics of various studied facies in cored sand interval of Memouniat Formation are grouped to four types A, B, C and D **(**Fig. 40**)**. Practical comparison of GR-SP curves with available core description shows that the SP curves sloping to the left **(**type A**)** correspond with interpreted channel sand sequences. In these sequences the sands are characterized by a sharp basal contact and of fining-upward fashion. The curve is generally smooth in the lower part and becomes more serrated toward the top, recoding an overall increase in shale lamination.

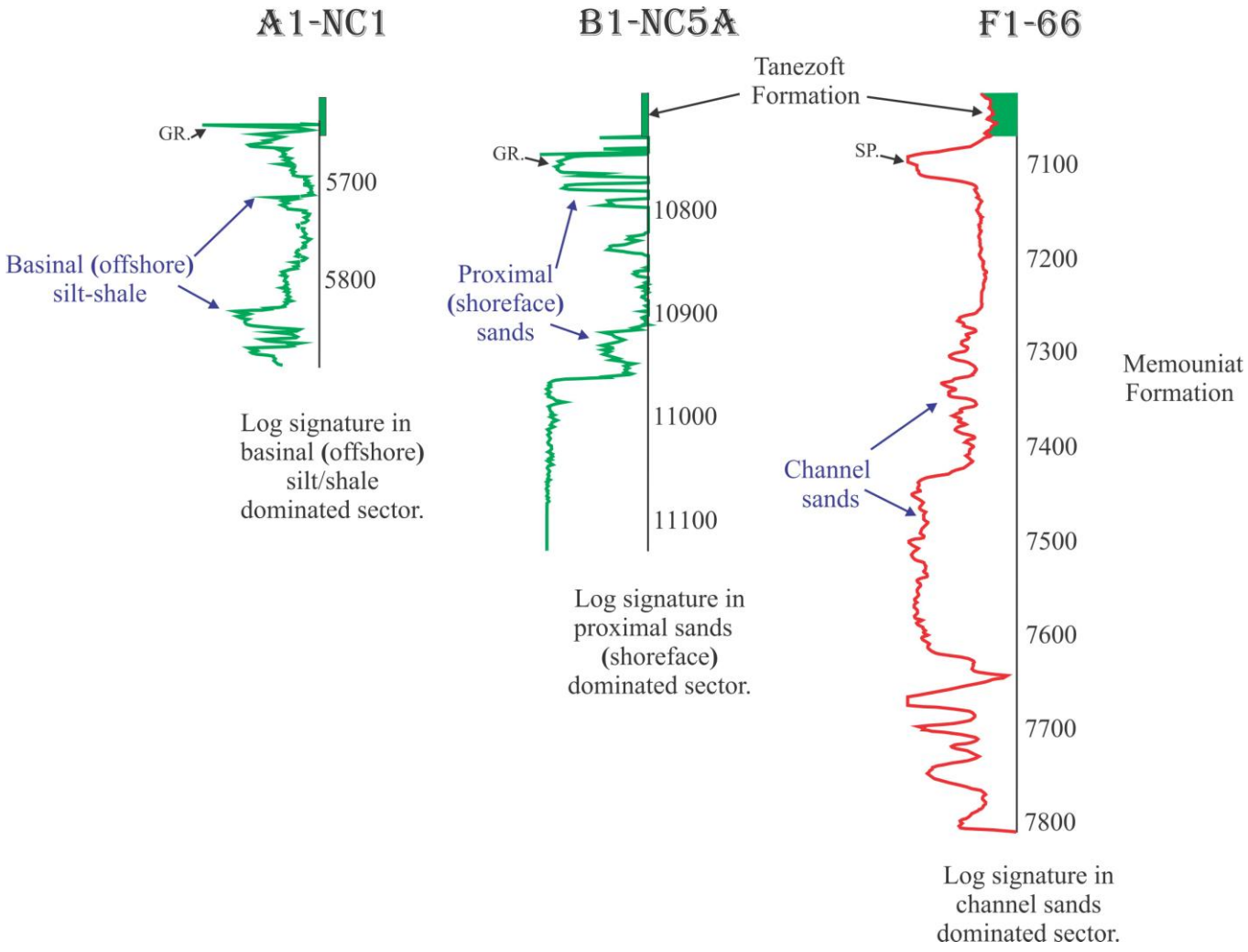

Figure 39. Well log types showing GR.-SP. log signatures of the Memouniat Formation in different studied sectors.

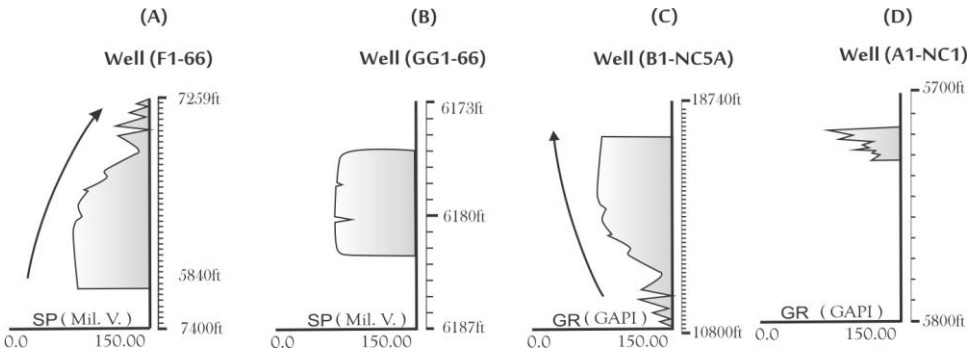

Figure 40. Different log signatures observed from available logs in the study area.

Eventually these channels were abandoned marking possible good porous and permeable sand at the base **(**clean sand**)**, as evidenced by some hydrocarbon shows at some intervals.

The blocky SP curve **(**B**)** may refer to stacked channels, having sharp base and top, characterized by overall same grain size with little variation in clay contents. They may be in general represent the best reservoir because of their less mud contents.

The GR curves sloping to the right **(**type C**)** correspond with beach, bars, coastal sands or deltaic deposits. These deposits are characterized by a sharp upper contact and of a gradational base which account for overall coarsening-upward grain size. The curve is generally serrated toward the bottom, recoding an overall increase in shaly laminations. Possible oil shows may be encountered at the top of sand unit.

The serrated **(**spiky**)** GR curve **(**D**)** showing occasionally small fining or coarsening log-signature. The serrated nature usually corresponds to the presence of shaly interbeds. Generally this shaly sand unit is lacking hydrocarbon shows as they are relatively of mud saturated.

The SP log characteristics are also investigated and occasionally compared with GR curves in most available wells. The SP curve is usually less definitive than the GR curves especially in wells **(** A1-NC118, B2-NC5A **)** and in some cases the trends of curve are even reversed in wells **(**C1-NC7A, D1-23**)**.

In general, the SP curve is less reliable than GR for interpreting depositional facies, it is affected by some factors such as:

1- Fluid formation salinity.

2- Diagenesis.

Chapter (5)
Petrography of Memouniat Formation

5.1 Detraital Composition

Thin sections from Memouniat Formation impregnated with blue epoxy resin and stained with Alizarin Red S and Potassium Ferricyanide for carbonate **(**Dickson 1965, Miller 1988**)** were studied under the polarizing microscope **(**Olympus BX41TS, made in Japan, 2004**)** to determine the main mineral composition of grains framework.

Modal point counting was performed for the seventeen thin sections **(**T.S. 1-T.S. 17**)** in order to determine the proportion of the different clastic grains in the Memouniat Formation. An average of 300 points per thin section were counted. The area of each thin section was invistigated using line-traverse method of Galehouse **(**1971**)**, with 2mm space in between each point counted, mineral grains and rock clasts were determined and characterized, while grain less than 0.2mm apparent diameter were counted as matrix. The result of this analysis is shown in table 2, in which the Memouniat sands have a very high monocrystalline quartz content, which account for about **(**92%**)** of the total sand grains.

The remaining grains consist mainly of rock fragments **(**6%**)** which include polycrystalline quartz of possible metamorphic origin, clay clasts, **(**and may be of some dolomite fragments**)**, sparse of feldspar grains traces **(**2%**)** may be seen at some places. Volcanic rock fragments are absent.

T.S. No	Framework grain composition (%)					Grain size	Cement type (%)			Lithofacies types
	Q.	F.	R.F.	Others	Matrix	mm	Sil.	Cal.	Clay	
1	97	2	1	0	0	>2	20	10	0	Channel
2	87	3	10	0	0	0.25	25	5	0	Channel
3	95	4	1	0	0	0.25	27	3	0	Channel
4	84	3	13	0	0	0.25-0.5	28	2	0	Channel
5	89	4	7	0	0	0.25-0.5	24	6	0	Channel
6	92	2	6	0	0	0.25 -0.125	26	4	0	Channel
7	94	2	4	0	1	0.125-0.0625	20	10	0	Basinal
8	92	4	4	1	2	0.25-0.125	25	3	2	Channel
9	88	2	10	4	3	0.125-0.625	18	2	10	Proximal
10	89	2	9	1	1	0.25-0.125	22	8	0	Proximal
11	96	3	1	0	0	0.125-0.0625	17	13	0	Basinal
12	97	1	2	0	0	0.0625	16	14	0	Basinal
13	89	3	8	1	1	0.5-0.25	12	11	7	Proximal
14	93	3	4	1	1	0.25-0.125	22	7	1	Proximal
15	92	0	8	2	4	0.0625	14	3	13	Proximal
16	86	5	9	0	0	0.125	17	12	1	Proximal
17	95	2	3	0	2	0.125-0.0625	16	14	0	Basinal

Table 2. Framework grain composition for the studied thin sections of Memouniat Formation, Hamada **(**Ghadames**)** Basin, NW Libya.

5.1.1 Quartz

Monocrystalline quartz is the most common mineral in the Memouniat Formation, ranging from 84% to 97%. The characteristic quartz grain size in studied sandstone units is rising from 0.125mm to >2mm for the channel fill sand facies, 0.0625mm to 0.5mm for proximal marine sand facies **(**shoreface**)**, and from 0.125mm to 0.0625mm for the basinal silt/shales facies.

Quartz grain usually show non-undulose straighted extinction of granitic origin **(**Folk, 1980**).** The undulatory extinction of quartz occurs as a result of deformation of the rock after its formation and that the greater the cumulative deformation the larger the angle, hence it is a useful indicator of the orogenic history of the rock **(**West**,** 1991**)**. However some undulose extinction were charactering polycrystalline quartz grains.

Interface of quartz grains is very well common through some grain-to-grain contact (Figs. 41, 42). and crystal overgrowth (Figs. 43, 44).

The monocrystalline quartz is occupies the major grain with different grain size depends on the distance from the origin rock and how much effected with transporting agents. In the studied thin sections the grain size of monocrystalline quartz grains changes from conglomeratic in lag deposits of some channels in channel fill sands sector especially in core # 11, well F1-66 characterized by quartzarenite (Figs. 41, 42) and to fine to medium grained in some other places (Figs. 45, 46). This differentiation reveals to changes in current regime from high current velocity to much more lower at the fine grain sands.

Quartz grains are heavely fractured as seen in Litharenite sandstone (Fig. 43) at 7087ft, may be of tectonic or diagenetic origin. Sublitharenite can be also characterizing sand facies in core #3 of well GG1-66 (Figs. 47-50) and in core #4 (Figs. 51, 52).

5.1.2 Feldspar

Feldspar grains are of minor constituent in the studied Memouniat Formation, if they present they considered as traces (2%). They are lath like to platy shape, range from 0.09mm to 0.18mm, with some features exhibit albite twining (Heinrich, 1965) (Figs. 53, 54).

Feldspar percentage in the channel fill sands (2%) is lower than that in the proximal (shoreface) sands (2.5%), but it is much lower in the basinal (offshore) silt/shale (1.2%). This differences in percentage in represented depositional environments may indicates that the feldspar grains are less persisted in the basinal (offshore) sector.

The nature of feldspar grains are much sensitive to weathering agents, that is come to their chemical composition. However the aggregates of this mineral in the studied thin sections in the study area are very low and sometime are completely altered to form clay matrix and then reworked to form the secondary porosity which in order may enhance reservoir characteristics of Memouniat Formation in Hamada (Ghadames) Basin.

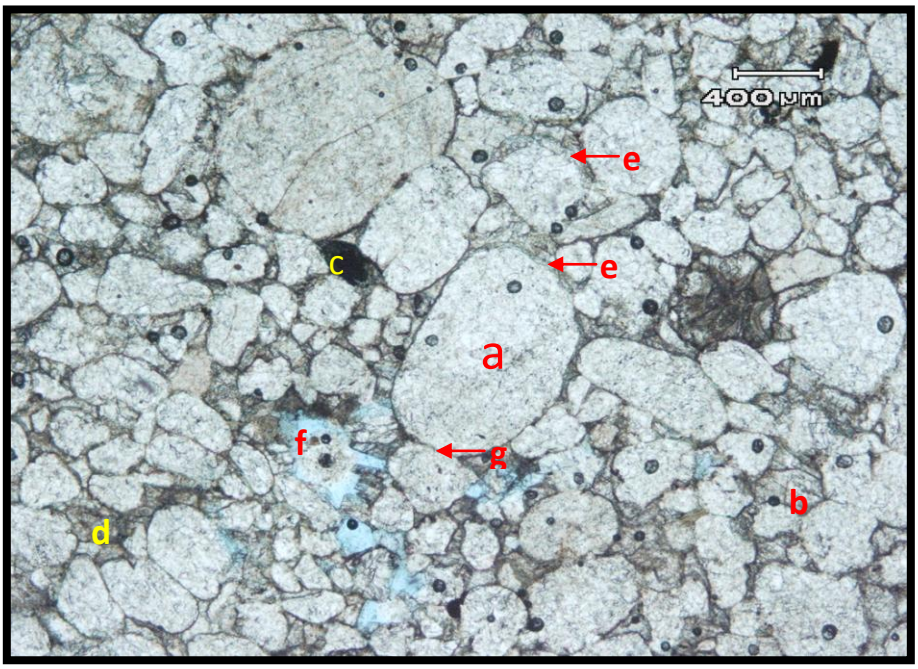

Figure 41. Thin section photomicrograph (1) of Quartzarenite in channel fill sands in Memouniat Formation, showing (a) quartz, (b) feldspar, (c) clay clasts, (d) calcite cement, (e) quartz overgrowth, (f) leaching porosity and (g) grain-to-grain contact. Core # 11 at 7598ft., well F1-66 NC8A (PPL).

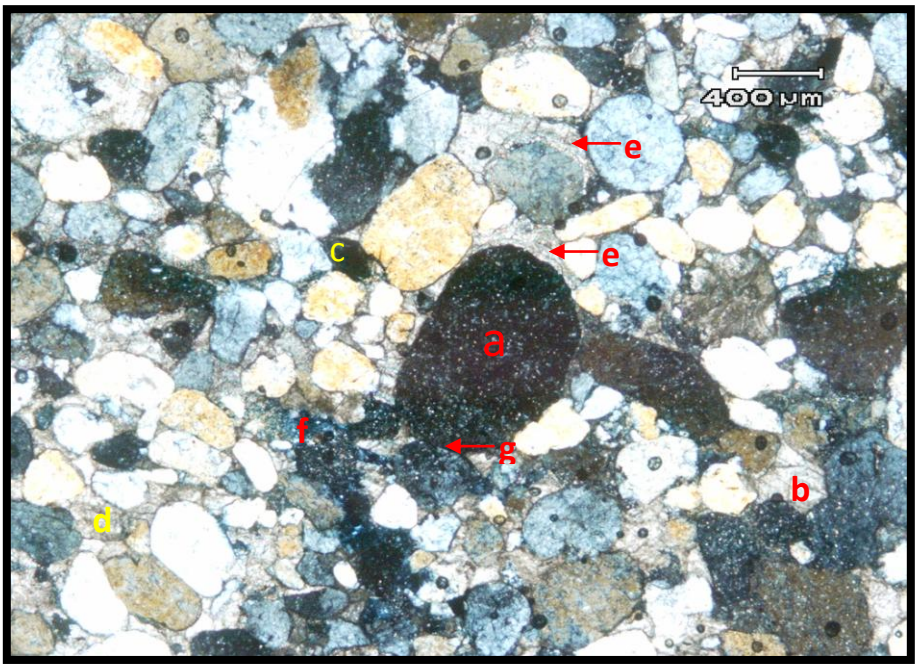

Figure 42. Thin section photomicrograph (1) of Quartzarenite in channel fill sands in Memouniat Formation, showing (a) quartz, (b) feldspar, (c) clay clasts, (d) calcite cement, (e) quartz overgrowth, (f) leaching porosity and (g) grain-to-grain contact. Core # 11 at 7598ft., well F1-66 NC8A (XPL).

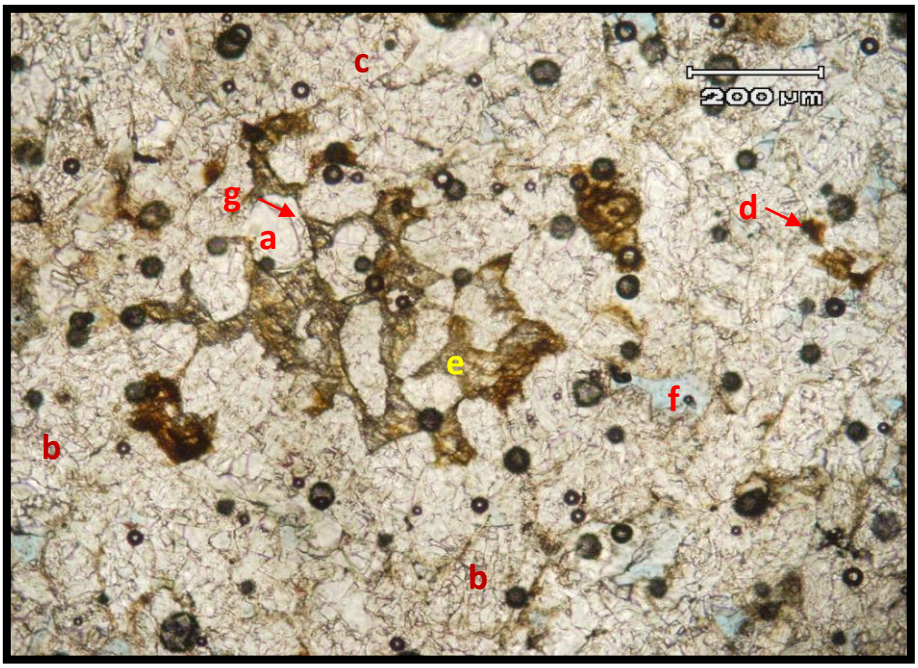

Figure 43. Thin section photomicrograph **(**2**)** of Sublitharenite in channel fill sands in Memouniat Formation, showing **(**a**)** quartz, **(**b**)** feldspar, **(**c**)** polycrystalline quartz **(**d**)** clay clasts, **(**e**)** partial calcite cement, **(**f**)** leaching porosity and **(**g**)** quartz overgrowth. Core # 10 at 7085-7088ft., well F1-66 NC8A **(**PPL**)**.

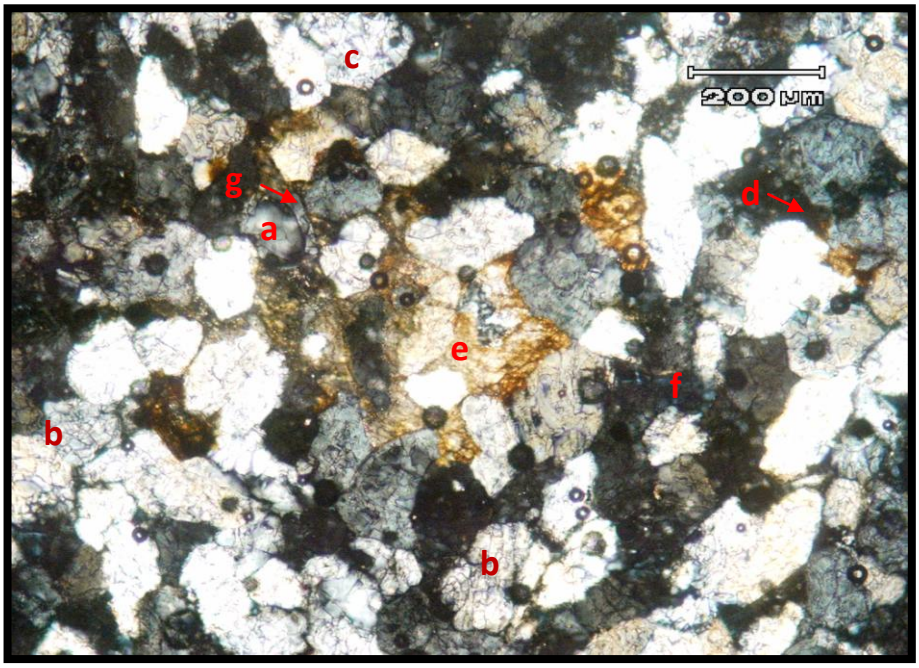

Figure 44. Thin section photomicrograph **(**2**)** of Sublitharenite in channel fill sands in Memouniat Formation, showing **(**a**)** quartz, **(**b**)** feldspar, **(**c**)** polycrystalline quartz**, (**d**)** clay clasts, **(**e**)** partial calcite cement, **(**f**)** leaching porosity and **(**g**)** quartz overgrowth. Core # 10 at 7085-7088ft., well F1-66 NC8A. **(**XPL**)**.

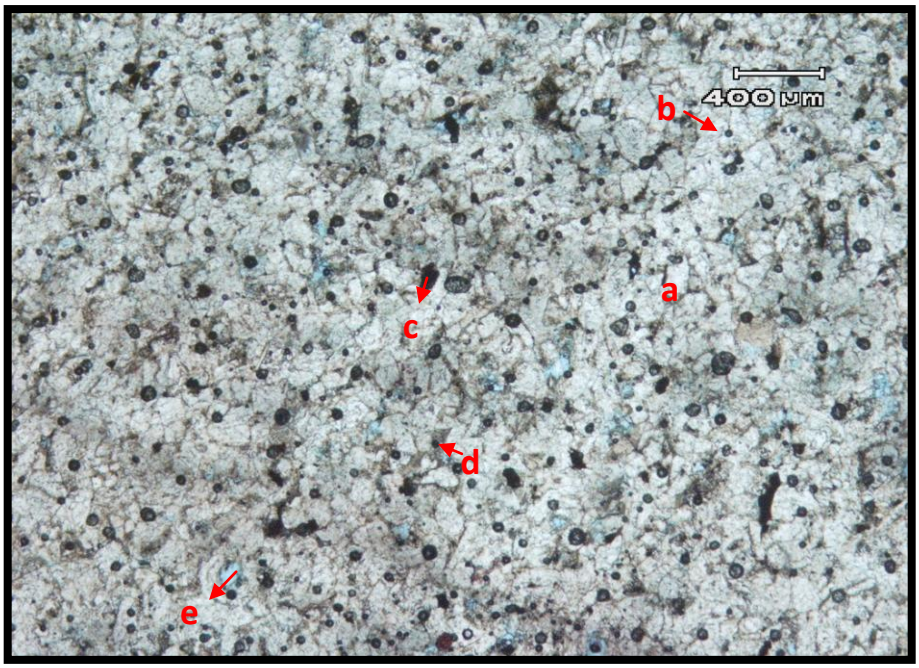

Figure 45. Thin section photomicrograph (3) of Quartzarenite in channel fill sands in Memouniat Formation, showing (a) quartz, (b) feldspar, (c) clay clasts, (d) calcite cement and (e) leaching porosity. Core # 11 at 7591-7594ft., well F1-66 NC8A (PPL).

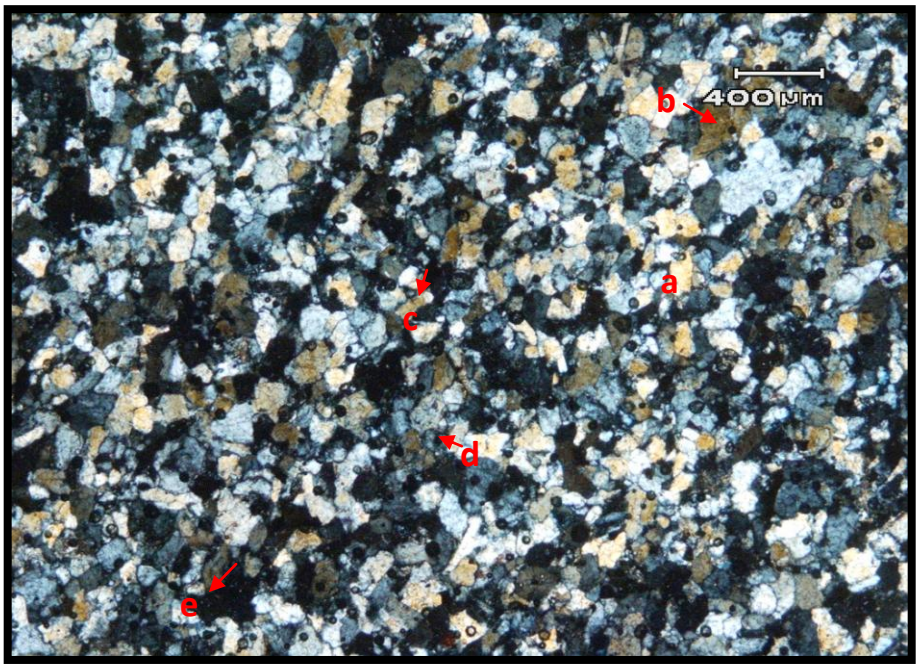

Figure 46. Thin section photomicrograph (3) of Quartzarenite in channel fill sands in Memouniat Formation, showing (a) quartz, (b) feldspar, (c) clay clasts, (d) calcite cement and (e) leaching porosity. Core # 11 at 7591-7594ft., well F1-66 NC8A (XPL).

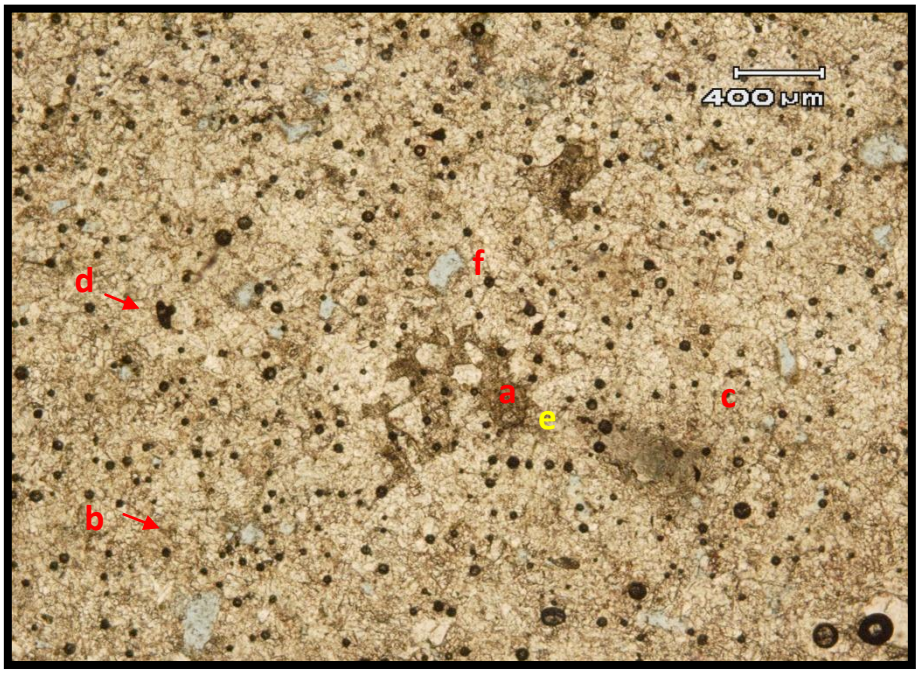

Figure 47. Thin section photomicrograph **(**4**)** of Sublitharenite in channel fill sands in Memouniat Formation, showing **(**a**)** quartz, **(**b**)** polycrystalline quartz, **(**c**)** feldspar, **(**d**)** clay clasts, **(**e**)** calcite cement and **(**f**)** leaching porosity. Core # 3 at 6181.84ft., well GG1-66 NC8A **(**PPL**)**.

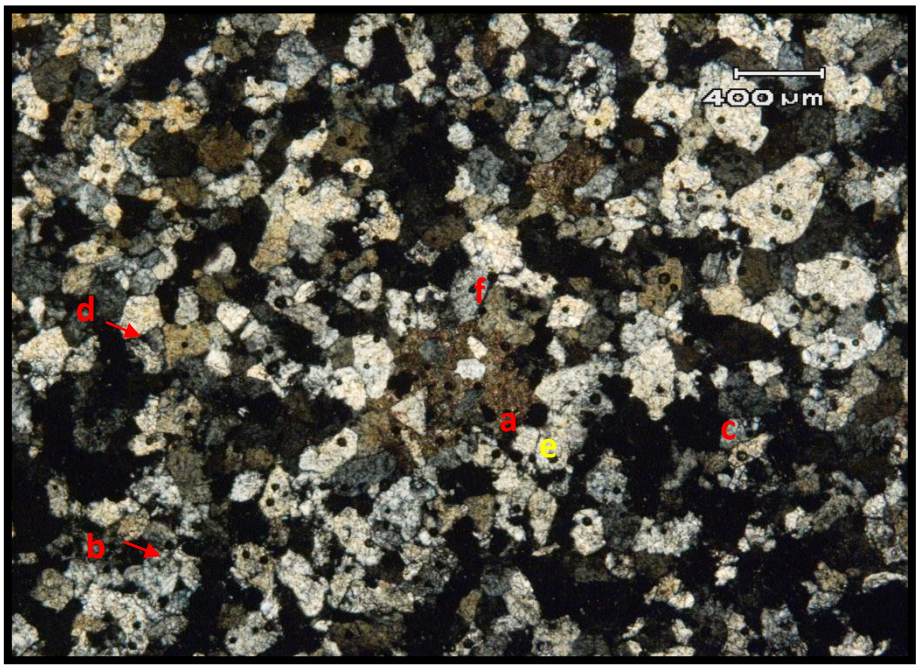

Figure 48. Thin section photomicrograph **(**4**)** of Sublitharenite in channel fill sands in Memouniat Formation, showing **(**a**)** quartz, **(**b**)** polycrystalline quartz, **(**c**)** feldspar, **(**d**)** clay clasts, **(**e**)** calcite cement and **(**f**)** leaching porosity. Core # 3 at 6181.84ft., well GG1-66 NC8A **(**XPL**)**.

Figure 49. Thin section photomicrograph **(**5**)** of Sublitharenite in channel fill sands in Memouniat Formation, showing **(**a**)** quartz, **(**b**)** feldspar, **(**c**)** polycrystalline quartz, **(**d**)** clay clasts and **(**e**)** calcite cement. Core # 3 at 6166.69ft., well GG1-66 NC8A **(**PPL**)**.

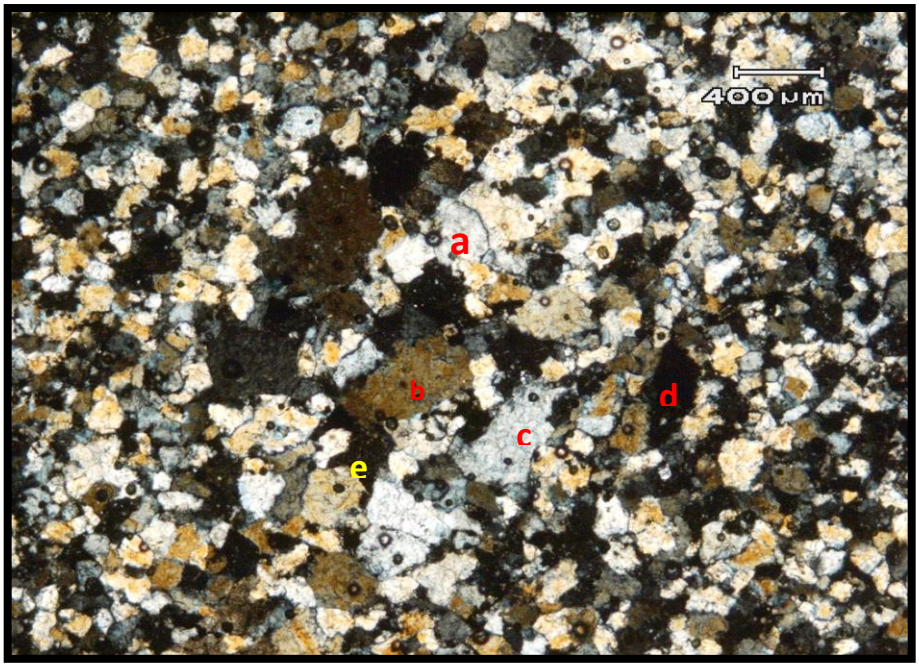

Figure 50. Thin section photomicrograph **(**5**)** of Sublitharenite in channel fill sands in Memouniat Formation, showing **(**a**)** quartz, **(**b**)** feldspar, **(**c**)** polycrystalline quartz, **(**d**)** clay clasts and **(**e**)** calcite cement. Core # 3 at 6166.69ft., well GG1-66 NC8A **(**XPL**)**.

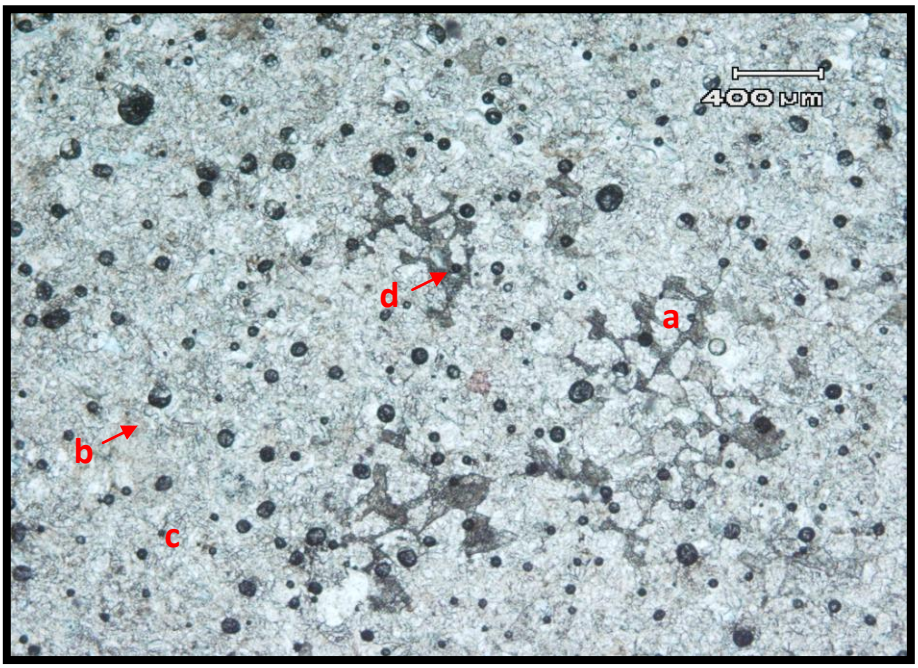

Figure 51. Thin section photomicrograph **(**6**)** of Sublitharenite in channel fill sands in Memouniat Formation, showing **(**a**)** quartz, **(**b**)** feldspar, **(**c**)** polycrystalline quartz and **(**d**)** calcite cement. Core # 4 at 6205.08ft., well GG1-66 NC8A **(**PPL**)**.

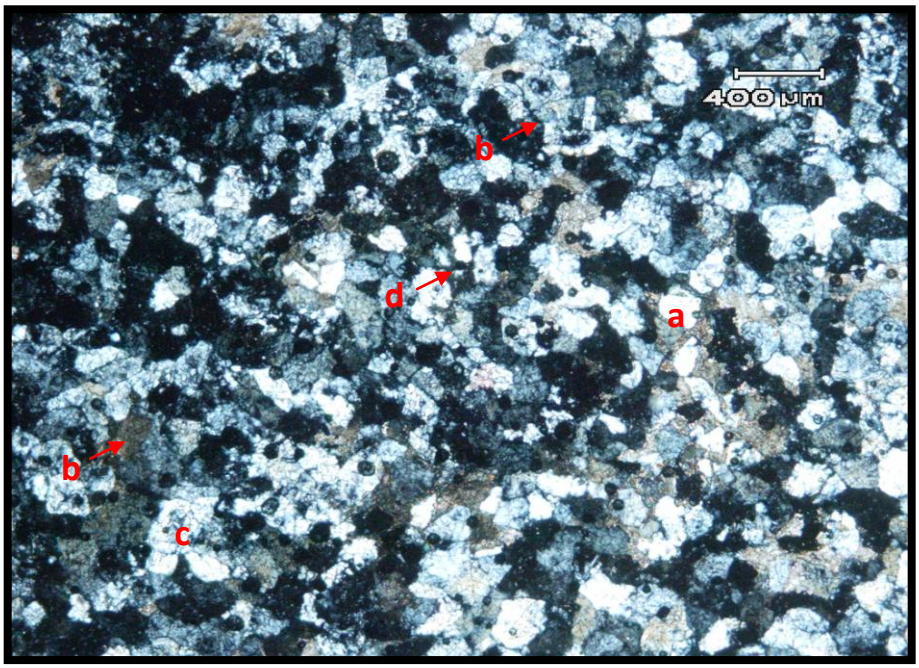

Figure 52. Thin section photomicrograph **(**6**)** of Sublitharenite in channel fill sands in Memouniat Formation, showing **(**a**)** quartz, **(**b**)** feldspar, **(**c**)** polycrystalline quartz and **(**d**)** calcite cement. Core # 4 at 6205.08ft., well GG1-66 NC8A **(**XPL**)**.

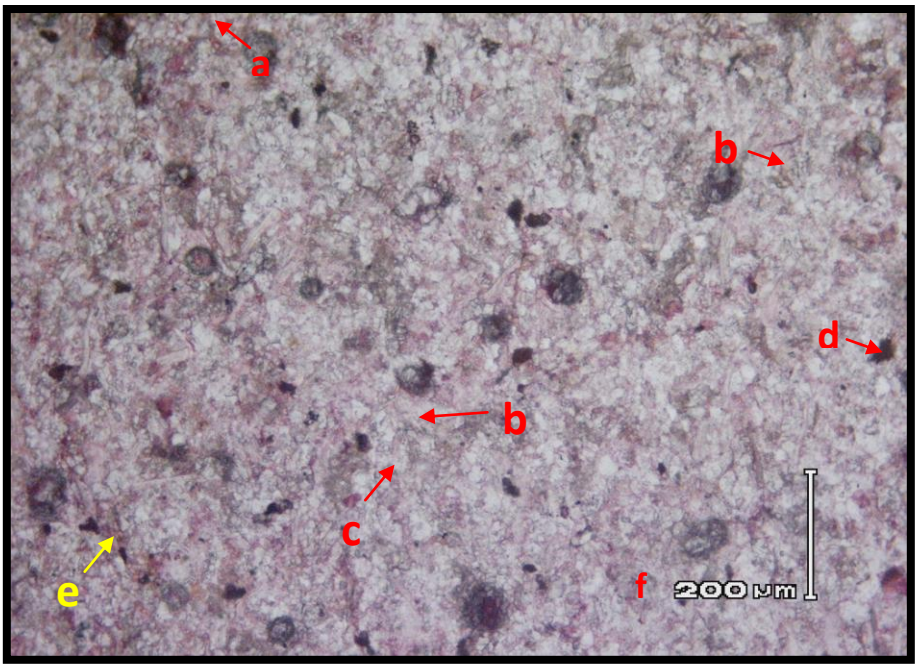

Figure 53. Thin section photomicrograph **(**7**)** of Sublitharenite in basinal silt/shale in Memouniat Formation, showing **(**a**)** quartz, **(**b**)** feldspar, **(**c**)** polycrystalline quartz, **(**d**)** clay clasts, **(**e**)** clay matrix and **(**f**)** calcite cement. Core # 15 at 6298.6ft., well D1-23 **(**PPL**)**.

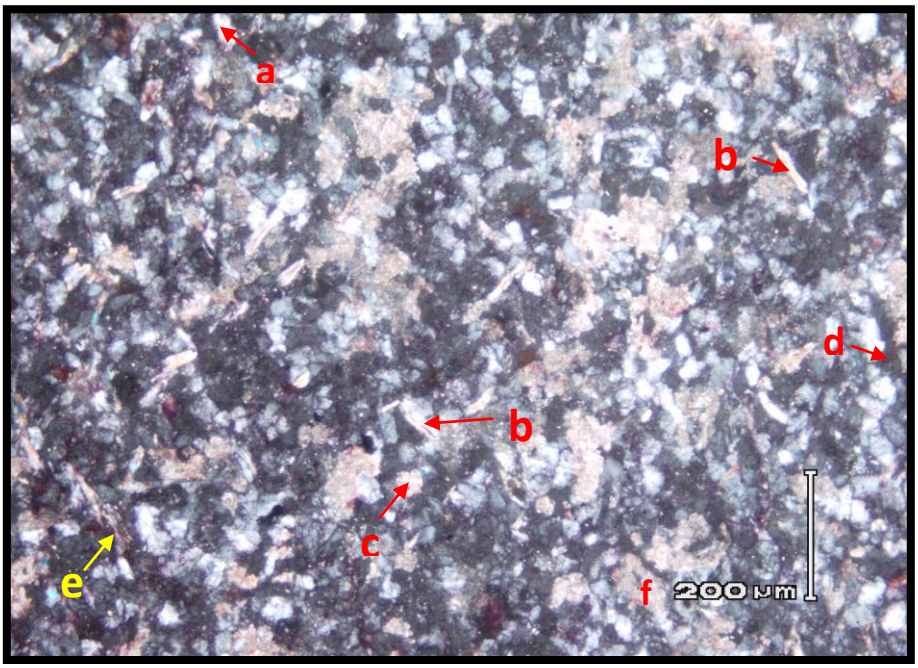

Figure 54. Thin section photomicrograph **(**7**)** of Sublitharenite in basinal silt/shale in Memouniat Formation, showing **(**a**)** quartz, **(**b**)** feldspar, **(**c**)** polycrystalline quartz, **(**d**)** clay clasts, **(**e**)** clay matrix and **(**f**)** calcite cement. Core # 15 at 6298.6ft., well D1-23 **(**XPL**)**.

5.1.3 Rock fragments

They are account for about (6%) of the detraital constituents where they are increasing from quartzarenite sandstone to litharenite sandstone. Metamorphic rock fragments are the dominant and representing the elongated and stretched polycrystalline quartz grains.

Clay clasts ranging from (0.048mm to 0.175mm) of light brown to dark grey grains enclosed between quartz grains (Figs. 55, 56). Some of clay clasts have been crushed between quartz grains which is importantly contribute to the matrix in the studied thin sections. Other accessory minerals as traces may be present like mica (Figs. 57-60).

The mica in Memouniat Formation can be found as trace or up to 4% locally. Predominately muscovite is present, which occurs as elongated flakes, easily identified by its parallel extinction and of platy nature, colorless in (PPL) and shows bright second-order color under (XPL). Occasionally appeared to be bent between rigid quartz grains (Fig. 57). The examined sandstone thin sections can be classified as sublitharenite to rare quartzarenite by using Folk sandstone classification (1980), (Fig. 61).

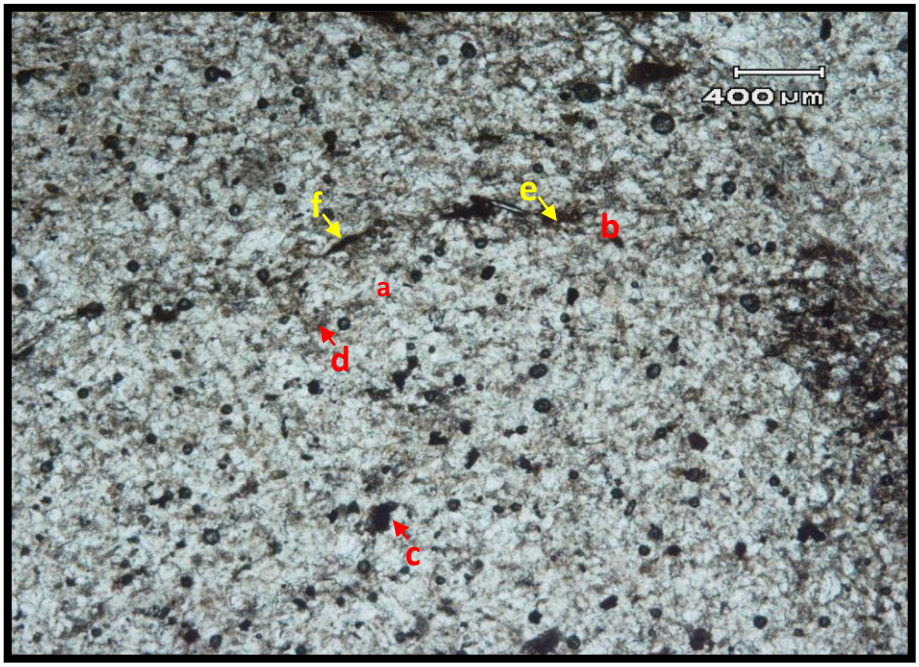

Figure 55. Thin section photomicrograph **(**8**)** of Sublitharenite in channel fill sands in Memouniat Formation, showing **(**a**)** quartz, **(**b**)** feldspar, **(**c**)** clay clasts, **(**d**)** calcite cement, **(**e**)** clay matrix and **(**f**)** mica flacks. Core # 4 at 6221.24ft., well GG1-66 NC8A **(**PPL**)**.

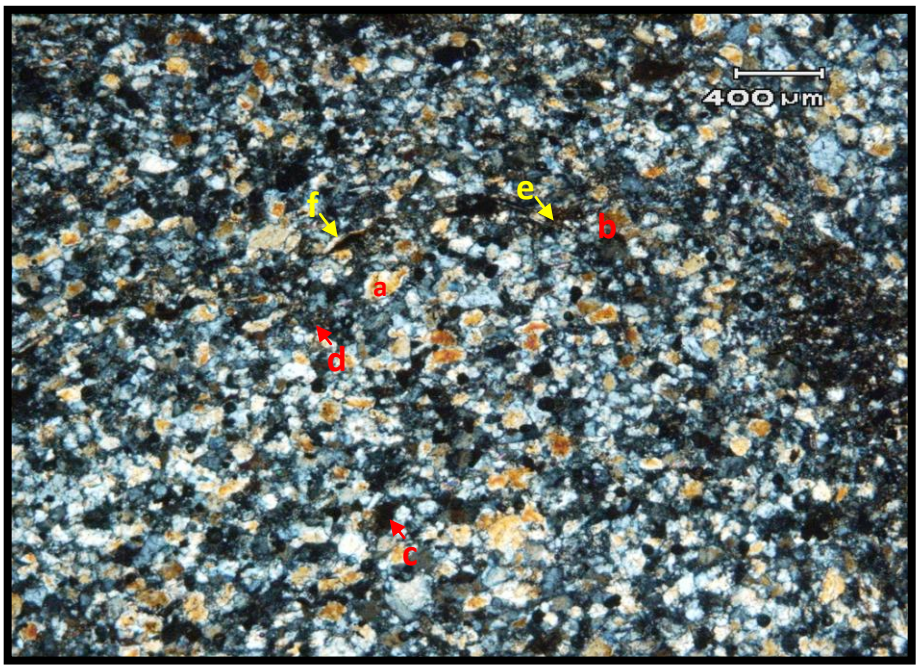

Figure 56. Thin section photomicrograph **(**8**)** of Sublitharenite in channel fill sands in Memouniat Formation, showing **(**a**)** quartz, **(**b**)** feldspar, **(**c**)** clay clasts, **(**d**)** calcite cement, **(**e**)** clay matrix and **(**f**)** mica flacks. Core # 4 at 6221.24ft., well GG1-66 NC8A **(**XPL**)**.

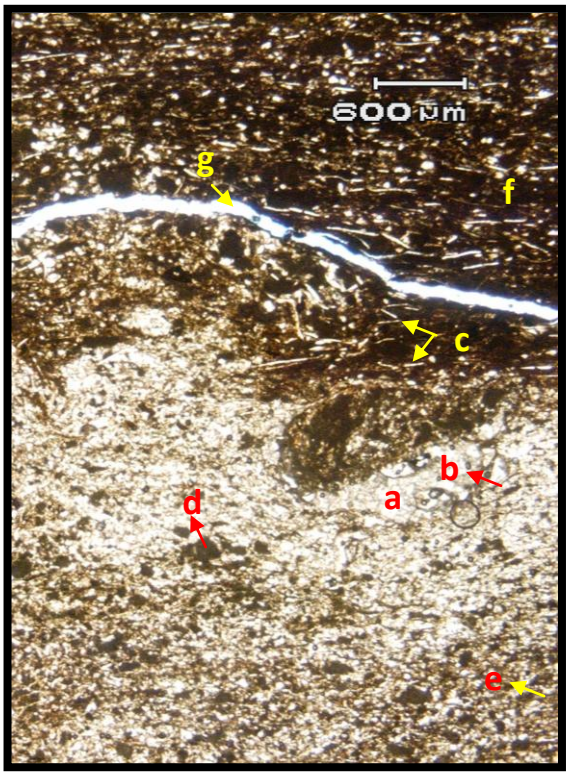

Figure 57. Thin section photomicrograph (9) of Sublitharenite in proximal sands in Memouniat Formation, showing (a) quartz, (b) feldspar, (c) mica flacks, (d) clay clasts, (e) calcite cement, (f) clay matrix and (g) fracture porosity. Core # 12 at 5838.3ft., well A1-NC1 (PPL).

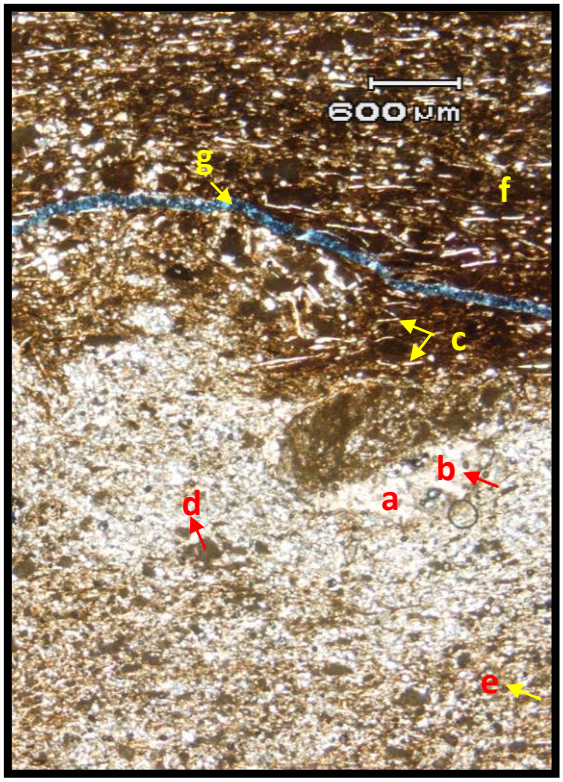

Figure 58. Thin section photomicrograph (9) of Sublitharenite in proximal sands in Memouniat Formation, showing (a) quartz, (b) feldspar, (c) mica flacks, (d) clay clasts, (e) calcite cement, (f) clay matrix and (g) fracture porosity. Core # 12 at 5838.3ft., well A1-NC1 (XPL).

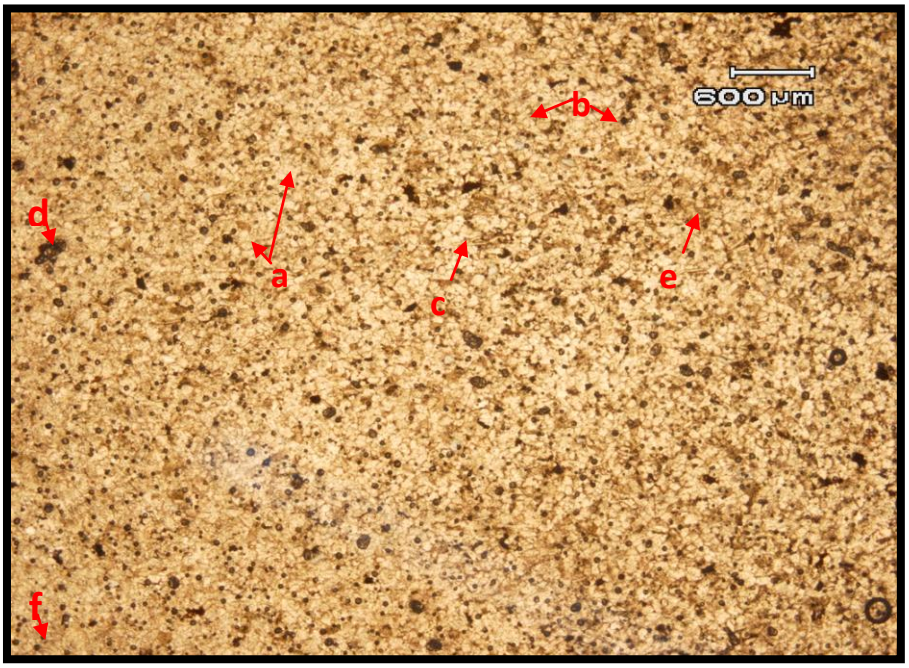

Figure 59. Thin section photomicrograph (10) of Sublitharenite in proximal sands in Memouniat Formation, showing (a) quartz, (b) feldspar, (c) mica flacks, (d) clay clasts, (e) calcite cement and (f) clay matrix. Core # 12 at 5835.2ft., well A1-NC1 (PPL).

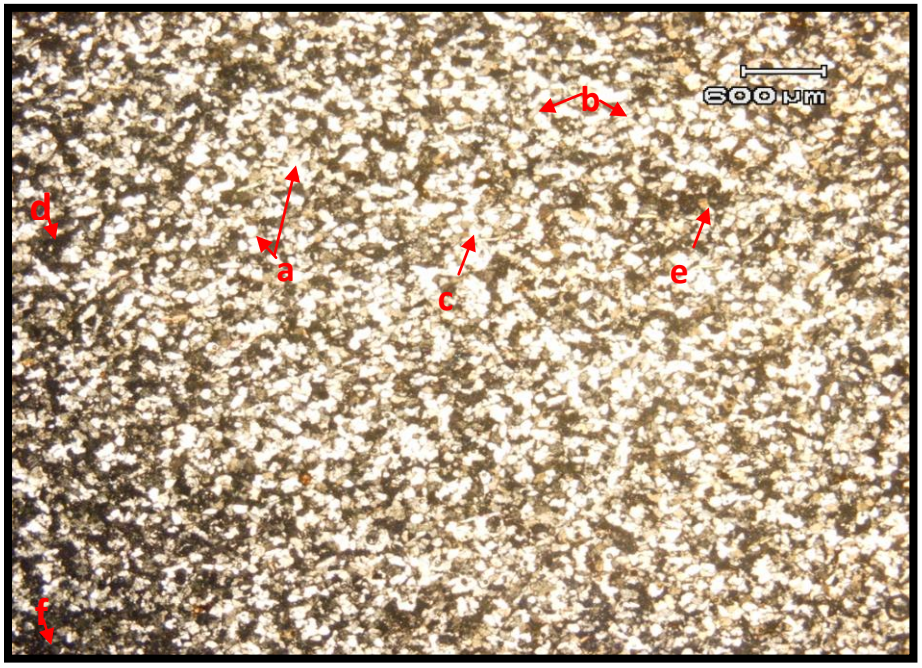

Figure 60. Thin section photomicrograph (10) of Sublitharenite in proximal sands in Memouniat Formation, showing (a) quartz, (b) feldspar, (c) mica flacks, (d) clay clasts, (e) calcite cement and (f) clay matrix. Core # 12 at 5835.2ft., well A1-NC1 (XPL).

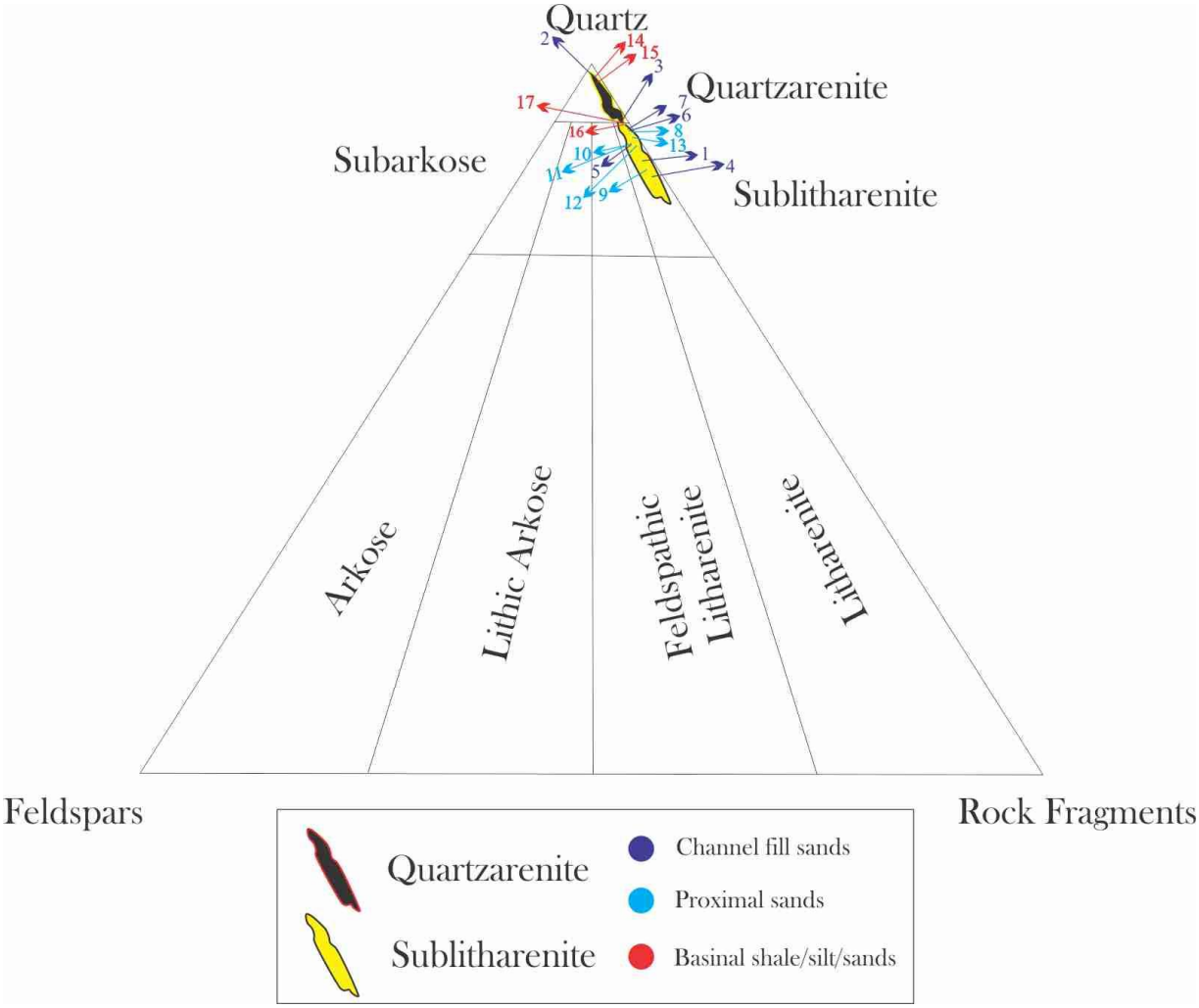

Figure 61. Triangle diagram showing detrital plots for the Memouniat Formation in the study area Hamada **(**Ghadames**)** Basin. **(**QRF classification of sandstones after Folk, 1980**)**

5.2 Authigenic minerals

5.2.1 Quartz overgrowth

The dominant cement is silicate through grain-to-grain contact, occasionally characterized by overgrowth fashion of quartz crystals of euhedral terminations **(**Fig. 41**),** especially in quartzarenite sandstone facies. Total estimated silicate cement from 12% to 28%. In general, the silica cement various with sand types **(**channel sands at depth 6181.84ft **)** and show some inverse relationship with carbonate cement and clay matrix **(**proximal sand at depth 5837.6ft and in basinal silt/shale at depth 6298.6ft**) (**Table 2**)**.

5.2..2 Carbonate cement

Carbonate cement is also recognized as patchy calcite to paikilotopic crystals filling pores **(**Fig. 43**)**, ranging from 2% to 14% in quartzarenite **(**Figs. 43,44, 62-65**)** to sublitharenite **(**Figs. 66-69**)** sandstone units.

Calcite cement in shallow marine sandstones normally cannot be derived from sources outside the sandstones owing to a lack of viable transport mechanisms for significant amounts of dissolved calcium carbonate. Within the sandstones the only significant source of calcite cement is usually biogenic carbonate, which is consequently considered to be the dominant source of calcite cement within shallow marine sandstones. Influx of carbon dioxide into a sandstone will not lead to precipitation of additional calcite cement unless a source of calcium other than biogenic carbonate is present, but the carbon isotopic composition of the calcite cement may be strongly affected **(**Walderhaug, and Bjorkum, 2009**)**.

Biogenic carbonate is less stable than calcite cement, and once a calcite cement nucleus has formed it will lower the concentration of dissolved calcite within its range of influence. Biogenic carbonate will then dissolve around the growing nucleus, diffuse down the concentration gradient and precipitate on the surface of the growing nucleus or concretion. This process will continue until the available biogenic carbonate is consumed or all porosity is filled with calcite cement **(**Walderhaug, and Bjorkum, 2009**)**.

5.2.3 Authigenic clay minerals

Clay minerals are of common weathering products of feldspar at humid and relatively high temperature condition **(**McGeary, 2004**)**. Clay cement may be encountered as pore filling illite or replacive occasionally replaces kaoilinaite in sandstone facies. Clay cement filling fractures and reduce porosity where it is much prominent at some places in proximal sand facies **(**Figs. 70-73**)** and basinal silt/shale **(**Figs. 74, 75**)** facies in the study area.

Figure 62. Thin section photomicrograph (11) of Quartzarenite in basinal silt/shale in Memouniat Formation, showing (a) quartz, (b) feldspar, (c) clay clasts and (d) pervasive calcite cement. Core # 15 at 6301.4ft., well D1-23 (PPL).

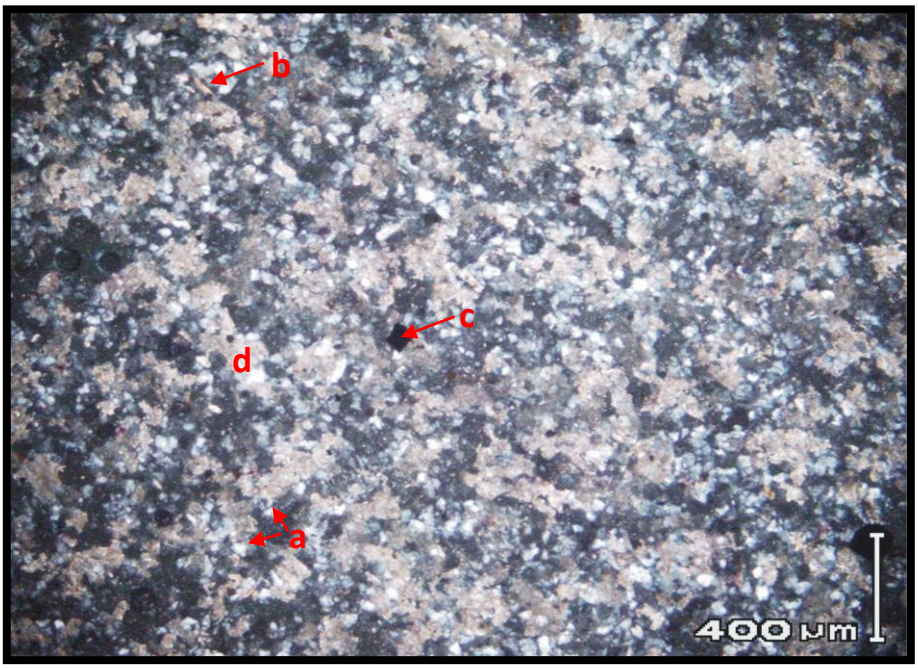

Figure 63. Thin section photomicrograph (11) of Quartzarenite in basinal silt/shale in Memouniat Formation, showing (a) quartz, (b) feldspar, (c) clay clasts and (d) pervasive calcite cement. Core # 15 at 6301.4ft., well D1-23 (XPL).

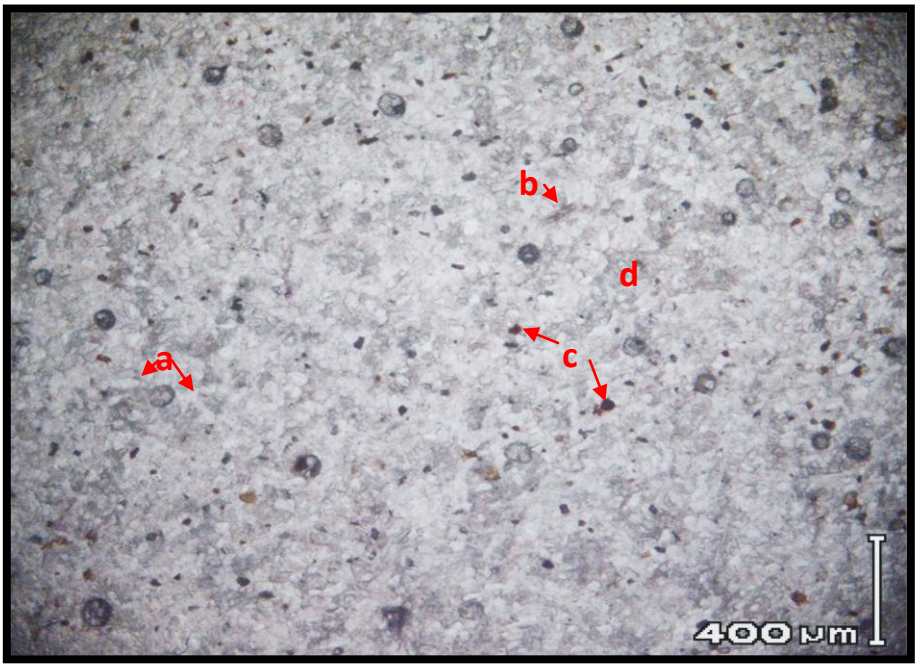

Figure 64. Thin section photomicrograph **(**12**)** of Quartzarenite in basinal silt/shale in Memouniat Formation, showing **(**a**)** quartz, **(**b**)** feldspar, **(**c**)** clay clasts and **(**d**)**, pervasive calcite cement. Core # 15 at 6302.3ft., well D1-23 **(**PPL**)**.

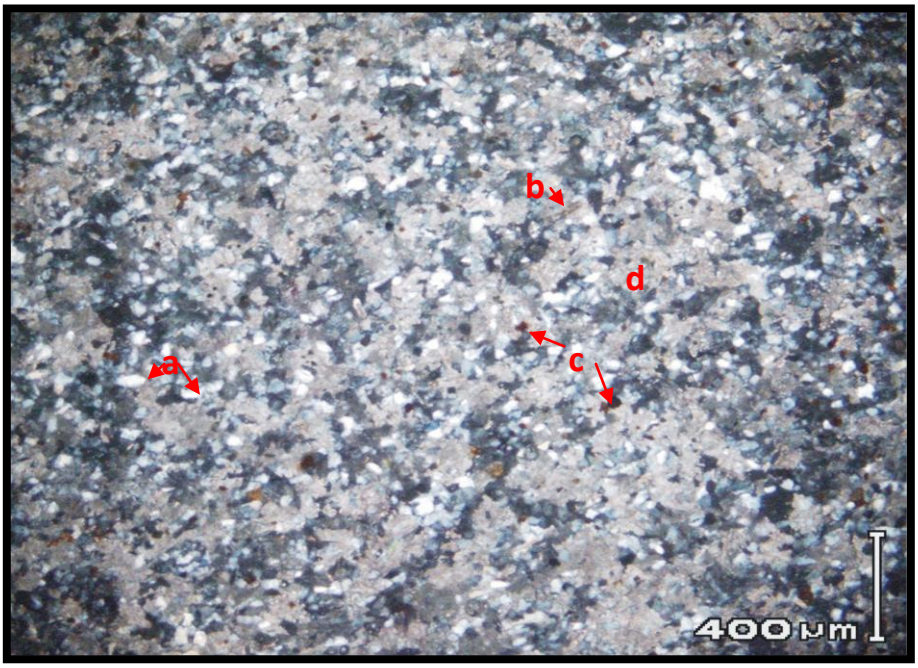

Figure 65. Thin section photomicrograph **(**12**)** of Quartzarenite in basinal silt/shale in Memouniat Formation, showing **(**a**)** quartz, **(**b**)** feldspar, **(**c**)** clay clasts and **(**d**)**, pervasive calcite cement. Core # 15 at 6302.3ft., well D1-23 **(**XPL**)**.

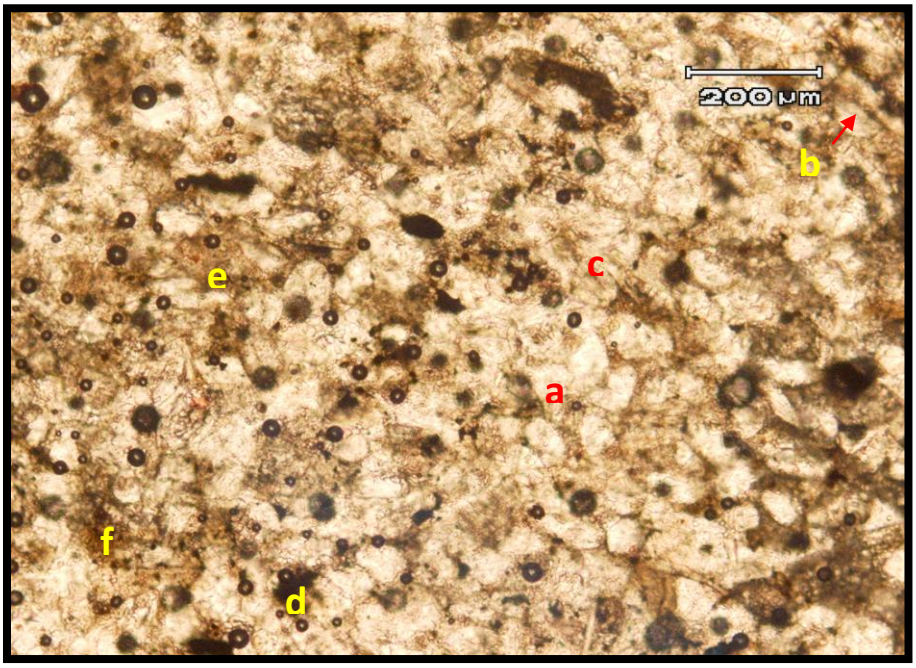

Figure 66. Thin section photomicrograph **(**13**)** of Sublitharenite in proximal sands in Memouniat Formation, showing **(**a**)** quartz, **(**b**)** feldspar, **(**c**)** mica flacks, **(**d**)** clay clasts, **(**e**)** calcite cement, **(**f**)** clay matrix. Core # 12 at 5837.6ft., well A1-NC1 **(**PPL**)**.

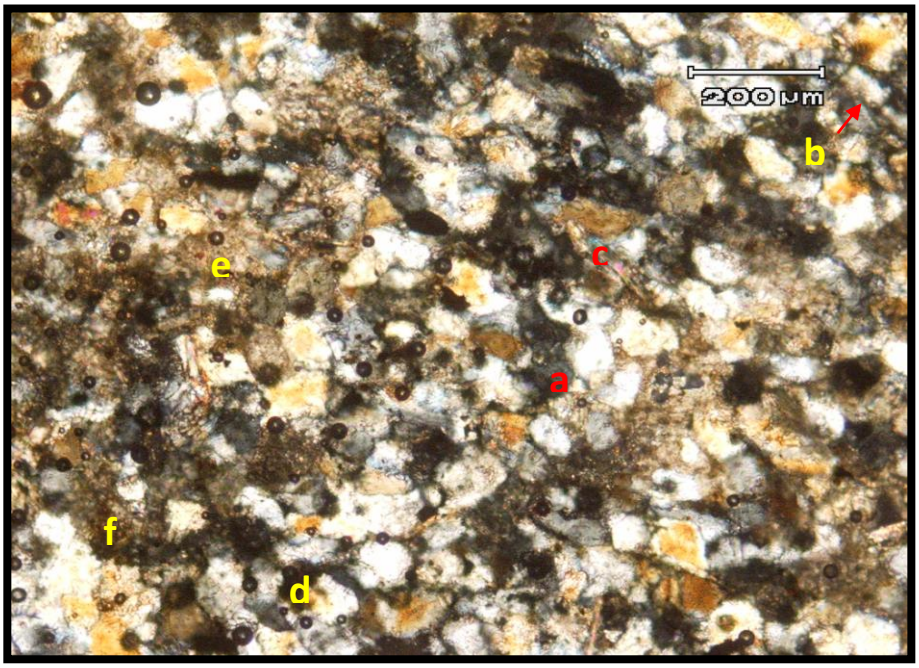

Figure 67. Thin section photomicrograph **(**13**)** of Sublitharenite in proximal sands in Memouniat Formation, showing **(**a**)** quartz, **(**b**)** feldspar, **(**c**)** mica flacks, **(**d**)** clay clasts, **(**e**)** calcite cement, **(**f**)** clay matrix. Core # 12 at 5837.6ft., well A1-NC1 **(**XPL**)**.

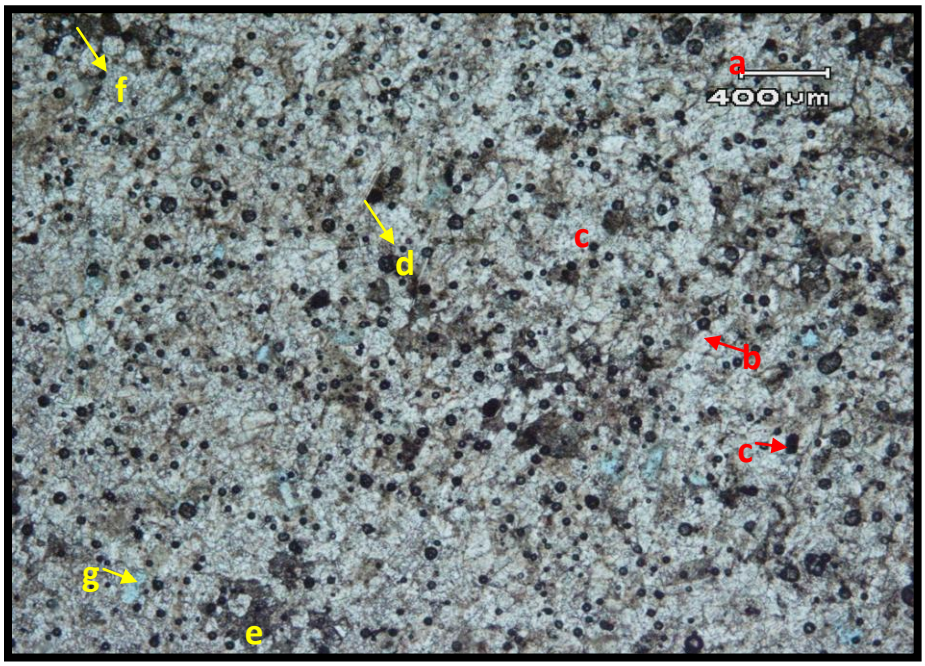

Figure 68. Thin section photomicrograph (14) of Sublitharenite in proximal sands in Memouniat Formation, showing (a) quartz, (b) feldspar, (c) clay clasts, (d) mica flacks, (e) pervasive calcite cement, (f) clay matrix and (g) leaching porosity. Core # 12 at 5830ft., well A1-NC1 (PPL).

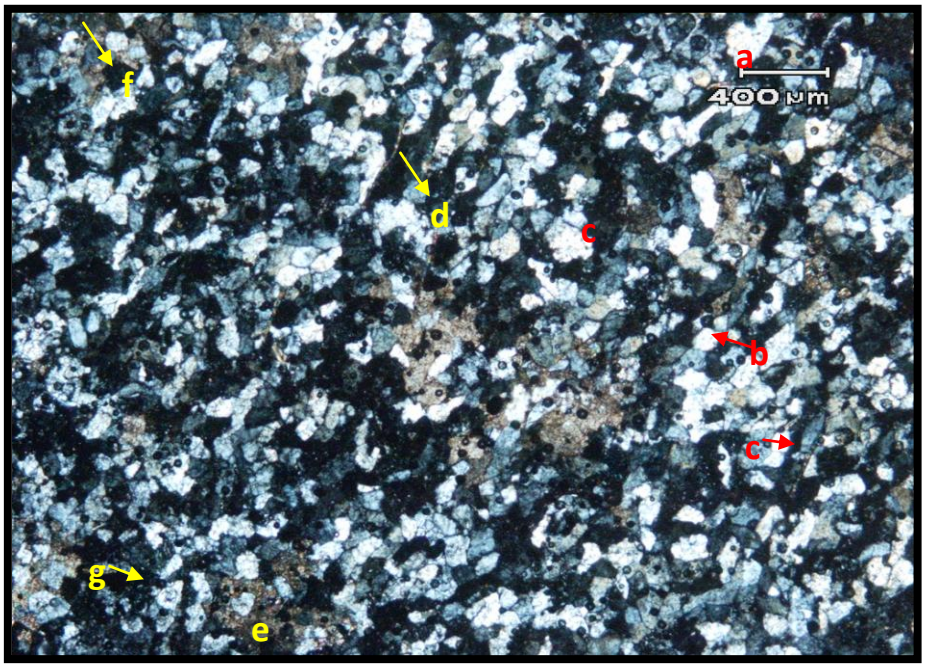

Figure 69. Thin section photomicrograph (14) of Sublitharenite in proximal sands in Memouniat Formation, showing (a) quartz, (b) feldspar, (c) clay clasts, (d) mica flacks, (e) pervasive calcite cement, (f) clay matrix and (g) leaching porosity. Core# 12 at 5830ft., well A1-NC1 (XPL).

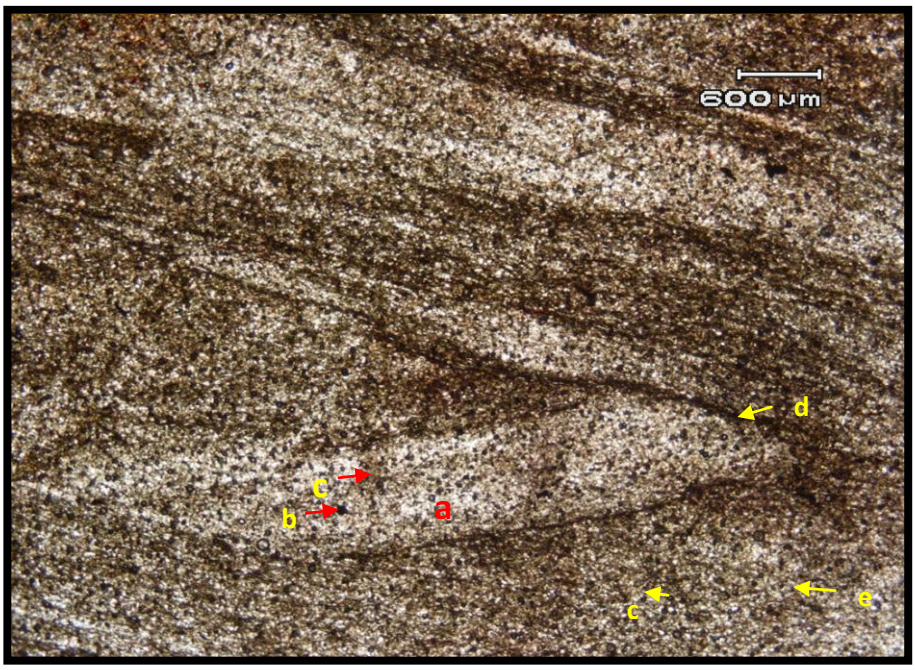

Figure 70. Thin section photomicrograph (15) of Sublitharenite in proximal sands in Memouniat Formation, showing (a) quartz, (b) clay clasts (c) calcite cement, (d) clay matrix and (e) mica flacks. Core # 11 at 5655.8ft., well A1-NC1 (PPL). Low angle truncation surface reflects periodic variation in wave energy condition.

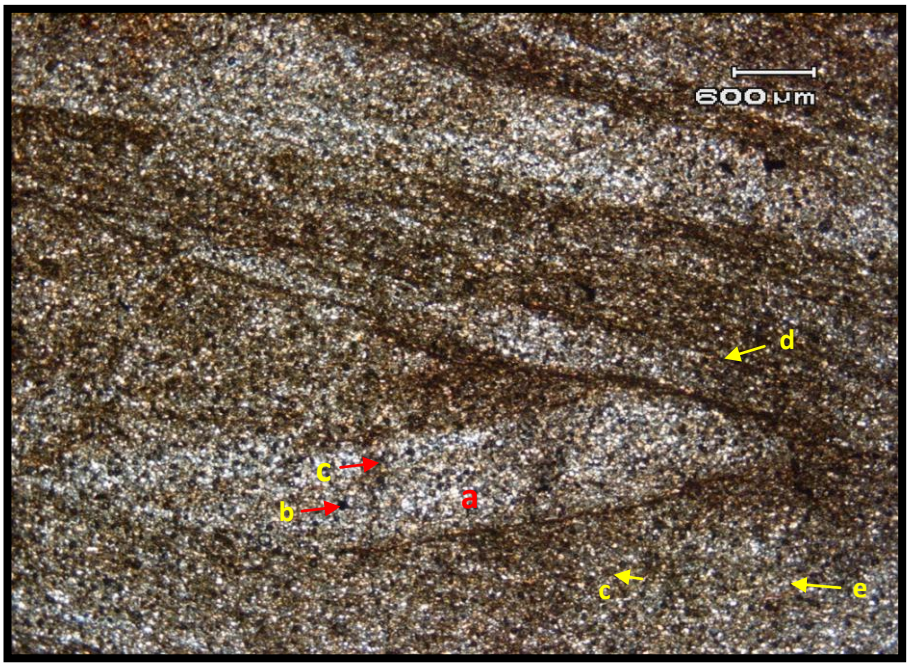

Figure 71. Thin section photomicrograph (15) of Sublitharenite in proximal sands in Memouniat Formation, showing (a) quartz, (b) clay clasts (c) calcite cement, (d) clay matrix and (e) mica flacks. Core # 11 at 5655.8ft., well A1-NC1 (XPL). Low angle truncation surface reflects periodic variation in wave energy condition.

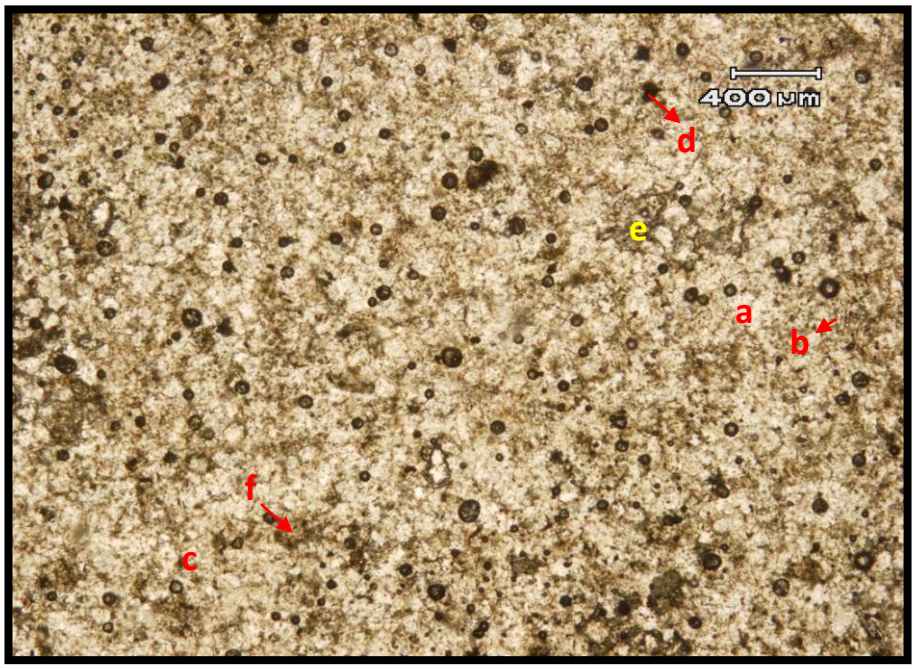

Figure 72. Thin section photomicrograph **(**16**)** of Sublitharenite in proximal sands in Memouniat Formation, showing **(**a**)** quartz, **(**b**)** feldspar, **(**c**)** polycrystalline quartz, **(**d**)** clay clasts, **(**e**)** calcite cement and **(**f**)** clay matrix. Core # 12 at 5842.11ft., well A1-NC1 **(**PPL**)**.

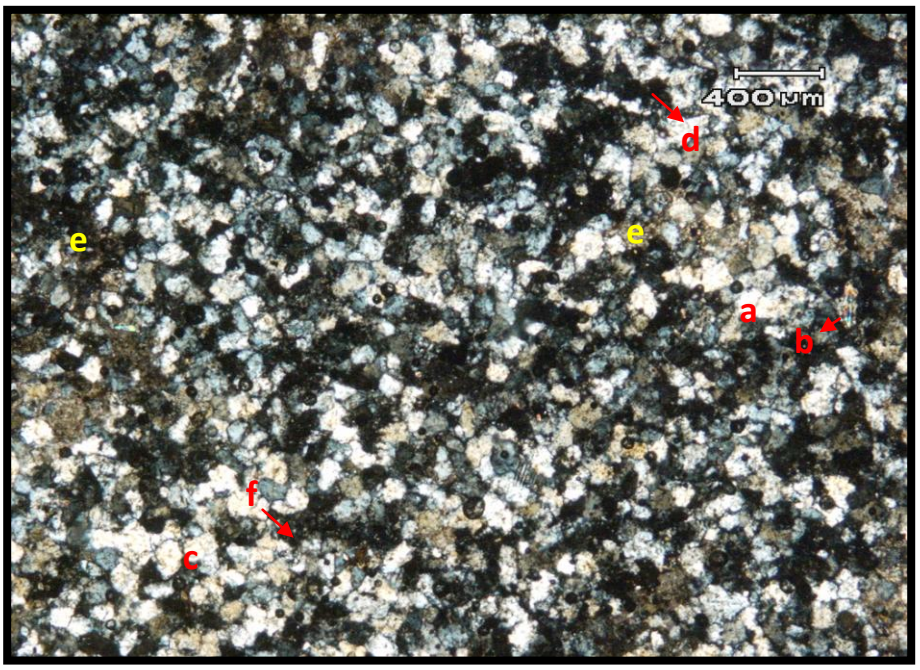

Figure 73. Thin section photomicrograph **(**16**)** of Sublitharenite in proximal sands in Memouniat Formation, showing **(**a**)** quartz, **(**b**)** feldspar, **(**c**)** polycrystalline quartz, **(**d**)** clay clasts, **(**e**)** calcite cement and **(**f**)** clay matrix. Core # 12 at 5842.11ft., well A1-NC1 **(**XPL**)**.

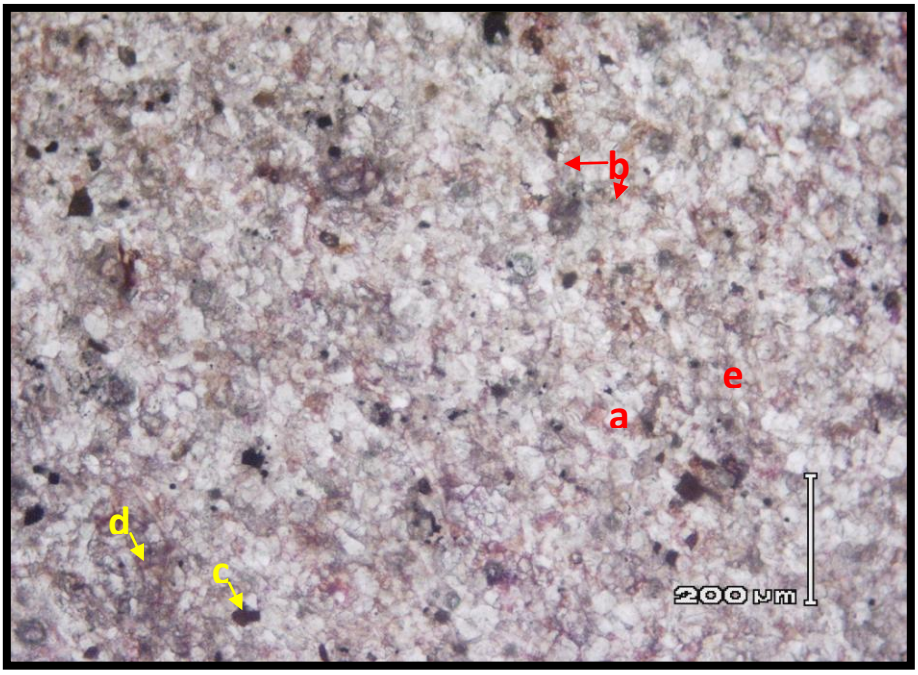

Figure 74. Thin section photomicrograph (17) of Quartzarenite in basinal silt/shale in Memouniat Formation, showing (a) quartz, (b) feldspar, (c) clay clasts, (d) clay matrix and (e) calcite cement. Core # 15 at 6298.3ft., well D1-23 (PPL).

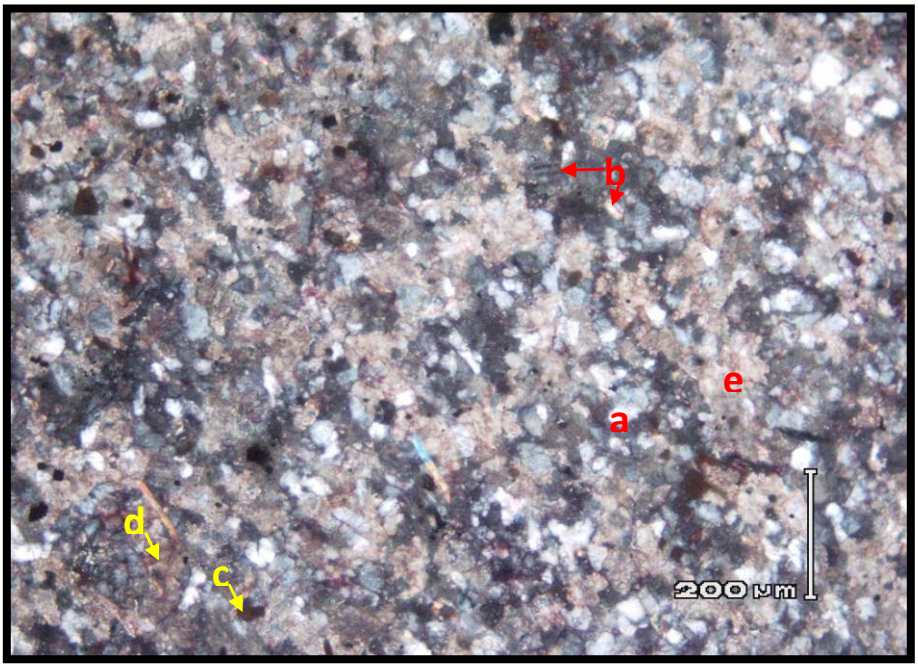

Figure 75. Thin section photomicrograph (17) of Quartzarenite in basinal silt/shale in Memouniat Formation, showing (a) quartz, (b) feldspar, (c) clay clasts, (d) clay matrix and (e) calcite cement. Core # 15 at 6298.3ft.. well D1-23 (XPL).

Chapter (6)
Paleogeography of Memouniat Formation

6.1 Stratigraphic cross section (Time stratigraphic unit)

The lateral relationship between identified facies in cores have been examined by constructing regional stratigraphic cross section **(**Fig. 76**)**. In this cross section traces of GR-log and/or SP-curve was used to define lithological changes at each control point.

Using GR-log characteristic and lithology the Memouniat Formation in the study area can be divided into three sectors **(**channel fill sand dominated sector, proximal sand dominated sector, and basinal offshore silt/shale dominated sector**)**. Whereas in each well sand and shale beds may occur interbedded at different levels.

The base of the persistent high radioactive shale of Tanezzuft Formation was chosen as a regional datum, as this horizon marks a rapid and wide spread transgression and it is believed to approximate a relatively flat paleosurface, and can be traced from well to well providing a meaningful stratigraphic relationship, within which observed facies are correlatable and can be examined in terms of lateral facies changes.

The lower limit of Memouniat Formation can be defined by Melez Chogran Shale at some locations **(**wells M1-66, F1-66, D1-23, and A1-NC1**)** whereas its presence across the correlatable wells could be speculative marking an arbitrary lower boundary.

Within the establishing stratigraphic framework **(**Fig. 76**)** the facies changes laterally from much channelized sandstone units to the south passes northward to a much transgressive high energetic marine sands, which eventually grades into a basinal offshore silt/shale facies.

Accompanying these regional basin-ward facies changes is a notable decrease in grain size of Memouniat Formation **(**northward**)**. Increasing distance from south to north reflects an increase in the shale sections **(**vertically**)** in each correlated well.

Hence, another vertical changes in facies regarding the development of some carbonate horizon especially in wells **(**B1-26, B1-NC5A, and A1-70**)** of the middle sector which may suggest subsequent transgression marking the beginning of this

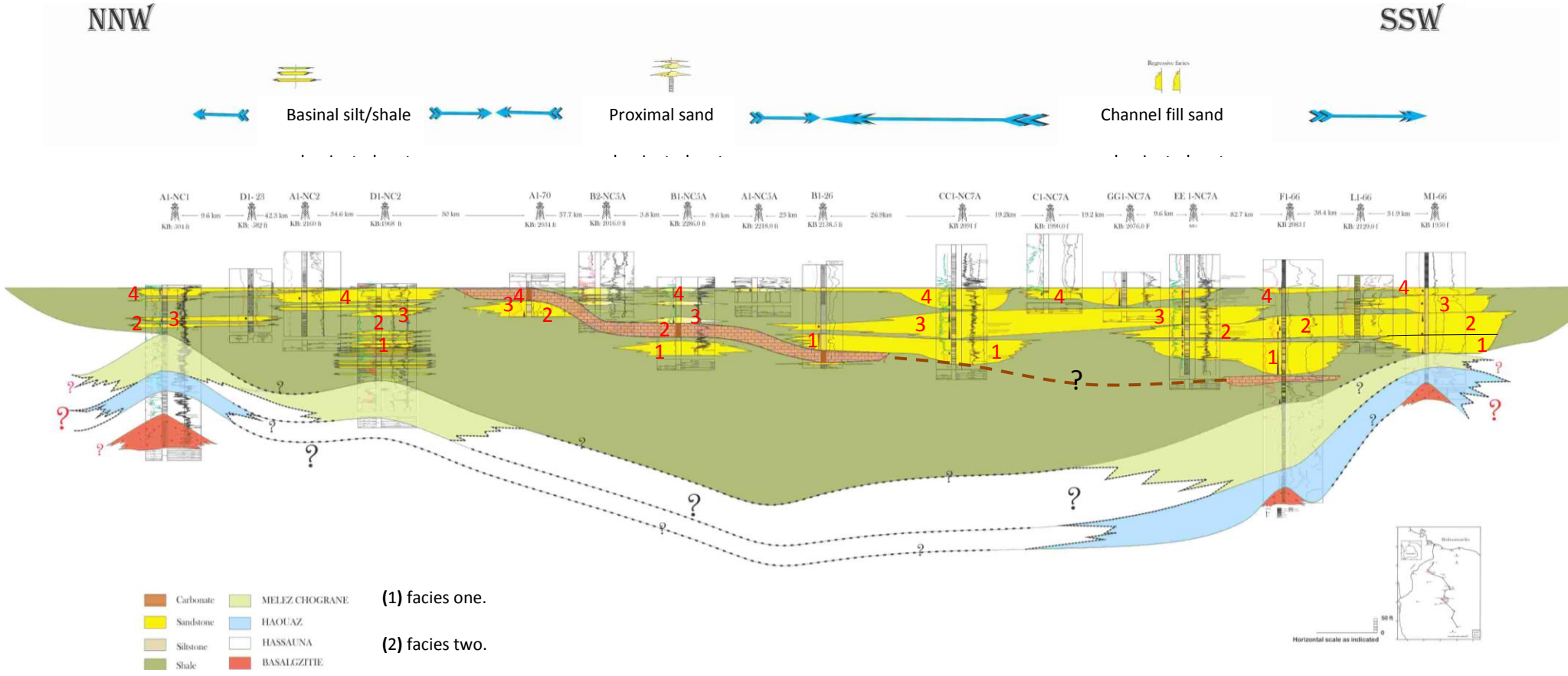

Figure 76. Regional stratigraphic cross-section, showing possible correlation of the selected Memouniat Formation, units **(**1-4**)** and their predominant sectors, Hamada **(**Ghadames**)** Basin, NW Libya.

horizon to much more marine reworked sand at the top. We have regarded this carbonate horizon or its equivalent in this study as a facies from Memouniat Formation, it appears to be infill topographic lows on the eroded and irregular Memouniat surface, and thins or absent over topographic highs. It may has an unconformable relationship with the overlying Tanezzuft Formation which truncates this carbonate horizon at some locations as in well A1-70.

Moreover its location appears to be either associated with shallow depth **(**wells A1-70, B2-NC7A and B1-NC7A**) (**Fig. 76**)** topping the Memouniat Formation whereas could be seen in deeper section of Memouniat Formation at great depth **(**well F1-66**)**. Its thickness reaches 85ft to the north and decreases to 40ft to the south and sometime completely missed, especially in the southern part of the basin at the vicinity of wells (M1-66, L1-66, EE1-NC7A and CC1-NC7A**)**. The discontinuity of this limestone may suggests that coastal inundation was active through valley incisions in southern part of the study area. This carbonate facies may be interpreted to comparatively shorter periods of localized carbonate production during episodes of marine inundation.

6.2 Fence diagram (Areal distribution of Memouniat facies)

The areal distribution of the recognized facies can be analyzed with the aid of a fence diagram **(**Fig. 77**)**. The usefulness and the advantage of using fence diagram in this study is that the lateral facies changes can be traced in different directions, moreover, the correlation lines can be looped between correlated wells to show or verify their accuracy.

In this diagram, the radioactive marker used in cross-section **(**Fig. 76**)** can be used and carried throughout the basin. This transgressive unit of great significance and may be considered as the deep-low relief topping the Memouniat Formation, whereas other transgressive shale units can be seen interbedded and widespread between Memouniat sands.

The main channels system that existed in the south are clearly revealed as they are changing character postulating the formation of proximal marine sands across the central **(**middle**)** mapped area and show some lateral extension and variations.

Interbedded silt and shale that may be assigned for basinal offshore silt/shale facies occur to the north or northwest, and are characterized by sedimentation in a relatively low basinal area.

6.3 Paleogeography of the study area:

The available wells used in this fence diagram **(**Fig. 77**)** are assumed to reveal the paleogeography of the studied area and allow facies changes and continuity. The coarse sands and their channel type increase southward, indicating that the source of these clastics present in that direction. The further marine fine sand , silt and shale are increasingly dominated the north and northwest.

The facies boundaries or **(**black solid lines**)** that separating these recognized facies and defining major sectors **(**channel predominated sector, wavy dominated sand proximal **(**shoreface**)** sector and basinal **(**offshore**)** silt/shale predominated sector**)** are basically depends on recognizable log motifs and available core samples of the studied facies where their dashed extensions are arbitrary.

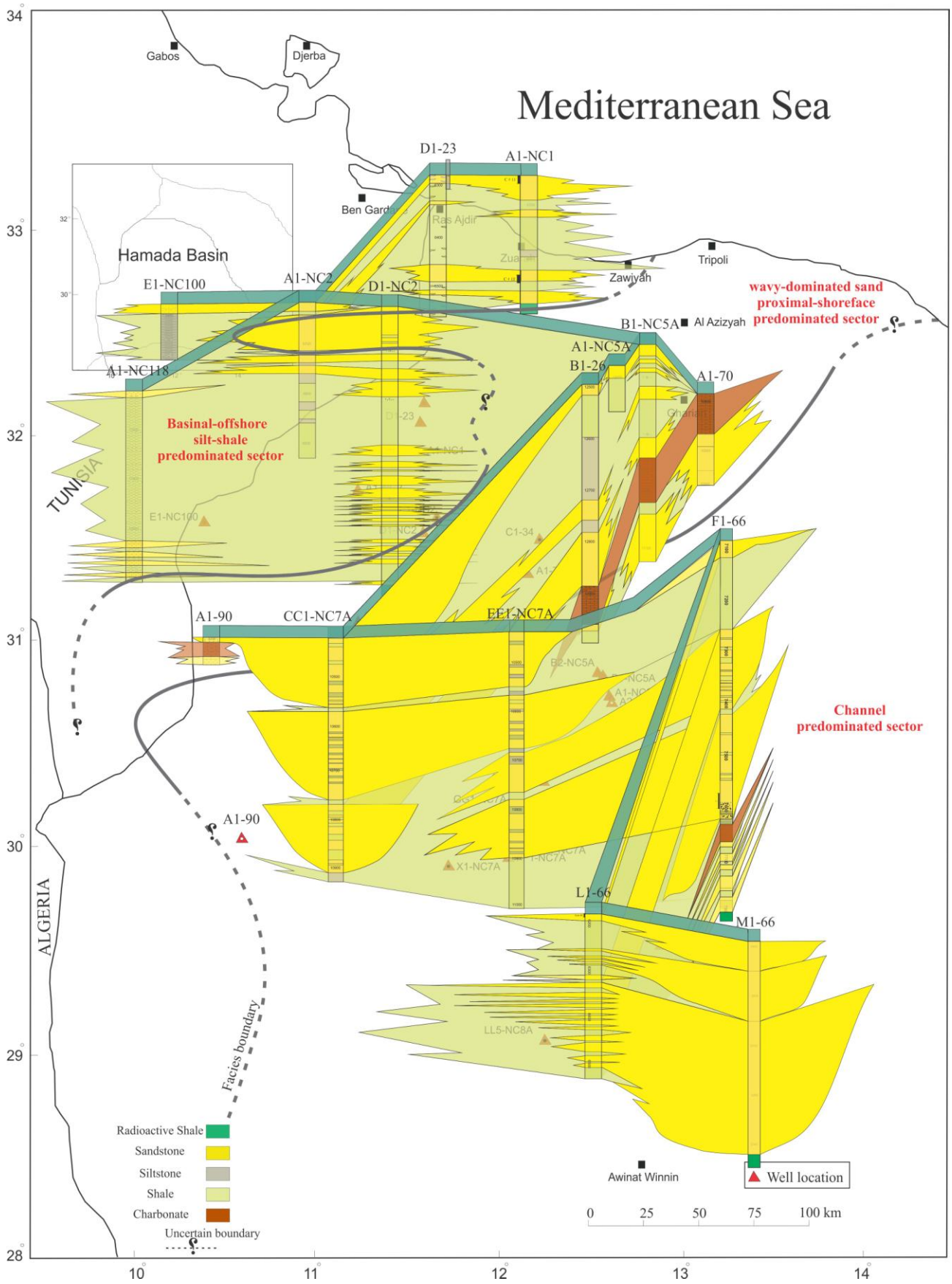

Figure 77. Areal distribution **(**Fence diagram**)** of the interpreted facies of Memouniat Formation, postulating also the paleogeography of the study area depicted from depositional facies changes. Hamada **(**Ghadames**)**. Basin, NW Libya.

6.4 Sandstone trend maps

Extensive reviewing of surface and subsurface studies are incorporated in our regional mapping efforts and interpretation included, Waring, (1976), Ryer et al. (1987), Gustason, (1988), Dolsom, (1991), Smith, (1992), Ryer, (1993), and Henry, and Al Dantorth (2002).

For the sake of showing the distribution of the correlated facies or units and detecting their trends, regarded sand units have been numbered and traced laterally to match their possible equivalent units from south to north (Fig. 76). With the available well control and by using net sand thickness and log- motifs for the selected sandstone units, net sandstone isopach and log facies maps can be generated for the studied numbered sandstone units across the basin.

6.4.1 Isopach maps for sand units 1-4.

Net sandstone isopach maps for units 1-4 were constructed (Figs. 78, 79, 80, 81) by measuring the thickness sandstone that recording a reading of 75 API or less on GR-log. However, the well control in the study area is not enough to map in details these sand units (1-4); this is because of the fact that some wells are not exist in some areas like NE and SW areas, also because of the wide spacing between studied wells (e.g. A1-90 and E1-NC100). Therefore, the isopach contour patterns will be seen in solid line when data are more abundant, while it will be dashed line where data are not certain or speculated. The isopach maps for facies 1-4 are showing regional trend as sands thin-out from southeast direction to northwest marking the deeper marginal edge of the basin.

6.4.1.1 Isopach map for unit (1).

In figure (78), unit one has a minimum thickness of about (20ft) in well (D1-NC2) and a maximum thickness of about (240ft) in well (F1-66). The patterns of isopach contour lines are displaying channel like behavior in the vicinity of wells (L1-66, F1-66, M1-66, EE1-NC7A and CC1-NC7A) as these wells are characterized by general fining-upward sequences of fluviatile-channel deposition (Fig. 76 and 77). The contour lines spacing are very wide and stable along the study area, which reflect gentle

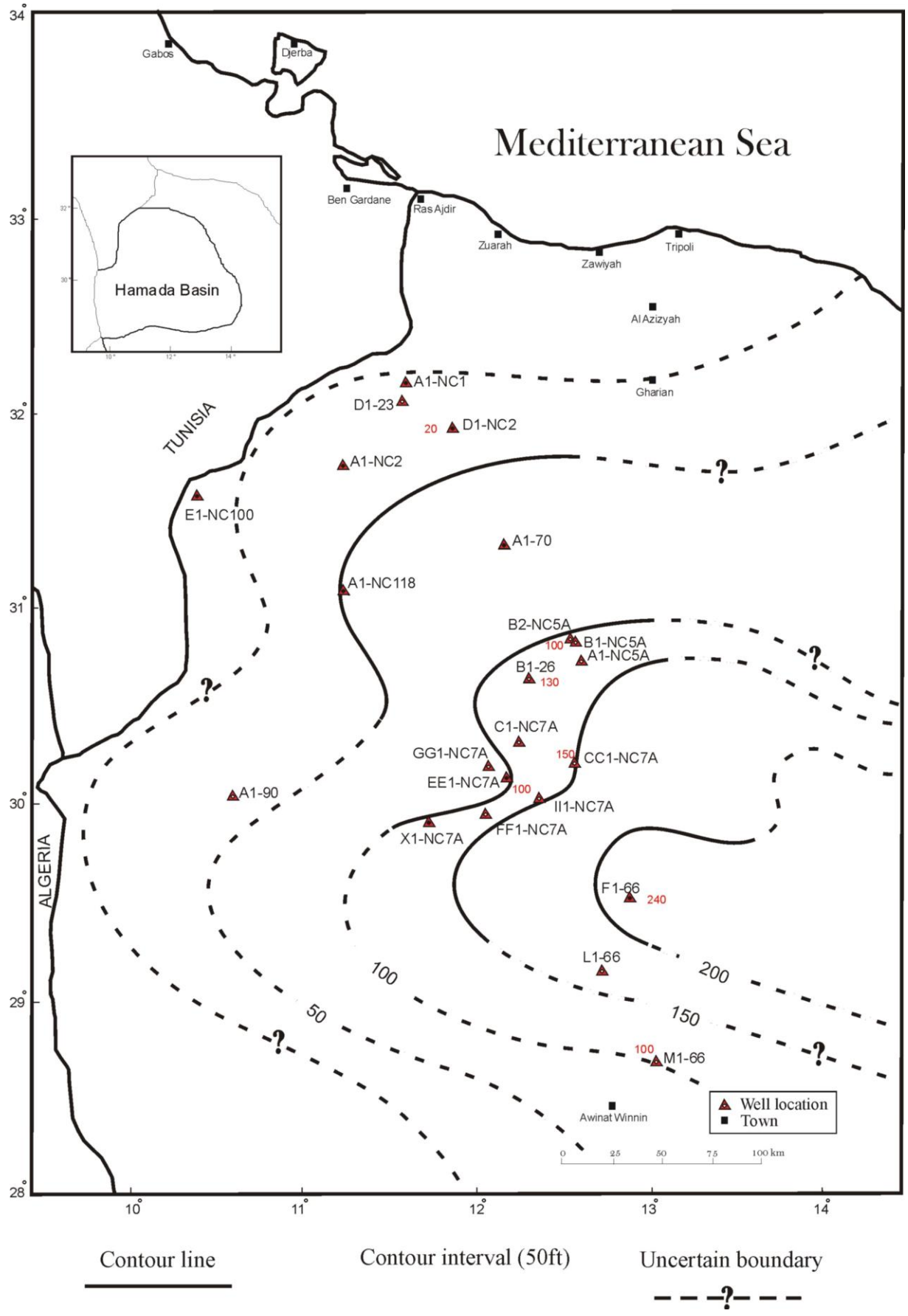

Figure 78. Isopach map of facies **(**1**)** for Memouniat Formation, Hamada **(**Ghadames**)** Basin.

slopping of the facies **(**1**)**. The proximal sands are thinner **(**70-50ft**)** and they are characterized by coarsening upward of transitional zone and of smooth loobate contours, which formed by the effects of changing channel caurses and incisions, In the NE and NW corners, contours are much more wider and less effected with these channels and appear to be much speculative. The basinal facies are toward the NW corner represent the minimum thickness of **(**20ft**)** in wells A1-NC2 and D1-NC2.

6.4.1.2 Isopach map for unit (2).

In figure **(**79**)**, unit two has a minimum thickness of about **(**20ft**)** in well **(**A1-NC1**)** and a maximum thickness of about **(**120ft**)** in well **(**F1-66**)**. The patterns of isopach contour lines are displaying channel like behavior in the vicinity of wells **(**L1-66, F1-66 and M1-66**)** as these wells are characterized by general fining-upward sequences of fluviatile-channel deposition. The phenomena of channel along facies **(**2**)** is existing in NE to middle part of the area, and represent strong power of incision. The contour spacing is different from much more wide in the east to much narrower to the west. The thickness of the proximal sands is about 60ft and going to be thinner in basinal silt/shale facies to about 20ft, both of these facies are characterized by loobate shape contour lines, which much more represented in the N and SW directions.

6.4.1.3 Isopach map for unit (3).

In figure **(**80**)**, unit three has a minimum thickness of about **(**40ft**)** in well **(**A1-NC1**)** and a maximum thickness of about **(**170ft**)** in well **(**CC1-NC7A**)**. The patterns of isopach contour lines are displaying low channel like behavior in the vicinity of wells **(**F1-66 and CC1-NC7A**)** as these wells are characterized by general fining-upward sequences of fluviatile-channel deposition, with low to high incision and occasionally of wide contour spacing. The proximal sands represent wide area of coarsening upward fashion of about 80ft thickness as in well **(**D1-NC2**)**, while the basinal area is much more narrower and thinner.

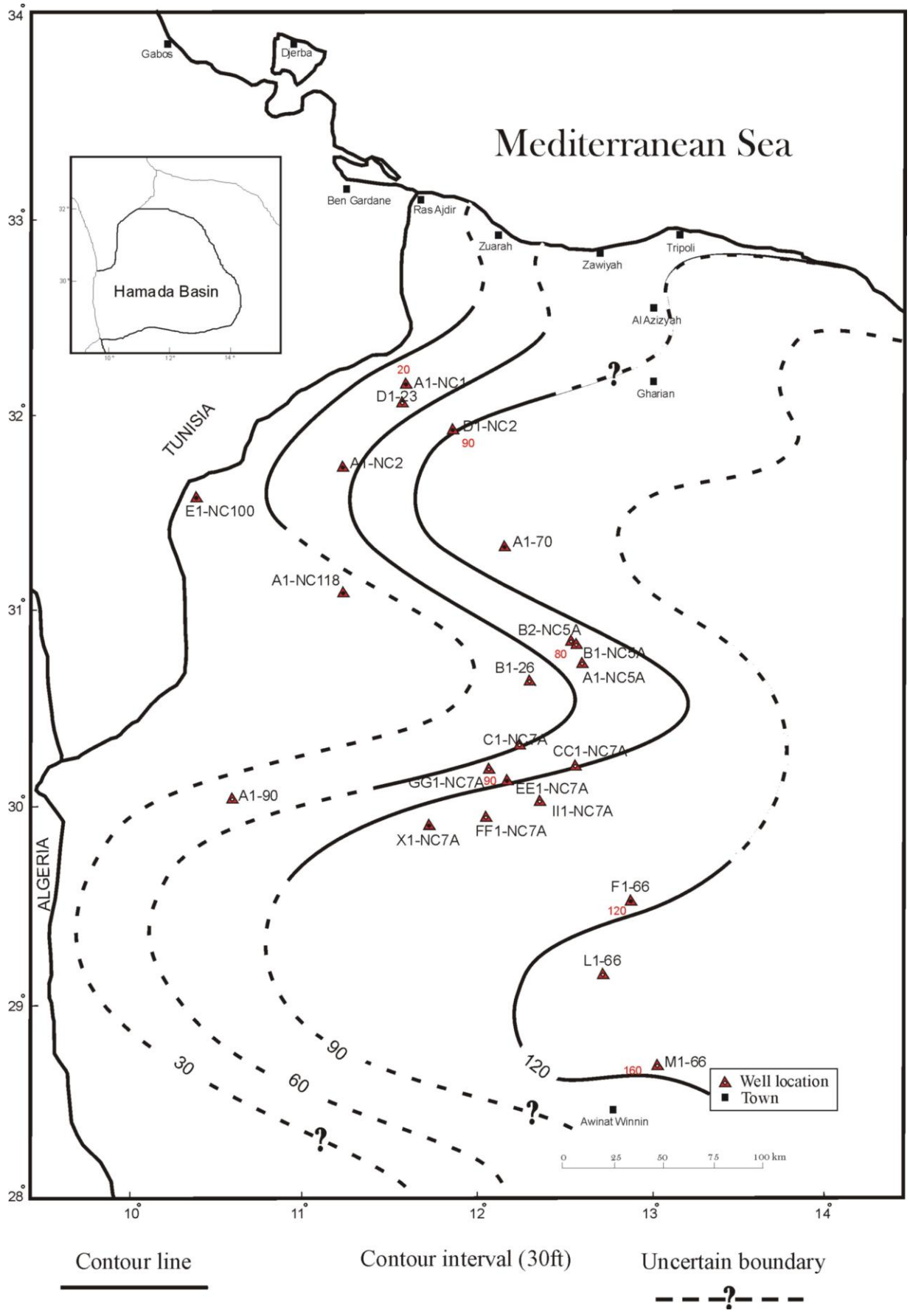

Figure 79. Isopach map of facies **(**2**)** for Memouniat Formation, Hamada **(**Ghadames**)** Basin.

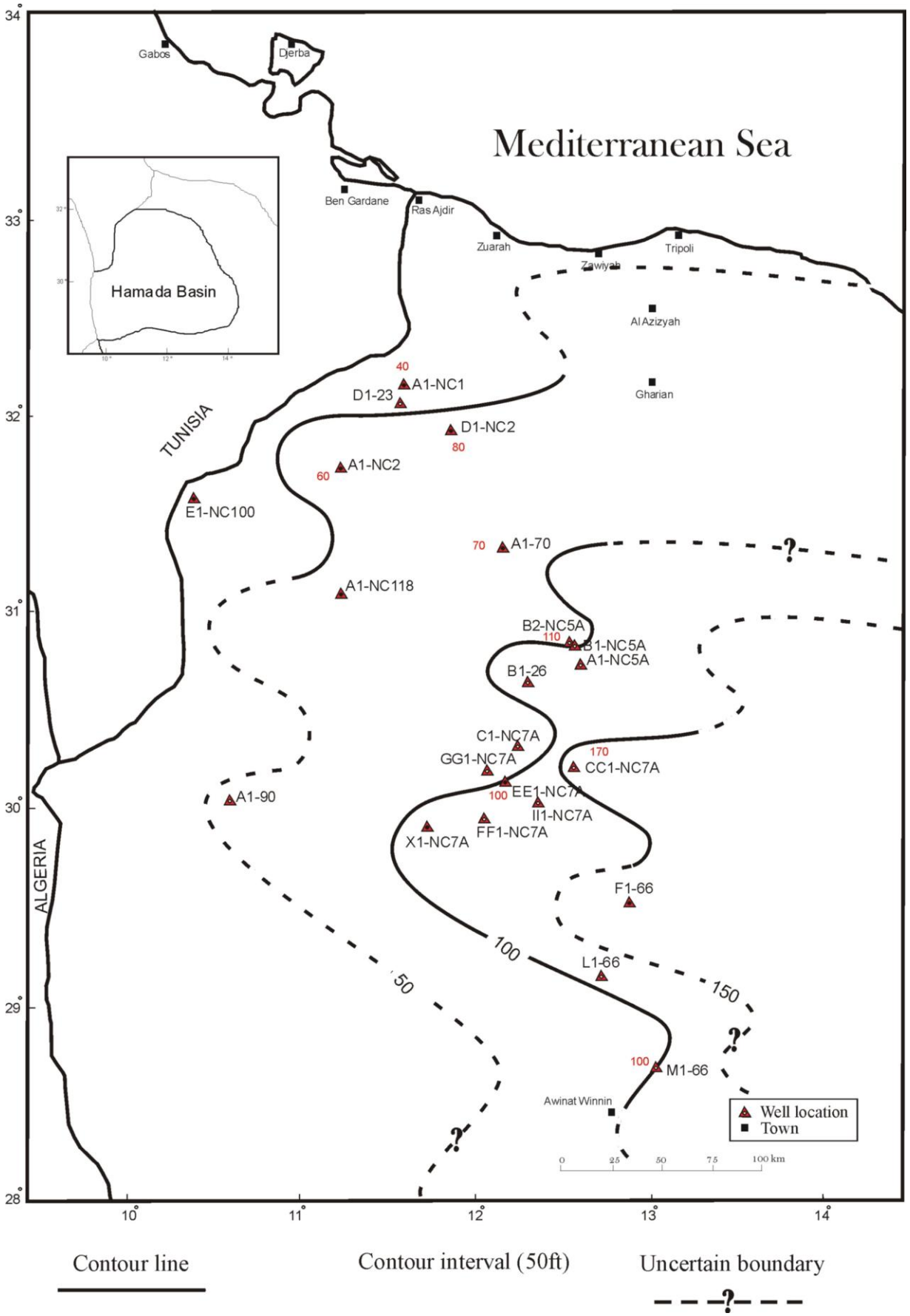

Figure 80. Isopach map of facies **(**3**)** for Memouniat Formation, Hamada **(**Ghadames**)** Basin.

6.4.1.4 Isopach map for unit (4).

In figure (81), unit four has a minimum thickness of about (20ft) in well (E1-NC100) and a maximum thickness of about (140ft) in well (CC1-NC7A). The patterns of isopach contour lines are displaying channel like behavior in the vicinity of well (CC1-NC7A). The shape of isopach contour lines can show a squeezed contour pattern which may suggest narrowing of the channel roots at some places, which reflect the effect of paleorelief on distribution of this unit. The proximal sands also it is representing limited area of (20-50ft) thickness, while the basinal silt/shale facies is much wider and covering large area with an approximate thickness of about 20ft.

From the isopach maps (Figs. 78, 79, 80 and 81) the areal distribution of these sands (1-4) is obviously changing from SE to NW corners as the depositional system changes (from SE to NW) from channel dominated sands to proximal (shoreface) sands to eventually silt/shale of basinal (offshore) end. So that the variation in thickness must be associated with areas of maximum sediment supply concentrated (thicker) to the SE and to much less (thinner) to the NW as probably high waves actions and currents may redistribute these sands and intensively reduced their thicknesses.

6.4.2 Log-Facies Maps for Units 1-4

Figures 82, 83, 84 and 85 are log facies maps for sandstone units 1-4, showing the different facies and their log shape characteristics which permit recognition of facies from each other (Serra, 1989) .

Actually log facies maps (Figs. 82, 83, 84 and 85) show that the channel sands and proximal shoreface sands are dominating the southern and central parts of the study area, while the most likely basinal (offshore) silt/shales are dominating the northern part of the study area. However, the carbonate facies are locally defining the NE/SW corners of the study area on the level of unit (2) (Fig. 83) and unit (4) (Fig. 85), and this may suggest its discontinuity and their depositional nature.

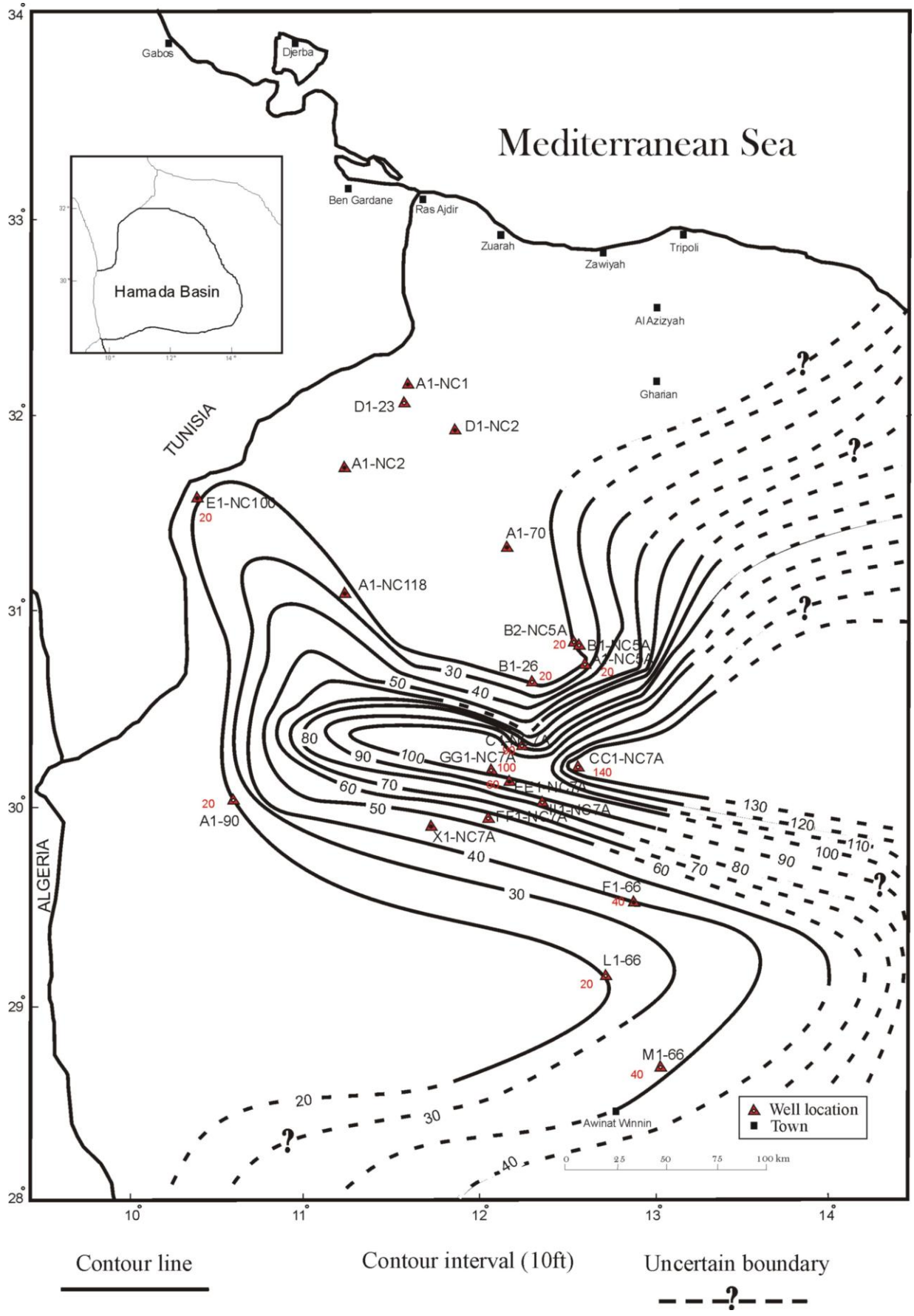

Figure 81. Isopach map of facies **(**4**)** for Memouniat Formation, Hamada **(**Ghadames**)** Basin.

Hence the integration of the log motif and net sandstone isopach maps for each mappable sandstone units may reveal their geometry and distribution. These maps should be contoured with the aid of the fence diagram **(**Fig. 77**)**.

As indicated in section **(**4.2, p. 35**)** the GR-log signature of channel sandstone is of bell shape characterizing by fining upward sequence serrated with shaly laminations at the upper part which effects on physical properties of the facies, sometimes characterized by blocky shape at some levels, which represent a good stacked sandstone unit to be drilled.

The sandstones of proximal sand is characterized by coarsening upward fashion of GR-log signature and of transitional base with the silt, shale lower units and of sharp remarkable top at the end of the unit. These sands reflecting high mode of depositional flow regime.

The offshore basinal silt/shale is characterized by spiky nature of log signature marking the northern most basin edge, having a thickness of 20ft and usually enclosed between marine shales as in wells D1-23 and A1-NC1, which suggest their marine offshore nature.

The mappable sandstone units 1-4 will be showing a lateral facies changes in transitional mode or even where the maps effectively may depict the main trends of their depositional system and also the direction from which clastics were derived.

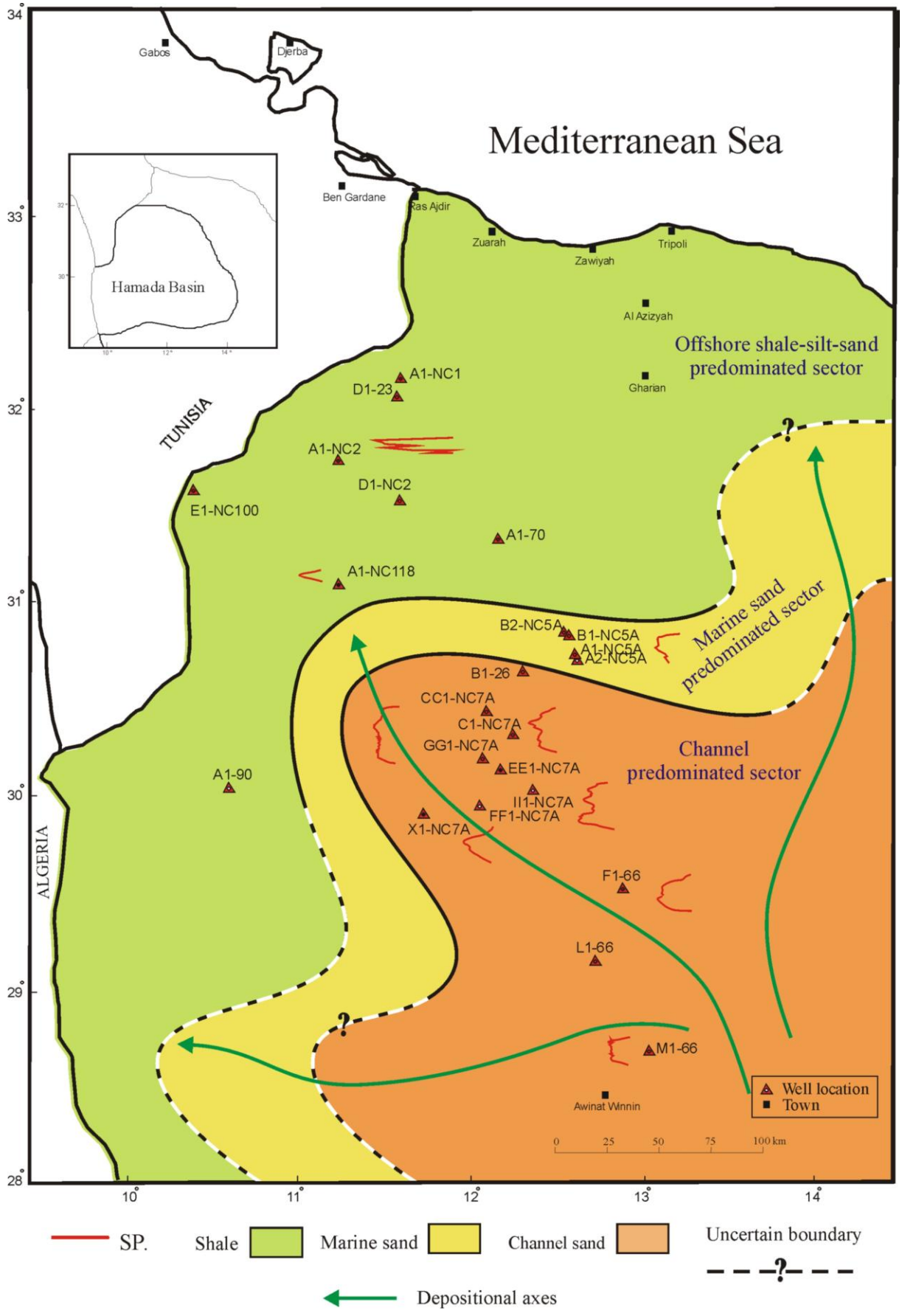

Figure 82. Log facies map of sand unit **(**1**)** for Memouniat Formation, Hamada **(**Ghadames**)** Basin.

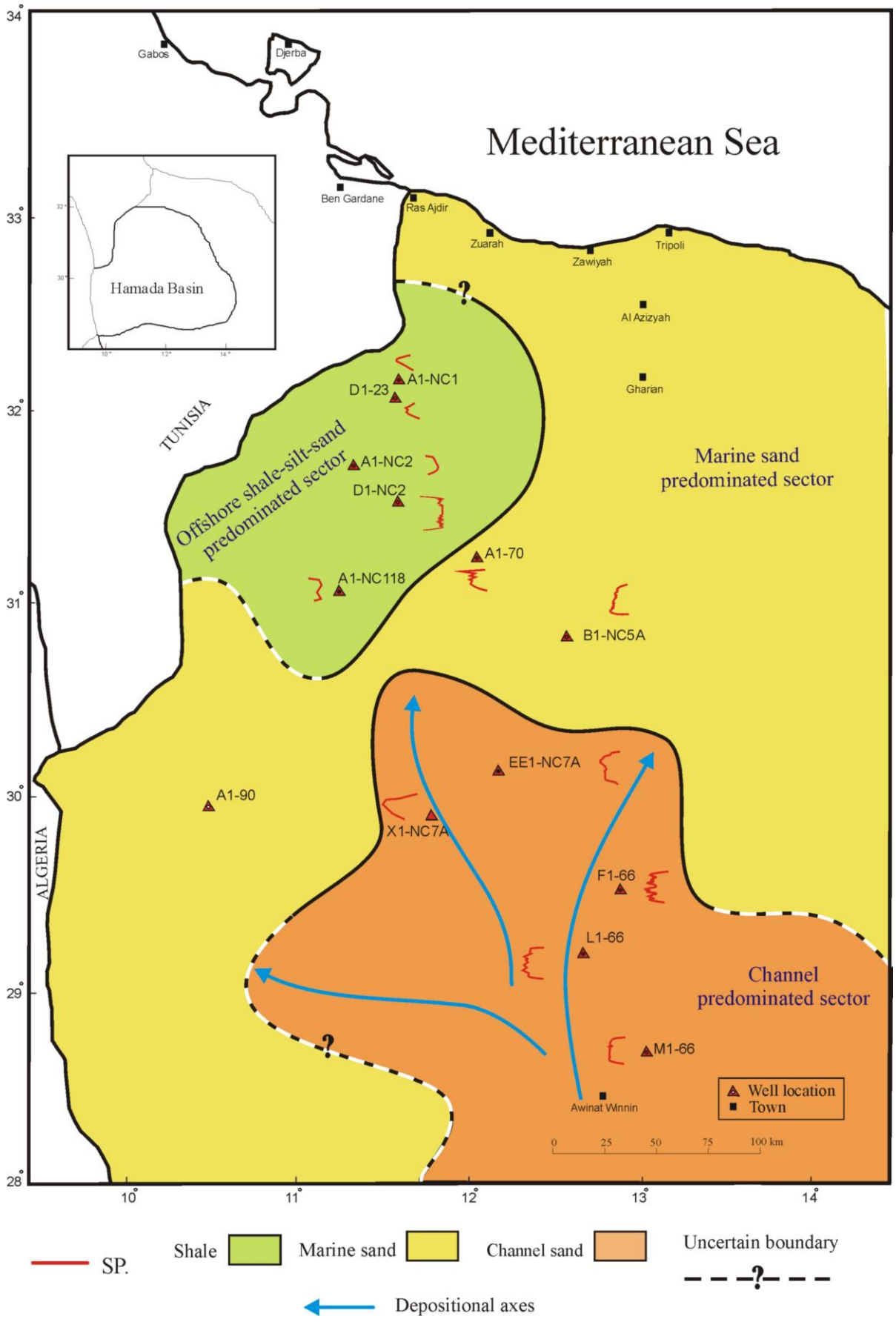

Figure 83. Log facies map of sand unit **(**2**)** for Memouniat Formation, Hamada **(**Ghadames**)** Basin.

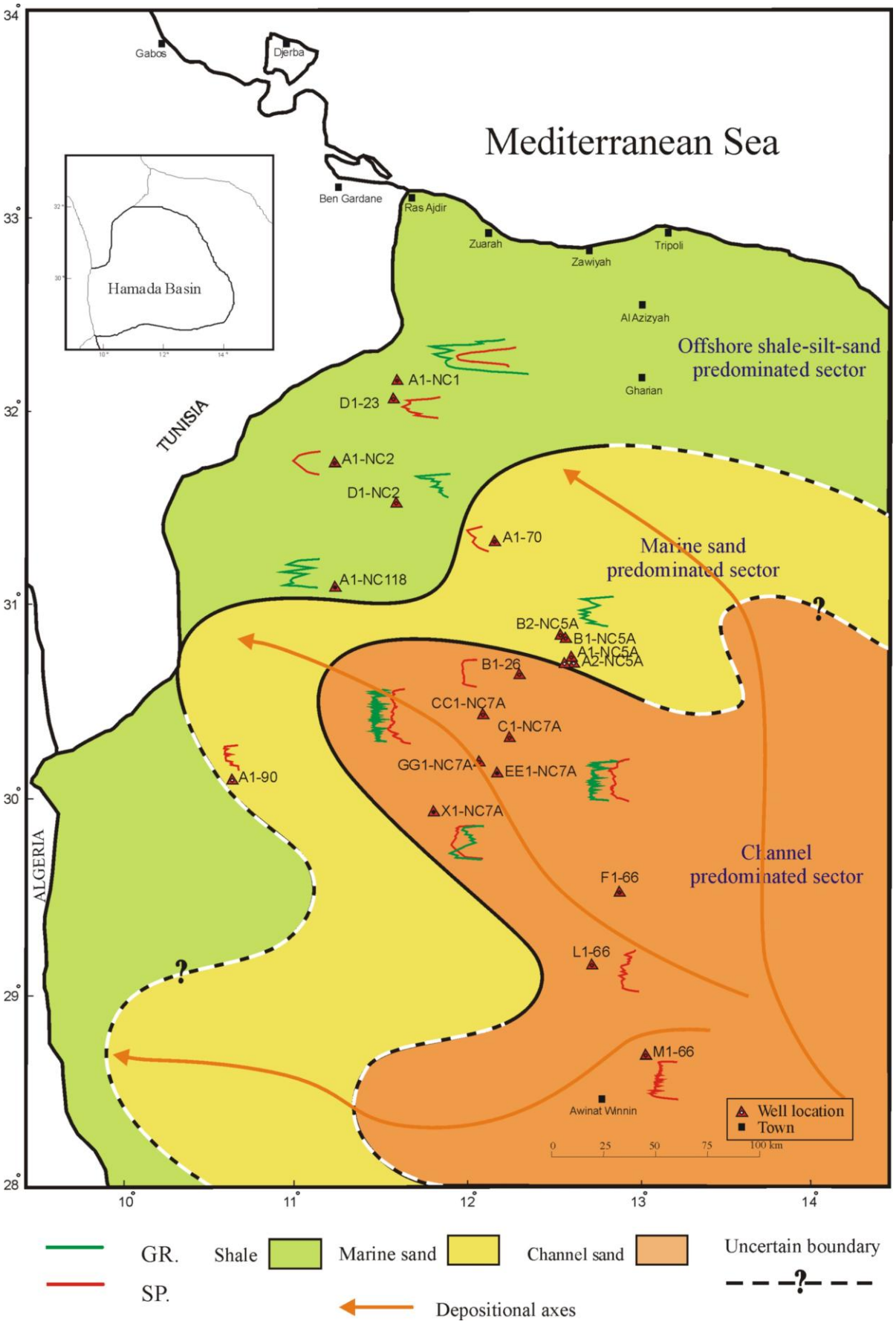

Figure 84. Log facies map of sand unit **(**3**)** for Memouniat Formation, Hamada **(**Ghadames**)** Basin.

Figure 85. Log facies map of sand unit **(**4**)** for Memouniat Formation, Hamada **(**Ghadames**)** Basin.

6.4.3 Superimposed Maps for Facies 1-4

The heterogeneity of Memouniat Formation can be seen laterally using sand axes map **(**Fig. 86**)** and can be seen vertically using composite facies map **(**Fig. 8**7)**. In this composite facies map penetration of different facies types **(**units**)** could be recovered. However, penetration of good stacking thickness present in each mapped unit is highly unlikely. This may relate to differential compaction and of different channel supply and shift of channel courses through time.

The channel shift could be obviously seen in **(**Fig. 86**)** which may be caused by intensive sedimentation in a relatively stable basin area **(**Blatt, Middleton and Murray, 1980**)**.

In the superimposed slice maps **(**Fig. 88**)**, the vertical sequence in any well can penetrate different sands at different locations. As a result one can conclude that the southern and central parts of the study area in the vicinity of wells M1-66, L1-66, F1-66, EE1-NC7A, GG1-66, NC7A, CC1- NC7A, A1- NC5A, B1-NC5A and B2-NC5A have probably the great chance to recover clean sandstones of channelized and shoreface facies. However, the northern part of the study area in the vicinity of the wells D1-NC2, A1- NC2, D1-23 and A1- NC1 will be characterized mostly by silty-shaly sandstones of basinal offshore facies.

By using figure 88, in case of selecting some areas to be drilled and penetrating the four horizons at locations **(**1, 2, 3, 4 and 5**)**, priority must be given to location **(**5), in spite of the fact that at this location less thickness **(**20-50ft**)** of the prospected sands **(**1-4**)** will be recovered, but of good reservoir characteristics represented by clean reworked sands of wave dominated sector in which winnowing out of the clay was very pronounced leaving behind the good clean coarser materials which may have a good secondary dissolutional porosity.

Location **(**2**)** must be penetrating good thick sequence of channel sands which may have good characteristics if the bottom coarse-grained part of the channel was recovered rather than the top fine-grained part; because the top most part of the channel may have some shale laminations which destroy the reservoir property of this sand unit. In fact this second priority location is characterized by primary porosity at the basal part of the channel which may partially filled with silica cement and reduce porosity.

Locations **(**1, 3, and 4**)** are of least priority because they are penetrating most likely the silty shale units which are of low quality, hence in these locations reservoir characterizations will be deteriorated.

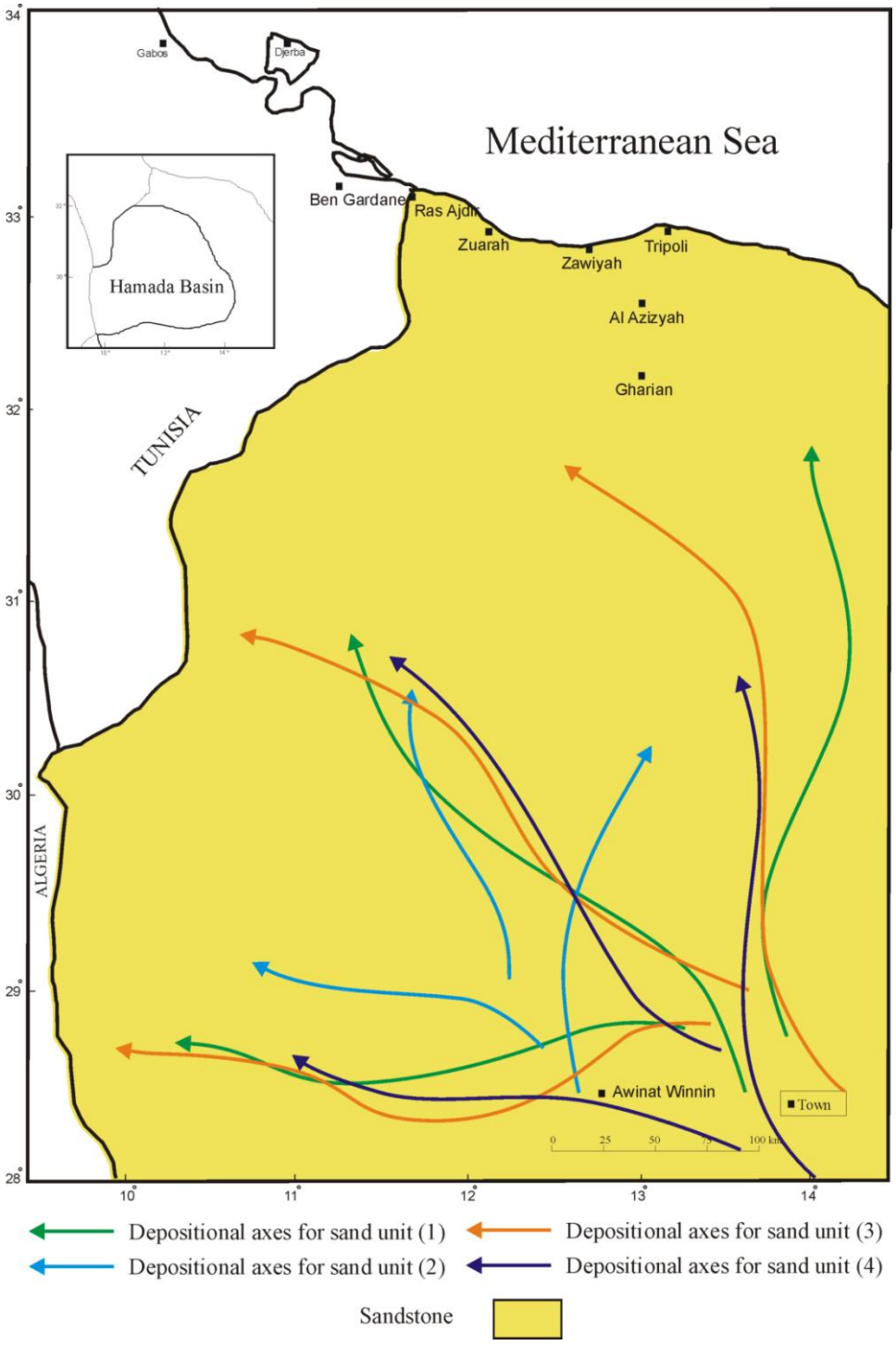

Figure 86. Depositional axes map for sand units 1-4 in the Memouniat Formation, Hamada **(**Ghadames**)** Basin.

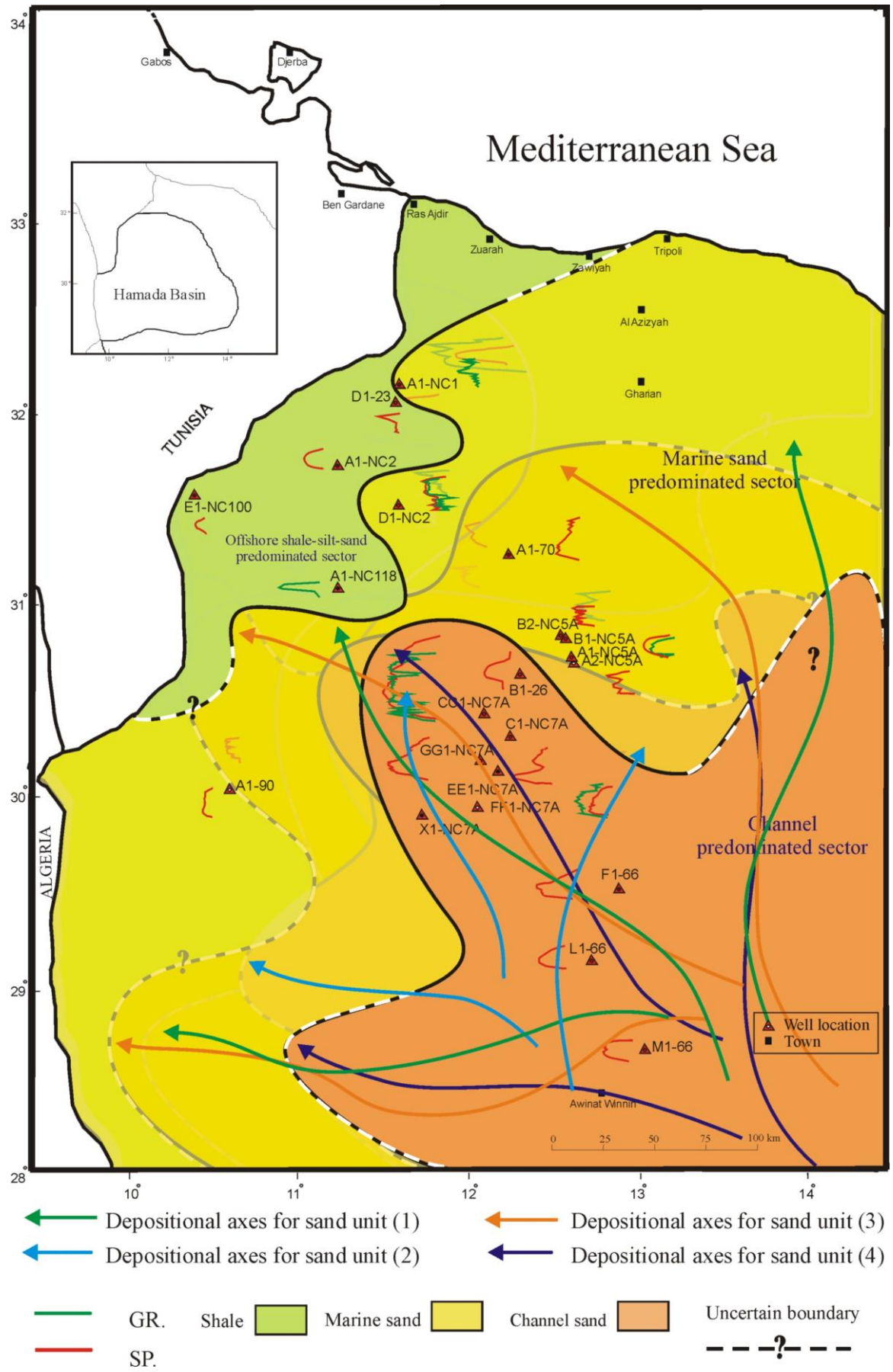

Figure 87. Composite facies map of Memouniat Formation, Hamada **(**Ghadames**)** Basin.

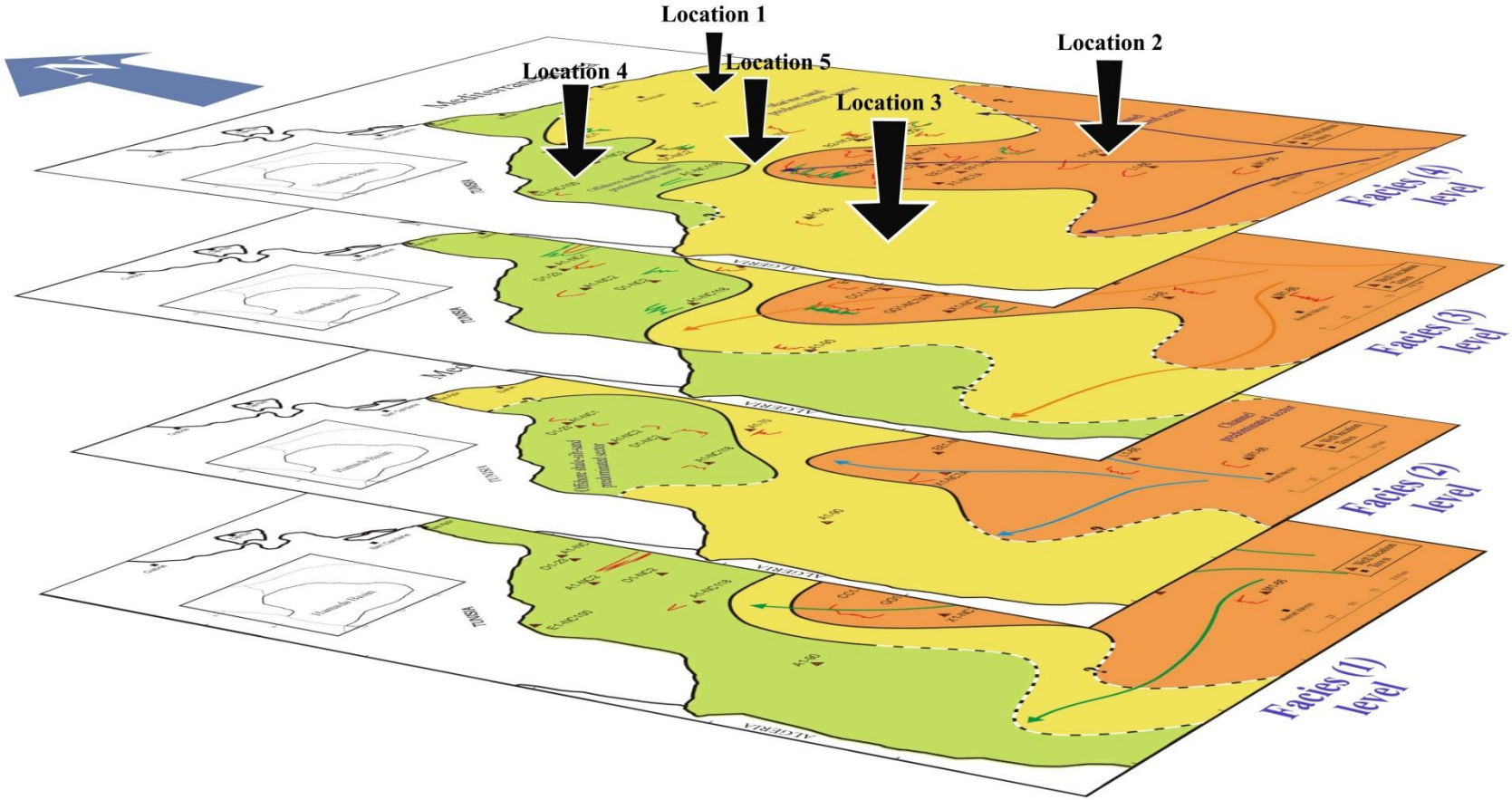

Fig. 88. Superimposed slice maps for studied facies 1-4 in the Memouniat Formation, Hamada **(**Ghadames**)** Basin. The vertical arrows at the top indicates the priority for better facies to be drilled.

Conclusions

Well-to-well correlation incorporating the facies data derived from cores and GR-log and SP-log characteristics have revealed that the Memouniat Formation in the area of study Hamada **(**Ghadames**)** Basin consists of mainly three depositional units bounded by time-stratigraphic markers. Within the established stratigraphic framework the identified facies change in a predictable fashion northwestward from channelized dominated sands to wavy laminated sands **(**proximal shoreface**)**, and eventually to basinal-offshore bioturbated silt/shale. The sands in the interpreted channels are coarse-grained and relatively thickly bedded than those in the proximal-shoreface and according to modal analysis through petrographic examination the Memouniat Formation have revealed that the average detrital composition of these sands is that of sublitharenite **(**Folk, 1980**)** with framework detrital grains averaging 92% monocrystalline quartz, 2% feldspar and 6% rock fragments.

Carbonate cement **(**calcite**)** was partially found in the channel-fill sands and proximal shoreface sands which increasing in occurrences in the basinal-offshore bioturbated silt/shale.

The depositional sand trends or axes of the mappable stratigraphic units **(**1-4**)** in the Memouniat Formation are offsets from those in the older units as a result of some differential compaction accompanying with changing channel courses through time. Therefore penetrating clean stacking maximum sand thickness present in each of the mapped units **(**1-4**)** is highly unlikely. Hence these sands are revealing its heterogeneity. The established composite facies map and the superimposed slice maps for the studied sand unit **(**1-4**)** are providing the basis for predicting regional facies distribution of Memouniat Formation throughout the Hamada **(**Ghadames**)** Basin.

The reliability of using wireline logs in presenting and defining the fundamental depositional facies also was investigated. The GR-log was found to be more accurate to the SP-log in identifying facies packages, making correlation and where cores were not available or where the primary sedimentary structures were obsecured by bioturbation or by unconsolidated nature of the sands.

Recommendation

This study has shown that an understanding of the facies distribution of Memouniat Formation and their possible depositional environments relationship through **(**cores, petrographic study, cross-section, fence diagram, isopach maps, facies maps and superimposed slice maps**)** is essential and to be pursued for an adequate assessment, evaluation and hence future exploration success of these sands interms of their facies development, quality and continuity.

Further study of these sands is very well needed regarding possible isolated structural culminations associated with available facies and some minor or major faults which may enhance locally the prospective sands of Memouniat Formation at some locations in the study area.

Future stratigraphic and sedimentological investigations are very well recommended for the carbonate unit characterizing the southwest and northeast portions of the study area at the vicinity of wells A1-90, D2-24, C1-NC143 to clearify its stratigraphic position and origin in the sequence.

Thus, on a basinwide basis, it is advantageous to establish both vertical and lateral distribution of facies in a manner illustrated in this study.

This information, along with knowledge of the tectonic history can be used to predict the distribution of Memouniat facies and their quality variations across the Hamada **(**Ghadames**)** Basin.

References

Attar, A. **(**1987**)**. Evolution structurale du bassin d'I1lizi. Internal Exploration Report 2575, Sonatrach, Algiers. In Geology and hydrocarbon occurrences in the Ghadames Basin, Algeria, Tunisia, Libya, eds. K. Echikh. **(**1998**)**, *Geological Society, London, Special Publications* v. 132; p. 109-129.

Ameed K. Ghori R. and Rajab A. Mohammed **(**2000**)**, Petroleum System Modelling in Ghadames Basin of NW Libya. In The Geology of Northwest Libya **(**2000**)**, eds. M. J. Salem, Khaled. M. Oun & Hussein M. Seddiq, p 245-259.

Belhaj, F. **(**1996**)**. Palaeozoic and Mesozoic stratigraphy of eastern Ghadamis and western Sirt Basins. *First Symposium on the Sedimentary Basins of Libya, Geology of the Sirt Basin.* vol. 1. ***(****eds. M.J. Salem, A.J. Mouzughi and O. S. Hammuda****)****,* Elsevier, Amsterdam, p. 57-96.

Bellini, E. and Massa, D. **(**1980**)**. A stratigraphic contribution to the Palaeozoic of the southern basins of Libya. *Second symposium on the Geology of Libya.* Vol. 1 **(***eds. M.J. Salem and M.T. Busrewil***)**, Academic Press, London,p. 3-56.

Bergstrom, S.M. and Massa, D. **(**1991**)**. Stratigraphic biogeographic significance of Upper Ordovician conodonts from northwestern Libya. *Third Symposium on the Geology of Libya.* vol. 4 ***(****eds. M.J. Salem, O.S. Hammuda and B.A. Eliagoubi****)****,* Elsevier, Amsterdam, p. 1323-1342.

Blatt, H. , Middleton, G. and Murray R., **(**1980**)**. Environments and facies, ancient costal deposits. In: Origin of sedimentary rocks, sec. ed, p. 673-689.

Boote, D. R. D., Clark-Lowes, D. D., Traut, M. W. **(**1998**)**. Palaeozoic petroleum systems of North Africa. In: *Petroleum. Geology of North Africa, **(****ed. D. S. Macgregor, R.T.J. Moody, D. D. Clark-Lowes****)****,* Geol. Soc. pecial Publication No. 132, p. 7-68.

Collomb, G.R. **(**1962**)**. Etude geologique du Jebel Fezzan et de sa bordure Palaeozoique. *Com. Fran, du Pet, Notes etMem.* no. 1, p. 7-35.

Dickson, T. A. D. **(**1965**)**. A modified staining techniques for carbonates in thin section. Nature, Vol. 205, 587 p.

Dolson J., (2) Muller D., (3) Evetts M. J., (4) and Stein J. A., (3),. (1991). Regional Paleotopographic Trends and Production, Muddy Sandstone (Lower Cretaceous), Central and Northern Rocky Monutainso, The American Association of Petroleum Geology Bulletin V. 75, No. 3 (March 1991), p. 409-435. Abstract.

Don Hallett, (2004). Petroleum Geology of Libya. 2nd impression, p. 277.

Echikh, K. (1992). *Geology and hydrocarbon potential of Ghadamis basin.* Internal Report, National Oil Company of Libya (NOC), Tripoli.

Echikh, K. (1998). Geology and hydrocarbon occurrences in the Ghadames Basin, Algeria, Tunisia, Libya. In: *Petroleum Geology of North Africa, (ed. D.S.Macgregor, R.T.J. Moody, D.D. Clark-Lowes),* Geol. Soc. Special Publication No. 132, p. 109-130.

Elfigih, O. B. (2000). Regional Diagenesis and its relation to facies change in the Upper Silurian Lower Acacus Formation, Hamada (Ghadames) Basin NW Libya. Ph.D. thesis, Memorial Univ., NFLD, Canada.

El Hawat, A.S., Bezan A., Obeidi A., and Barghathi H. (2003). The Upper Ordovician-Lower Silurian Succession of Western Libya. Sequence Stratigraphy and Glacioeustatic- Tectonic Scenario. In the Geology of Northwest Libya, Salem and Oun (eds.), ESSL, Tripoli, Vol 1, p. 65-78.

Folk, R. L., (1980). Petrography of Sedimentary Rocks. Hemphill publishing company, Austin, Texas, p. 184.

Galehause, J. S. (1971). point counting (Ch. 16), In procedures in sedimentary petrology (ed. Carver, R. E., univ. and Gorgia Athens, Georgia, p. 385-406.

Gustason E. R., Wheeler D. A., ., Ryer T. A (1988). Structural Control on Paleovalley Development, Muddy Sandstone, Powder River Basin, Wyoming. AAPG Search and Discovery Article #91033©1988 AAPG Rocky Mountain Section, Bismarck, North Dakota, 21-24 August 1988. Abstract.

Havlicec, V. and Massa, D. (1973). Brachiopodes del Ordovician superieur de Libye occidentale, implications stratigraphiques regionales. *Geobios,* vol. 6, p. 267-290.

Heinrich E. Wm., **(**1965**)**. Microscopic Identification of Minerals. Professor of Minorology, the University of Michigan Ann Arbor, Michgan, p. 334.

Henry S. G., Al Danforth[2] **(**1**)** Geolearn LLC, Houston, **(**2002**)**. Application of Paleogeographic Maps for New Play Development in West Africa, AAPG Annual Meeting March 10-13, 2002 Houston, Texas.

Howlett, P. **(**2000**)**. Trapping Style in the Ghadamis **(**Berkine**)** Basin of Algeria, Libya and Tunisia. *Second Symposium on the Sedimentary basins of Libya. The Geology of Northwest Libya.* Book of abstracts, p. 361.

Jean-Loup Rubinoo, Remy Anfrayo , Christina Blanpiedo , Jean-Franconis Ghienne[2] and Gianreto Manatschal[2] **(**2000**)**, Meander Belt Complex within the lower Memouniat Formation in Western Al Qarqaf Area, Libya. In The Geology of Northwest Libya **(**2000**)**, eds. M. J. Salem, Khaled. M. Oun & Hussein M. Seddiq, p. 3 -18.

Klitzsch, E. **(**1971**)**. The Structure development of part of north Africa since Cambrian time. First Symposium on the Geology of Libya (ed. C. Gray). Faculty of Science, University of Libya, Tripoli.

Luning, S., Craig, J., Loydell, D.K., Storch, P. and Fitches, B. **(**2000a**)**. Lowermost Silurian 'hot shales' in north Africa and Arabia: regional distribution and depositional model. *Earth Science Reviews,* vol. 49, p. 121-200.

Marco Vecoli, Marco Tongiorgi, Marco Quintavalle and Dominique Massa **(**2000**)**, Palynological Contribution to the Cambro-Ordovician Stratigraphy of NW Ghadames Basin **(**Libya and Tunisia**)**. In The Geology of Northwest Libya **(**2000**)**, eds. M. J. Salem, Khaled. M. Oun & Hussein M. Seddiq, p. 253-266.

Massa, D. and Collomb, G. R. **(**1960**)**. Observations nouvelles sur la region d'Aouinet Ouenine et du Djebel Fezzan (Libye). *Proc. 21st Int. Geol. Congr.* (Norden), p. 12, 65-73.

Massa, D., Coquel, R., Loboziak, S. and Taugourdeau-Lantz, J. **(**1980**)**. Essai de synthese stratigraphique et palynologique du Carbonifere en Libye occidentale. *Ann. Soc. Geol. Nord.* Vol. 99, p. 429-442.

Massa, D. **(**1988**)**. *Paleozoique de Libye Occidentale- Stratigraphie et paleogeographie.* Doctoral thesis, Univ. Nice, p. 520.

McGeary D., Plummer C. C., Carlson D. H. **(**2004**)**. Physical Geology Earth Revealed. Californiaa State University at Sacramento. p. 301.

Miller, J., **(**1988**)**. Microscopical techniques chapter **(**4**)**. In techniques in sedimentology, **(**ed. Tuckes, M., 1988**),** p. 96-101.

Reading, H. G., **(**1978**)**. Sedimentary Environments and Facies. Elsevie, New York, 557 P. Don Hallett, **(**2002**)**. Petroleum Geology of Libya.

Rubino, J. L., Anfray, R., Blanpied, C., Ghienne, J. F., and Manatschal, G., **(**2000**)**. Meander Belt Complex within the Lower Mamuniyat Formation in Western Al Qarqaf Area, Libya. *Second Symposium on the Sedimentary basins of Libya. The Geology of Northwest Libya.* Abstracts, p. 3.

Ryer T. A., McClurg J. J., Muller M.t M. **(**1987**)**. Dakota-Bear River Paleoenvironments, Depositional History and Shoreline Trends-Implications for Foreland Basin Paleotectonics, Southwestern Green River Basin and Southern Wyoming Overthrust Belt. The Thrust Belt Revisited; 38th Annual Field Conference Guidebook, 1987, p. 179 - 206. Abstract.

Ryer, Thomas a., **(**1993**).** The Upper Cretaceous Ferron Sandstone of Central Utah: An overview, The Aries Group, Inc., Louisville, Co. Abstract.

Serra, O. **(**1989**)**. Sedimentary environments from wireline logs (Shlumberger), 2nd ed., p. 243.

Sikander, A.H. **(**2000**)**. The geology, structure and hydrocarbon potential of the Ghadamis and Murzuq Basins an overview (Abstract). *Second Symposium on the Sedimentary basins of Libya. The Geology of Northwest Libya.* Book of abstracts, p. 281.

Smith L. N., **(**1992**)**. Stratigraphy, Sediment Dispersal and Paleogeography of The Lower Eocene San Jose Formation, San Juan Basin, New Mexico and Colorado. New Mexico Geological Society Guidbook. 43rd Field Conference. San Juan IV. 1992.

Tucker M. E., **(**1991**)**. Sedimentary Petrology, An Introduction to the Origin of Sedimentary Rocks, eds. A. Hallam. sec. ed, p. 19.

Vaslett, **(**1990**)**. Petroleum Geology of North Africa, Cambrian - Ordovician.

Walderhaug, O. and Bjorkum, P. A. (2009) Calcite Cement in Shallow Marine Sandstones: Growth Mechanisms and Geometry, in Carbonate Cementation in Sandstones: Distribution Patterns and Geochemical Evolution (ed S. Morad), Blackwell Publishing Ltd., Oxford, UK. doi: 10.1002/9781444304893.ch8.

Wanis E. **(**2000**)**, Geology Evolution of Ghadames Basin-Impact on Hydrocarbon Prospectivity. In The Geology of Northwest Libya **(**2000**)**, eds. M. J. Salem, Khaled. M. Oun & Hussein M. Seddiq, p. 327-350.

Waringo J., **(**1976**)**. Regional Distribution of Environments of The Muddy Sandstone, Southeastern Montana. Geology and Energy Resources of the Powder River; 28th Annual Field Conference Guidebook, 1976 Pages 83 - 96. Introduction.

West G. **(**1991**)**. A note on undulatory extinction of quartz in granite. The Geological Society. Abstract.

Youssif and Abugares **(**2000**)**, The Petroleum Geology of the Palaeozoic Clastic of the Murauq Basin, Al Atshan Saddle and the Southern Part of the Ghadames Basin, Libya. In The Geology of Northwest Libya **(**2000**)**, eds. M. J. Salem, Khaled. M. Oun & Hussein M. Seddiq, p. 213-244.